Pancreatic Cancer - Early Detection, Prognostic Factors, and Treatment

Ansari, Daniel

2014

Bulletin No. 149 from the Department of Surgery, Clinical Sciences Lund,
Lund University, Sweden

Pancreatic Cancer

Early Detection, Prognostic Factors, and Treatment

Daniel Ansari, MD

LUND
UNIVERSITY

DOCTORAL DISSERTATION
by due permission of the Faculty of Medicine, Lund University, Sweden.

To be defended at Lecture Room 4, Main building, Skåne University Hospital,
Lund, September 26, 2014, at 1:00 pm.

Faculty opponent

Professor Helmut Friess, Department of General Surgery, The University Hospital
Rechts der Isar, Technical University Munich, Munich, Germany

Supervisor: Professor Roland Andersson

Co-supervisor: Associate Professor Bodil Andersson

Co-supervisor: Professor György Marko-Varga

Organization	Document name
LUND UNIVERSITY	DOCTORAL DISSERTATION
Department of Surgery, Skåne University Hospital	Date of issue: September 26, 2014
Author: Daniel Ansari, MD	Sponsoring organization

Title and subtitle: Pancreatic cancer – early detection, prognostic factors, and treatment

Abstract

Background: Pancreatic cancer is the fourth leading cause of cancer-related death. Only about 6% of patients are alive 5 years after diagnosis. One reason for this low survival rate is that most patients are diagnosed at a late stage, when the tumor has spread to surrounding tissues or distant organs. Less than 20% of cases are diagnosed at an early stage that allows them to undergo potentially curative surgery. However, even for patients with a tumor that has been surgically removed, local and systemic recurrence is common and the median survival is only 17-23 months. This underscores the importance to identify factors that can predict postresection survival. With technical advances and centralization of care, pancreatic surgery has become a safe procedure. The future optimal treatment for pancreatic cancer is dependent on increased understanding of tumor biology and development of individualized and systemic treatment. Previous experimental studies have reported that mucins, especially the MUC4 mucin, may confer resistance to the chemotherapeutic agent gemcitabine and may serve as targets for the development of novel types of intervention.

Aim: The aim of the thesis was to investigate strategies to improve management of pancreatic cancer, with special reference to early detection, prognostic factors, and treatment.

Methods: In paper I, 27 prospectively collected serum samples from resectable pancreatic cancer (n=9), benign pancreatic disease (n=9), and healthy controls (n=9) were analyzed by high definition mass spectrometry ($HDMS^E$). In paper II, an artificial neural network (ANN) model was constructed on 84 pancreatic cancer patients undergoing surgical resection. In paper III, we investigated the effects of transition from a low- to a high volume-center for pancreaticoduodenectomy in 221 patients. In paper IV, the grade of concordance in terms of MUC4 expression was examined in 17 tissue sections from primary pancreatic cancer and matched lymph node metastases. In paper V, pancreatic xenograft tumors were generated in 15 immunodeficient mice by subcutaneous injection of MUC4+ human pancreatic cancer cell lines; Capan-1, HPAF-II, or CD18/HPAF. In paper VI, a 76-member combined epigenetics and phosphatase small-molecule inhibitor library was screened against Capan-1 (MUC4+) and Panc-1 (MUC4-) cells, followed by high content screening of protein expression.

Results/Conclusion: 134 differentially expressed serum proteins were identified, of which 40 proteins showed a significant up-regulation in the pancreatic cancer group. Pancreatic disease link associations could be made for BAZ2A, CDK13, DAPK1, DST, EXOSC3, INHBE, KAT2B, KIF20B, SMC1B, and SPAG5, by pathway network linkages to p53, the most frequently altered tumor suppressor in pancreatic cancer (I). An ANN survival model was developed, identifying 7 risk factors. The C-index for the model was 0.79, and it performed significantly better than the Cox regression (II). We experienced improved surgical results for pancreaticoduodenectomy after the transition to a high-volume center (≥25 procedures/year), including decreased operative duration, blood loss, hemorrhagic complications, reoperations, and hospital stay. There was also a tendency toward reduced operative mortality, from 4% to 0% (III). MUC4 positivity was detected in most primary pancreatic cancer tissues, as well as in matched metastatic lymph nodes (15/17 vs. 14/17), with a high concordance level (82%) (IV). The tumor incidence was 100% in the xenograft model. The median MUC4 count was found to be highest in Capan-1 tumors. α-SMA and collagen extent were also highest in Capan-1 tumors (V). Apicidin (a histone deacetylase inhibitor) had potent antiproliferative activity against Capan-1 cells and significantly reduced the expression of MUC4 and its transcription factor HNF4α. The combined treatment of apicidin and gemcitabine synergistically inhibited growth of Capan-1 cells (VI).

Key words: artificial neural networks, apicidin, centralization, early detection, epigenetics, high definition mass spectrometry, MUC4, pancreatic cancer, pancreaticoduodenectomy, prognostic factors, xenograft model, treatment

Classification system and/or index terms (if any)

Supplementary bibliographical information | Language: English

ISSN and key title: 1652-8220 | ISBN: 978-91-7619-032-6

Recipient's notes | Number of pages 180 | Price

Security classification

Pancreatic Cancer

Early Detection, Prognostic Factors, and Treatment

Daniel Ansari, MD

LUND
UNIVERSITY

Department of Surgery, Clinical Sciences Lund
Skåne University Hospital, Lund, Sweden
ISBN 978-91-7619-023-6
ISSN 1652-8220

Front cover illustration and Figure 1 courtesy and copyright of Anders Flood

Printed in Sweden by Media-Tryck, Lund University
Lund 2014

Contents

“Chance favors the prepared mind”

Louis Pasteur

List of publications

The thesis is based on the following papers, which are referred to in the text by their Roman numerals. The papers are appended at the end of the thesis.

I. Ansari D, Andersson R, Bauden MP, Andersson B, Connolly J, Welinder C, Sasor A, Marko-Varga G. Protein deep sequencing applied to biobank samples from patients with pancreatic cancer. Journal of Cancer Research and Clinical Oncology 2014; In press.

II. Ansari D, Nilsson J, Andersson R, Regnér S, Tingstedt B, Andersson B. Artificial neural networks predict survival from pancreatic cancer after radical surgery. American Journal of Surgery 2013;205:1-7.

III. Ansari D, Williamsson C, Tingstedt B, Andersson B, Lindell G, Andersson R. Pancreaticoduodenectomy - the transition from a low- to a high-volume center. Scandinavian Journal of Gastroenterology 2014;49:481-4.

IV. Ansari D, Urey C, Gundewar C, Bauden MP, Andersson R. Comparison of MUC4 expression in primary pancreatic cancer and paired lymph node metastases. Scandinavian Journal of Gastroenterology 2013;48:1183-7.

V. Ansari D, Bauden MP, Sasor A, Gundewar C, Andersson R. Analysis of MUC4 expression in human pancreatic cancer xenografts in immunodeficient mice. Anticancer Research 2014;34:3905-10.

VI. Ansari D, Urey C, Said Hilmersson K, Bauden MP, Ek F, Olsson R, Andersson R. Apicidin sensitizes pancreatic cancer cells to gemcitabine by epigenetically regulating MUC4 expression. Anticancer Research 2014; In press.

Thesis résumé

STUDY	QUESTION	METHODS	RESULTS & CONCLUSION
I 	Can protein deep sequencing aid in the discovery of serum biomarkers for pancreatic cancer?	Prospective serum study. 27 serum samples from resectable pancreatic cancer (n=9), benign pancreatic disease (n=9), and healthy controls (n=9), 2012-2013. Sample preparation followed by high definition mass spectrometry ($HDMS^E$) analysis.	134 differentially expressed proteins were identified, of which 40 proteins showed a significant up-regulation in the pancreatic cancer group. 10 protein candidates were linked to the tumor suppressor p53 by protein network analyses.
II 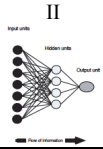	Can an artificial neural network (ANN) model predict long-term survival in pancreatic cancer?	Retrospective chart review. 84 pancreatic cancer patients undergoing surgical resection, 1995-2010. A ten-fold cross-validated feed-forward ANN was created and trained.	7 risk variables readily available in the clinic were identified. The discriminatory power for predicting survival determined with the C-index was 0.79 for the ANN and 0.67 for Cox regression.
III 	Does the transition from a low- to high-volume center for pancreatico-duodenectomy (PD) improve surgical outcome?	Retrospective chart review. 221 patients undergoing PD for pancreatic cancer and other periampullary tumors, 2000-2012.	Operative duration, blood loss, hemorrhagic complications, reoperations, and length of stay decreased after the transition to a high-volume center. Tendency toward reduced operative mortality, from 4% to 0%.
IV 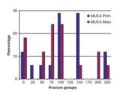	What is the grade of concordance in terms of MUC4 expression between primary pancreatic cancer and paired lymph nodes metastases?	Retrospective tissue study. 17 tissue sections from primary pancreatic cancer and matched lymph node metastases, 1999-2009. MUC4 immunostaining was performed.	MUC4 positivity was detected in most primary tumors and metastatic lesions (15/17 vs. 14/17) with a high level of concordance (82%). This suggests that MUC4 expression is retained during pancreatic cancer progression and could serve as target also for pancreatic cancer cell dissemination.
V 	Can a biologically relevant in vivo model of pancreatic cancer be generated that is suitable for the study of MUC4-directed therapy?	Experimental animal study. Pancreatic xenograft tumors were generated in 15 immunodeficient mice by subcutaneous injection of MUC4+ human pancreatic cancer cell lines; Capan-1, HPAF-II, or CD18/HPAF.	Tumor incidence was 100%. The median MUC4 count was highest in Capan-1 tumors. α-SMA and collagen extent were also highest in Capan-1 tumors.
VI 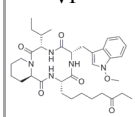	Can epigenetic control of MUC4 expression sensitize pancreatic cancer cells to gemcitabine treatment?	Experimental in vitro study. A 76-member combined epigenetics and phosphatase small-molecule inhibitor library was screened for antiproliferative activity against Capan-1 (MUC4+) and Panc-1 (MUC4-) cells, followed by high content screening of protein expression.	Apicidin (a histone deacetylase inhibitor) showed the greatest antiproliferative activity in Capan-1 cells and significantly reduced the expression of MUC4 and its transcription factor HNF4α. The combined treatment with apicidin and gemcitabine synergistically inhibited growth of Capan-1 cells.

Abstract

Background: Pancreatic cancer is the fourth leading cause of cancer-related death. Only about 6% of patients are alive 5 years after diagnosis. One reason for this low survival rate is that most patients are diagnosed at a late stage, when the tumor has spread to surrounding tissues or distant organs. Less than 20% of cases are diagnosed at an early stage that allows them to undergo potentially curative surgery. However, even for patients with a tumor that has been surgically removed, local and systemic recurrence is common and the median survival is only 17-23 months. This underscores the importance to identify factors that can predict postresection survival. With technical advances and centralization of care, pancreatic surgery has become a safe procedure. The future optimal treatment for pancreatic cancer is dependent on increased understanding of tumor biology and development of individualized and systemic treatment. Previous experimental studies have reported that mucins, especially the MUC4 mucin, may confer resistance to the chemotherapeutic agent gemcitabine and may serve as targets for the development of novel types of intervention.

Aim: The aim of the thesis was to investigate strategies to improve management of pancreatic cancer, with special reference to early detection, prognostic factors, and treatment.

Methods: In paper I, 27 prospectively collected serum samples from resectable pancreatic cancer (n=9), benign pancreatic disease (n=9), and healthy controls (n=9) were analyzed by high definition mass spectrometry ($HDMS^E$). In paper II, an artificial neural network (ANN) model was constructed on 84 pancreatic cancer patients undergoing surgical resection. In paper III, we investigated the effects of transition from a low- to a high volume-center for pancreaticoduodenectomy in 221 patients. In paper IV, the grade of concordance in terms of MUC4 expression was examined in 17 tissue sections from primary pancreatic cancer and matched lymph node metastases. In paper V, pancreatic xenograft tumors were generated in 15 immunodeficient mice by subcutaneous injection of MUC4+ human pancreatic cancer cell lines; Capan-1, HPAF-II, or CD18/HPAF. In paper VI, a 76-member combined epigenetics and phosphatase small-molecule inhibitor library was screened against Capan-1 (MUC4+) and Panc-1 (MUC4-) cells, followed by high content screening of protein expression.

Results/Conclusion: 134 differentially expressed serum proteins were identified, of which 40 proteins showed a significant up-regulation in the pancreatic cancer group. Pancreatic disease link associations could be made for BAZ2A, CDK13, DAPK1, DST, EXOSC3, INHBE, KAT2B, KIF20B, SMC1B, and SPAG5, by pathway network linkages to p53, the most frequently altered tumor suppressor in pancreatic cancer (I). An ANN survival model was developed, identifying 7 risk factors. The C-index for the model was 0.79, and it performed significantly better than the Cox regression (II). We experienced improved surgical results for pancreaticoduodenectomy after the transition to a high-volume center (≥25 procedures/year), including decreased operative duration, blood loss, hemorrhagic complications, reoperations, and hospital stay. There was also a tendency toward reduced operative mortality, from 4% to 0% (III). MUC4 positivity was detected in most primary pancreatic cancer tissues, as well as in matched metastatic lymph nodes (15/17 vs. 14/17), with a high concordance level (82%) (IV). The tumor incidence was 100% in the xenograft model. The median MUC4 count was found to be highest in Capan-1 tumors. α-SMA and collagen extent were also highest in Capan-1 tumors (V). Apicidin (a histone deacetylase inhibitor) had potent antiproliferative activity against Capan-1 cells and significantly reduced the expression of MUC4 and its transcription factor HNF4α. The combined treatment of apicidin and gemcitabine synergistically inhibited growth of Capan-1 cells (VI).

Populärvetenskaplig sammanfattning

Pankreascancer, cancer i bukspottkörteln, är den fjärde vanligaste orsaken till död i cancer och årligen insjuknar cirka 1000 patienter i Sverige. Överlevnaden är kort med en 5-årsöverlevnad på endast 6 procent. Pankreascancer orsakar, förutom lidande, också betydande kostnader för såväl den medicinska vården, som förluster för samhället, exempelvis i form av förtida död.

Eftersom symtomen vid pankreascancer är vaga och ofta uppträder i ett sent skede av sjukdomen finns det ett stort behov av att förbättra den tidiga diagnostiken. Idag finns inga godkända diagnostiska biomarkörer för pankreascancer. Genom att söka efter proteinsekvenser i blodprov med s.k. masspektrometri kan nya biomarkörer för pankreascancer identifieras. Dessa markörer skulle kunna användas inom sjukvården för att i ett tidigt skede upptäcka om en patient bär på en tumör i pankreas innan den har spridit sig till andra organ. Då ökar möjligheten att bota patienten med operation.

Det är väsentligt med en korrekt bedömning av prognosen för varje patient för att styra val av behandling. Det finns flera prognostiska modeller beskrivna i litteraturen, men det saknas fortfarande ett etablerat prognostiskt system. Nuvarande stadieindelning, s.k. TNM-klassifikationen tar inte hänsyn till faktorer utöver T-stadium (primärtumörens storlek och utbredning), N-stadium (spridning till regionala lymfkörtlar) och M-stadium (förekomst av fjärrmetastaser). För patienter som genomgår kirurgi är TNM-indelningen inte tillräckligt pålitlig för att förutsäga den enskilde patientens prognos efter operation. En modell för prediktering av överlevnad kan baseras på s.k. artificiella neurala nätverk, en avancerad datoriserad optimeringsmodell som kan analysera icke-linjära samband.

Pankreascancer är svårbehandlad och det finns därmed en stor potential för terapiförbättringar. Kirurgin (Whipples operation) har successivt förfinats och dödsfall i samband med operation har minskat och är idag några enstaka procent. Det är visat att centralisering av pankreaskirurgi till högvolymscentra har haft en viktig roll i detta. Cytostatika (cellgifter) kan ges som efterbehandling efter kirurgi eller som behandling när tumören växer så att den inte kan opereras. Tyvärr är resistens mot cytostatika ett vanligt problem och fortsatta förbättringar av resultaten kräver ökad förståelse av tumörbiologin och ny typ av individanpassad behandling. MUC4 är ett cellyteprotein som ofta finns i vävnad från patienter med pankreascancer men som saknas i normal pankreas. Detta protein har i tidigare experimentella studier kunnat kopplas till

cytostatikaresistens. Terapi riktad mot MUC4 kan därför utgöra en framtida behandlingsstrategi mot pankreascancer.

I delarbete I studerades värdet av masspektrometri för att påvisa proteinmarkörer i serum tidigt i förloppet vid pankreascancer. Vid en jämförelse mellan operabel pankreascancer, godartade pankreassjukdomar och friska individer, identifierades 134 serumproteiner som kunde särskilja grupperna från varandra, varav 40 proteiner var uppreglerade vid pankreascancer. Flera av dessa proteiner kunde via interaktionsanalyser kopplas till p53, ett protein som har en central roll vid uppkomst av pankreascancer. Resultaten från denna studie är ett viktigt steg i utvecklingen av ett enkelt blodbaserat diagnostiskt test för pankreascancer.

I delarbete II utvecklades en algoritm för prognostisering av pankreascancer med hjälp av artificiella neurala nätverk. Riskfaktorer tillgängliga i daglig klinisk praxis och som bidrar till sämre prognos vid pankreascancer identifierades och rangordnades. En modell togs fram som hade bättre prediktionsförmåga än traditionell statistik analys.

I delarbete III kartlades alla patienter som genomgått Whipples operation i Lund under perioden 2000-2012. Totalt 221 patienter inkluderades. Resultaten visade att sedan övergången till högvolymskirurgi (definierat som 25 eller fler operationer per år) har de operativa resultaten förbättrats vad gäller blodförlust vid operation, operationstid, blödningskomplikationer, risk för reoperation och vårdtid. Operativ mortalitet minskade från 4 till 0 procent.

I delarbete IV studerades uttrycket av MUC4 i vävnad från primär pankreascancer och matchade lymfkörtelmetastaser. Resultaten visade att majoriteten av primärtumörerna uttryckte MUC4 och att detta uttryck bibehölls i metastaserna, vilket talar för att MUC4 är ett potentiellt behandlingsmål även vid metastaserande sjukdom.

I delarbete V utfördes experimentella djurstudier genom transplantation av pankreastumörcellinjer i immundefekta möss i syfte att arbeta vidare med MUC4-proteinet. Tumörer från en av cellinjerna (Capan-1) uttryckte mest MUC4 och bedömdes därför bäst lämpad för fortsatta studier.

I delarbete VI undersöktes den tillväxthämmande effekten av olika s.k. epigenetiska läkemedel på pankreascancerceller. Apicidin, en s.k. HDAC-hämmare visade sig mest effektivt och potentierade även effekten av det vanliga pankreascancermedlet gemcitabin genom att nedreglera MUC4 i cancercellinjen Capan-1.

Abbreviations

2-DE	two-dimensional gel electrophoresis
5-FU	fluorouracil
α-SMA	α-smooth muscle actin
ADH	alcohol dehydrogenase
AMOP	adhesion-associated domain in MUC4 and other proteins
ANN	artificial neural network
ASA	American Society of Anesthesiologists
BAZ2A	bromodomain adjacent to zinc finger domain protein 2A
BMI	body mass index
BPD	benign pancreatic disease
BPI	base peak intensity
BSA	bovine serum albumin
CCK	cholecystokinin
CA 19-9	carbohydrate antigen 19-9
CAF	cancer associated fibroblast
CD	cytoplasmic tail domain
CDK13	cyclin-dependent kinase 13
C-index	concordance index
CEA	carcinoembryonic antigen
CT	computed tomography
DAB	diaminobenzidine
DAPI	4',6-diamidino-2-phenylindole
DAPK1	death-associated protein kinase 1

DGE	delayed gastric emptying
DPBS	Dulbecco's phosphate-buffered saline
DST	bullous pemphigoid antigen 1, isoforms 6/9/10
EDTA	ethylenediaminetetraacetic acid
EGF	epidermal growth factor
EMT	epithelial-mesenchymal transition
ESI	electrospray ionization
EXOSC3	exosome component 3
FDA	Food and Drug Administration
FFPE	formalin fixed paraffin embedded
FOXA2	forkhead box A2
FWHM	full width at half maximum
GATA6	GATA-binding factor 6
H	healthy
H-score	histochemical score
H&E	hematoxylin and eosin
HCS	high content screening
$HDMS^E$	high definition mass spectrometry
HNF4α	hepatocyte nuclear factor 4 alpha
HRP	horseradish peroxidase
INHBE	inhibin beta E chain
IPMN	intraductal papillary mucinous neoplasm
ISGPF	International Study Group on Pancreatic Fistula
ISGPS	International Study Group of Pancreatic Surgery
KAT2B	histone acetyltransferase KAT2B
KIF20B	kinesin-like protein KIF20B
KM	Kaplan-Meier
LC-MS/MS	liquid chromatography tandem mass spectrometry
LD_{50}	lethal dose 50
MS	mass spectrometry

MUC4	mucin 4
NIDO	nidogen
p53	tumor protein 53
PanIN	pancreatic intraepithelial neoplasia
PANTHER	protein annotation through evolutionary relationship
PC	pancreatic cancer
PCA	principal component analysis
QC	quality control
ROC	receiver operating characteristic
RP	reversed phase
RSD	relative standard deviation
SMC1B	structural maintenance of chromosomes protein 1B
SPAG5	astrin
STRING	search tool for the retrieval of interacting genes/proteins
TBS	tris-buffered saline
TM	transmembrane
TNM	tumor-node-metastasis
TR	tandem repeat
UPLC	ultra performance liquid chromatography
vWD	von Willebrand factor D

Chapter 1 Introduction

1.1 The past and present of pancreatic cancer

The earliest known description of pancreatic cancer was provided in 1761 by Giovanni Battista Morgagni, an Italian pathologist at the University of Padua [1]. In his autopsy studies he reported the presence of lesions in the pancreas, but the lack of a microscope and a detailed histological report cast doubts on the supposed cancer diagnosis. In 1858, Jacob Mendez Da Costa, a Philadelphia clinician-pathologist, revisited Morgagni's original work and made a substantial contribution to the subject of pancreatic neoplasia by recording several cases of pancreatic cancer with one of these cases having a microscopic diagnosis of adenocarcinoma [2].

Forty years later, in 1898, the Italian surgeon Alessandro Codivilla performed the first reported attempt at a pancreaticoduodenectomy for a tumor involving the head of the pancreas, but this patient did not survive the postoperative period [3]. The same year, 1898, William Stewart Halsted from Johns Hopkins Hospital performed the first successful resection for ampullary cancer by excising portions of the duodenum and pancreas [4]. Once Emil Theodor Kocher, a Swiss surgeon, established his classical technique of a more extensive pancreaticoduodenal exposure (the Kocher maneuver) in 1903, several attempts were made at pancreatic resection [5]. In 1912, Walther Carl Eduard Kausch, a German surgeon, performed the first successful pancreaticoduodenectomy in two stages [6]. Two years later, Georg Hirschel described the first successful pancreaticoduodenectomy in one stage [7]. Some 21 years later, in 1935, Allen Oldfather Whipple presented the results of a two-stage procedure involving resection of the head of the pancreas and duodenum for ampullary carcinoma, which renewed the interest in pancreatic surgery [8]. Whipple and his colleagues were among the first to use silk instead of catgut, which was easily dissolved by pancreatic enzymes. In all, Whipple reported 37 pancreaticoduodenectomies in his career with the operation evolving from a two-stage to a one-stage procedure [9, 10]. Whipple is generally credited with popularizing the operation that still bears his name. In 1937, Alexander Brunschwig extended the indication for pancreaticoduodenectomy to include cancer of the head of the pancreas [11].

During the 1960s and 1970s pancreaticoduodenectomy was performed in small numbers because of a hospital mortality of approximately 25% [12]. However, during the 1980s and 1990s, a dramatic decline in hospital mortality was realized in a number of centers, and in recent years it has been demonstrated that with concentration of experience the mortality rate could be reduced to below 5% [12-15].

While major advances have been made in the surgical management of pancreatic cancer since the era of Whipple, the principal surgical goal remains the same. This includes removal of all gross and microscopic disease within the pancreas, a so-called margin-negative or R0 resection [16, 17].

Although pancreatic surgery nowadays can be performed more safely, only 10-20% of all pancreatic cancer patients are diagnosed at an early stage, that allows them to be candidates for curative resection. Even for patients with a tumor that has been surgically removed the median survival is only 17-23 months [18]. Treatment for patients with advanced disease still remains largely palliative. The anti-tumor activity of fluorouracil (5-FU) in pancreatic cancer was reported as far back as the 1960s [19]. In 1997, gemcitabine emerged as a new reference treatment in advanced pancreatic cancer with alleviation of some disease-related symptoms and a slight survival advantage over 5-FU treatment [20]. FOLFIRINOX (folinic acid, 5-FU, irinotecan, and oxaliplatin) [21] or nab-paclitaxel in combination with gemcitabine [22] have both improved survival for pancreatic cancer patients compared with gemcitabine alone, but the median survival for both are still less than 1 year.

In the light of the observation that mortality rates for all major cancer sites have decreased in recent years, it is discouraging that pancreatic cancer death rates have not improved. The lack of early detection and effective treatment, as well as an increased incidence due to changes in risk factors such as tobacco use and obesity are contributing factors to this scenario [23-27]. Pancreatic cancer is currently the fourth leading cause of death from cancer with a cumulative 5-year survival rate of only 6% [28]. If no substantial breakthroughs are made in the coming years, pancreatic cancer is projected to become the number two cause of cancer-related death, preceded only by lung cancer [24]. A major barrier to the management of pancreatic cancer is the resistance to existing chemotherapeutic agents. Gemcitabine resistance in pancreatic cancer has been associated with several mechanisms including alteration of apoptosis regulating genes [29], low expression of nucleoside transporters or reduced levels of metabolic enzymes [30], and recently mucin 4 (MUC4) overexpression [31-33]. This knowledge is of great importance when developing novel types of intervention. To substantially improve pancreatic cancer survival rates, early detection strategies, a better understanding of tumor biology, and novel therapeutic approaches are urgently needed. Novel OMICS technologies such as proteomics may render new protein biomarkers, aiding in pancreatic cancer research and clinical care.

1.2 Pancreas – anatomy and physiology

The pancreas is a retroperitoneal organ that measures 15-20 cm in length and weighs about 75-100 grams [34]. The normal pancreas has a yellow color and a lobulated appearance. The pancreas is anatomically divided into four sections: head, neck, body, and tail. The head of the pancreas lies in the C-loop of the duodenum (Figure 1). The uncinate process is a projection from the inferior portion of the pancreatic head that is wedged between the superior mesenteric vessels and the aorta. The pancreatic neck connects the head and body of the pancreas and is located anterior to the portal vein, which is formed by the confluence of the superior mesenteric and splenic veins. The body of the pancreas continues to the left from the pancreatic neck. The tail is the narrowest part of the pancreas and extends toward the splenic hilum. The pancreatic duct (duct of Wirsung) runs transversely through the substance of the pancreas and joins the common bile duct, after which both ducts empty into the duodenum at the major duodenal papilla. An accessory pancreatic duct (duct of Santorini) is sometimes present, which communicates with the pancreatic duct and opens independently into the duodenum at the minor duodenal papilla.

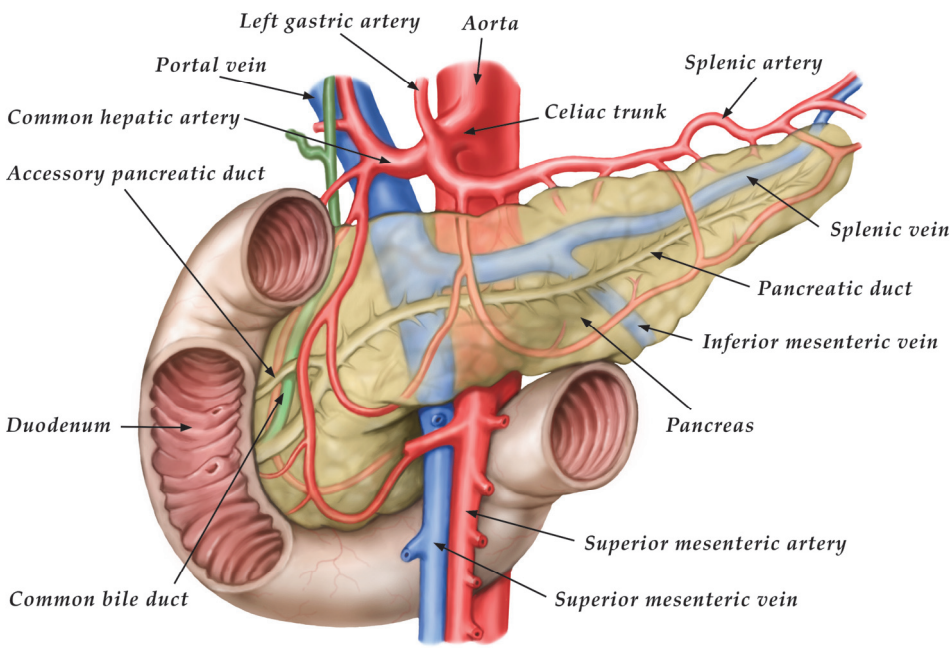

Figure 1. Anatomy of the pancreas.

The arterial blood supply to the pancreas arises from the celiac trunk and superior mesenteric artery. The primary branches of the celiac trunk are the common

hepatic, splenic, and left gastric arteries. The common hepatic artery divides into the hepatic artery proper and the gastroduodenal artery. The gastroduodenal artery gives off branches, the anterior and posterior superior pancreaticoduodenal arteries, which together with the anterior and posterior inferior pancreaticoduodenal arteries, originating from the superior mesenteric artery, form arterial arcades that supply the pancreatic head. The splenic artery gives rise to several important vessels, including the dorsal pancreatic artery, the pancreatic magna, and the caudal pancreatic artery, which represent the major vascular supply to the body and tail of the pancreas.

The venous effluents from the pancreas drain into the portal vein. The venous drainage of the head of the pancreas is through small branches of the superior mesenteric and portal veins, and the body and tail drain into small branches of the splenic vein. The inferior mesenteric vein enters the splenic vein posterior to the pancreatic body, but it does not drain the pancreas.

The pancreas has an extensive lymphatic system. Major lymphatic routes include pancreaticoduodenal lymph nodes, and lymph nodes in the hepatoduodenal ligament, as well as pyloric, middle colic, hepatic, and splenic lymph nodes, with final drainage into celiac, superior mesenteric, para-aortic, and aorto-caval lymph nodes [35].

Both sympathetic and parasympathetic nerve fibers innervate the pancreas. Sympathetic innervation comes from the thoracic splanchnic nerves via the celiac and superior mesenteric plexuses. Parasympathetic nerve fibers to the pancreas are contained in the vagus nerve via its celiac branch. Parasympathetic nerves stimulate pancreatic secretion, whereas sympathetic nerves are largely inhibitory. Afferent sensory nerve fibers in the pancreatic parenchyma can transmit pain of pancreatic origin [36].

The pancreas is a mixed type of gland having both exocrine and endocrine functions. The exocrine pancreas constitutes approximately 85% of the total pancreatic mass. The functional unit of the exocrine pancreas is the acinus (Figure 2). Each acinus is comprised of a single layer of acinar cells arranged in a circular formation. The ductal system begins with the centroacinar cells, situated in the center of the acinus, and proceeds through progressively larger ducts, termed intercalated, intralobular, interlobular, and major ducts in increasing order of size.

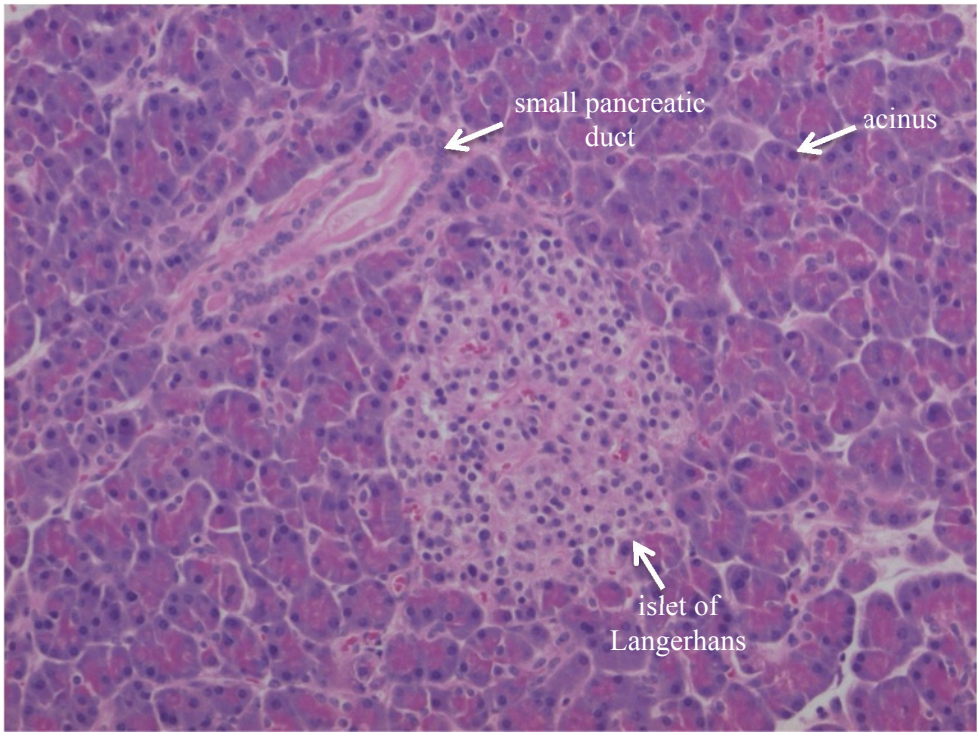

Figure 2. Normal pancreas morphology. The microscopic field shows lobules composed of acini, a small pancreatic duct, and islet of Langerhans.

The exocrine pancreatic secretion has two main components, i.e. the digestive enzyme secretions from the acinar cells and the aqueous electrolyte secretions originating from the ductal cells.

Acinar cells contain zymogen granules in the apical region of the cytoplasm that contain pancreatic enzymes that are released by exocytosis when needed. Enzymes that are excreted include the endopeptidases (trypsinogen, chymotrypsinogen, and proelastase) and the exopeptidases (procarboxypeptidase A and B). Other secreted enzymes are amylase, lipase, and colipase. All peptidases are excreted into the ductal system as inactive precursors. Once in the duodenum, trypsinogen is converted to the active form, trypsin, by interaction with duodenal mucosal enterokinase. Trypsin, in turn, then activates the other excreted peptidases. In contrast to the peptidases, the enzymes amylase and lipase are excreted into the ductal system in their active forms. The functions of the different pancreatic digestive enzymes are summarized in Table 1.

Pancreatic enzymes function best in a neutral or slightly alkaline environment. The alkaline ($NaHCO_3$)-rich fluid secreted by the ductal cells serves to neutralize the acidic chyme caused by highly acidic gastric contents that are emptied into the duodenal lumen.

The release of the two hormones cholecystokinin (CCK) and secretin in response to chyme in the duodenum play a central role in regulating exocrine pancreatic secretion. A small amount of parasympathetically induced pancreatic secretion occurs in the cephalic portion of digestion. CCK stimulates the acinar cells to secrete large amounts of digestive enzymes. Secretin stimulates ductal cells to increase their secretion of aqueous $NaHCO_3$ solution. The presence of fats and proteins in the duodenal lumen is the main stimulus for CCK release, while the primary stimulus for secretin release is the acid in the duodenum.

Table 1. The role of pancreatic enzymes in digestion [37].

ENZYMES	FUNCTION	
Protease	Digests proteins	Proteins $\xrightarrow[\text{Chymotrypsin}]{\text{Trypsin}}$ Peptides $\xrightarrow{\text{Carboxypeptidase}}$ Amino acids
Amylase	Digests carbohydrates	Starch $\xrightarrow{\text{Amylase}}$ Maltose
Lipase	Digests fats	Fats $\xrightarrow{\text{Lipase, bile salts}}$ Monoglycerides and fatty acids

The endocrine pancreas constitutes only about 2% of the pancreatic mass. More than 90% of pancreatic endocrine cells are found in islets of Langerhans (Figure 2). There are four main cell types found in the islets. The α-cells produce glucagon, which directs cells in the body to release glucose into the blood stream. The β-cells produce insulin, which directs cells in the body to accept glucose from the blood stream. The δ-cells produce somatostatin, which suppresses insulin and glucagon production, as well as release of gastric and digestive enzymes. The PP-cells are found not only in the islets, but also scattered within the exocrine part of the pancreas. Its polypeptide secretion exerts a number of gastrointestinal effects, such as stimulation of secretion of gastric and intestinal enzymes and inhibition of intestinal motility.

The remainder of the pancreas, accounting for approximately 13% of the mass, is composed of connective tissue, nerves, and blood vessels [38].

1.3 Pancreatic cancer pathophysiology

The term pancreatic cancer is meant to imply adenocarcinoma arising from the ductal epithelium in the exocrine portion of the gland. Ductal adenocarcinoma is the most common neoplasm in the pancreas, representing 85% of all pancreatic

neoplasms. Little is known about the causes of pancreatic cancer. The most commonly reported risk factors are smoking, obesity, family history, chronic pancreatitis, diabetes mellitus, and pancreatic cysts [39]. The peak incidence of pancreatic cancer occurs between 60 and 80 years of age. Patients below the age of 50 years are rare and constitute about 5-10% of all cases [40].

Pancreatic cancer evolves through precursor lesions, most typically pancreatic intraepithelial neoplasias (PanINs), acquiring clonally selected genetic and epigenetic alterations along the way (Figure 3). Pancreatic cancer can also less frequently evolve from intraductal papillary mucinous neoplasms (IPMNs) or mucinous cystic neoplasms.

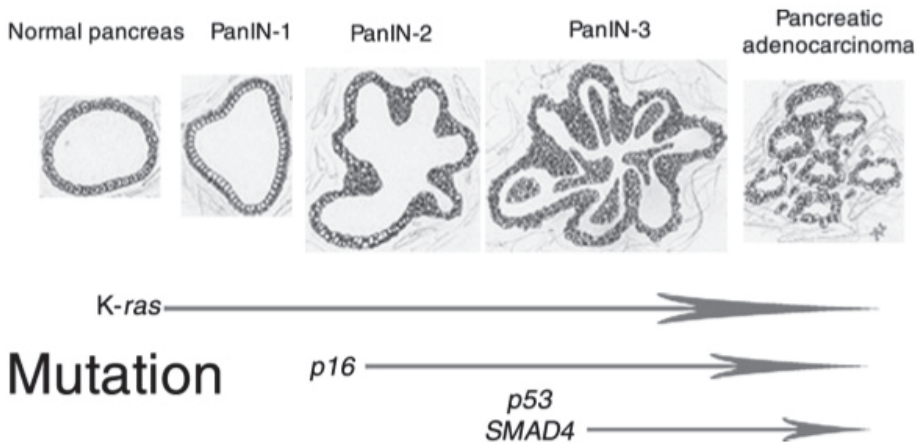

Figure 3. Genetic alterations during pancreatic cancer development. The tumor suppressor p53 is inactivated in most ductal adenocarcinomas and is one of the critical barriers blocking progression of PanIN initiated by K-ras. Printed with permission [41].

Macroscopically, most ductal adenocarcinomas are white and dense masses. Some may show central necrosis with hemorrhage. Microscopically, ductal adenocarcinomas grow in more or less glandular patterns within abundant desmoplastic stroma (Figure 4). The tumor often invades retroperitoneal fatty tissue, veins, and nerves, and it is rare to find a ductal adenocarcinoma that is limited to the pancreas at the time of diagnosis. Extension into neighboring organs or peritoneum is seen in advanced cases. The tumor may also spread via lymphatic channels to the pleura and lungs. Hematogenous metastases occur to the liver, lungs, and occasionally to the adrenals, kidneys, bones, brain, and skin [42].

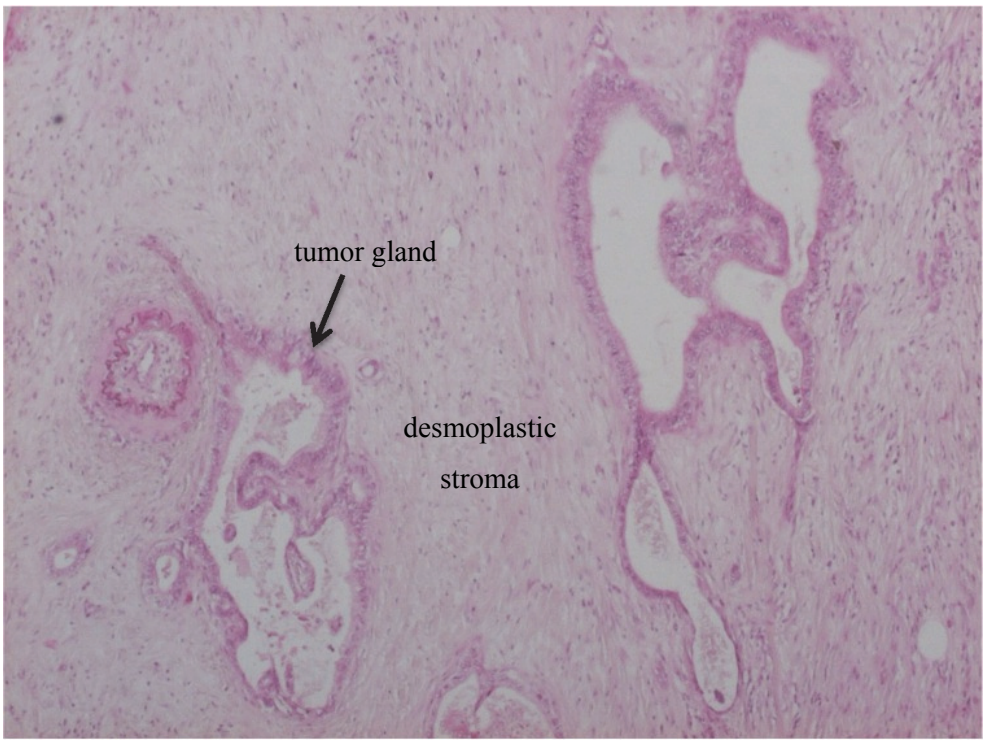

Figure 4. Moderately differentiated ductal adenocarcinoma with irregular gland formation and desmoplastic stromal reaction.

1.4 Diagnosis

1.4.1 Clinical presentation

The symptoms of pancreatic cancer often appear late in the course of the disease, thus making early detection difficult. The majority of tumors are located in the head of the pancreas and eventually cause obstructive jaundice due to direct compression of the common bile duct. Such patients may notice yellowing of their skin and eyes, darkening of their urine, and pale-colored stools. Abdominal pain radiating to the back is another presenting symptom and may be indicative of extensive nerve infiltration by the tumor [43]. Dramatic weight loss is frequent and is usually part of a particularly severe form of cachexia or wasting syndrome [44]. New-onset diabetes mellitus type 2 should alert the physician to a possible underlying pancreatic cancer [45]. Obstruction of the main pancreatic duct may lead to episodes of pancreatitis [46]. Depression has been reported to be more common in pancreatic cancer than in other malignancies [47].

Physical examination is often inconclusive but may prompt the initiation of additional diagnostic steps. Physical signs may include jaundice and vague abdominal discomfort in the upper quadrants. A palpable gallbladder (Courvoisier's sign) may be present in one third of patients [48]. Additional clinical findings are usually indicative of advanced stage disease such as hepatomegaly, ascites, temporal wasting, or a palpable abdominal mass. Other less common findings include left supraclavicular adenopathy (Virchow's node), periumbilical adenopathy (Sister Mary Joseph's node), and perirectal drop metastases (Blumer's shelf) [49]. Migratory thrombophlebitis (Trousseau's sign) and venous thrombosis may be manifestations of pancreatic cancer but may also occur in other types of cancer [50].

1.4.2 Imaging

Computed tomography (CT) with a pancreatic protocol is the most validated initial diagnostic imaging modality for pancreatic cancer. This technique allows visualization of the primary tumor and its relation to surrounding vessels and organs and whether there is any tumor spread to distant sites. Pancreatic cancer is characterized by poor enhancement compared with that of the surrounding pancreatic parenchyma due to the presence of abundant fibrous stroma and hypovascularity (Figure 5) [51]. Magnetic resonance imaging or endoscopic ultrasound may be considered as additional modalities if diagnostic difficulties persist after CT. Cytological diagnosis is not usually required in patients with an apparently resectable pancreatic tumor, and a negative fine needle aspiration biopsy does not exclude an adenocarcinoma due to the possibility of sampling error. Moreover, there is a risk of tumor seeding in the needle track, although this risk may be lower with endoscopic ultrasound-guided fine needle aspiration. Cytological diagnosis is generally restricted to patients with unresectable disease to achieve a histological diagnosis before initiating chemotherapy [52].

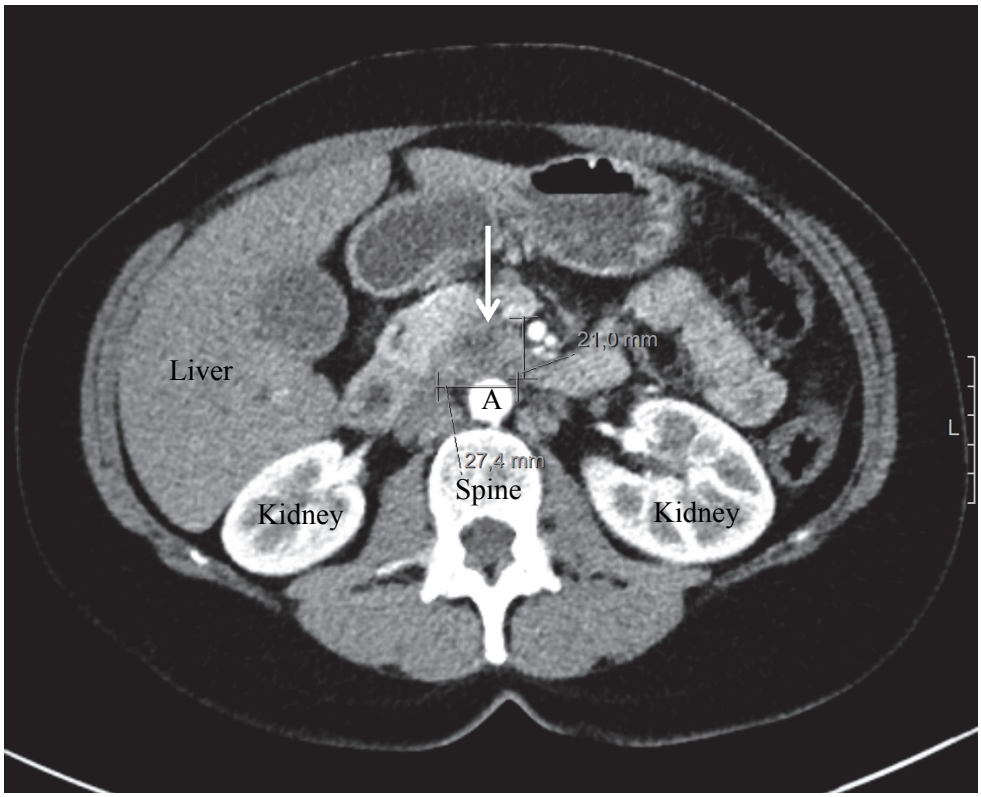

Figure 5. Preoperative CT scan of a patient with pancreatic cancer (arrow) that shows a low-attenuation mass in the head of the pancreas in close proximity to the aorta but without definite vascular involvement. A, aorta.

1.4.3 Current serum biomarkers

There is a great need to identify useful biomarkers for pancreatic cancer to help detect early-stage, operable disease. Recent genomic sequencing data indicate a 15-year interval for pancreatic cancer genetic progression from initiation to metastatic stage, indicating a sufficient window for early detection [53].

Carbohydrate antigen 19-9 (CA 19-9), a sialylated Lewis (a) antigen, is the only US Food and Drug Administration (FDA) approved biomarker for pancreatic cancer. CA 19-9 can be quantitatively measured in serum and may aid in monitoring recurrence and disease progression in pancreatic cancer patients [54]. CA 19-9 has been reported to have a sensitivity and specificity of about 80% for pancreatic cancer diagnosis [55] which is superior to other markers, including CEA, CA-50, and DUPAN-2 [42, 55, 56]. However, CA 19-9 is not recommended for use as a screening test for pancreatic cancer. The reason is its low positive predictive value and the fact that benign causes and all forms of biliary obstruction

can increase CA 19-9 levels [55, 57]. Moreover, approximately 10% of the population do not have the enzyme activity genotype (le/le) and consequently cannot synthesize CA 19-9 [16].

The likely practical future of screening for pancreatic cancer will involve a panel of blood biomarkers, followed by second-level abdominal imaging to confirm a positive biomarker result [39]. It is possible that a biomarker panel could have applicability not only in screening, but also in other aspects of patient management such as assessment of patient prognosis (prognostic biomarkers) or defining responders to a specific treatment (predictive biomarkers). The question of who to screen has received increased attention in recent years. Selecting individuals based risk factors, putting the patient safety first, is one strategy that is commonly accepted. Screening may thus be applied in a selected population such as those with a family history of the disease, new-onset diabetes mellitus, or a pancreatic cyst [58].

Blood is the most accessible and least invasive biofluid for biomarker discovery, and has the potential to significantly improve clinical management of the patient. However, given the low abundance in serum and plasma of known cancer biomarkers [59], new proteomic technologies are constantly being developed and refined to provide sufficient depth of analysis for biomarker quantification.

1.4.4 Principles and applications of mass spectrometry in pancreatic cancer

Proteomics is defined as the large-scale study of proteins, including information on abundances, their variations and modifications, along with their interacting partners and networks [60]. Currently, mass spectrometry is the workhorse in protein analysis. Mass spectrometry is an analytical technique that generates gas-phase ions of molecules present in a sample, which are separated according to their mass-to-charge ratios (m/z) and then detected. Recent advances in mass spectrometry techniques have enabled the investigation of protein expression profiles in complex protein mixtures, and the identification and quantification of disease-perturbed proteins. Either global expression profiling is made, or targeted protein sequencing and analysis. Traditionally, protein separation and comparison by two-dimensional gel electrophoresis (2-DE), followed by mass spectrometry-based identification, has been the main method used in proteomics studies [61]. However, 2-DE is limited by factors such as being experimentally laborious, and being difficult to perform reproducibly and consequently challenging for high-throughput analysis [62]. As an alternative to the 2-DE approach, ‘bottom-up’ shotgun proteomics has emerged. The shotgun approach uses a proteolytic enzyme such as trypsin to generate peptides that can be analyzed with liquid chromatography coupled with tandem mass spectrometry (LC-MS/MS), which

combines the physical separation capabilities of liquid chromatography with the mass analysis capabilities of mass spectrometry [63-65]. However, given the complexity of the serum and plasma proteome only a few studies have investigated the use of shotgun proteomics for the discovery of pancreatic cancer biomarkers in blood [66]. To reach beyond the limitations of conventional mass spectrometry, the use of high definition mass spectrometry ($HDMS^E$) can provide the extra dimension of high-efficiency ion mobility separation to achieve deeper proteome coverage [67].

1.5 Prognosis

1.5.1 Stages of pancreatic cancer

Clinical staging is performed according to the TNM classification and categorizes patients into 3 stages: resectable, locally advanced, and metastatic disease (Table 2) [46]. CT provides about 70-85% accuracy for prediction of resectability [68, 69]. Positron emission tomography can be helpful if metastases are suspected such as for indeterminate lesions by CT [70]. Laparoscopy can spot e.g. peritoneal metastases but is not undertaken routinely, but occasionally in tumors of the body and tail of the pancreas.

Staging dictates the most appropriate initial treatment. The median survival time of resectable pancreatic cancer with adjuvant chemotherapy is 17-23 months, while the median survival is 8-14 months for locally advanced pancreatic cancer, and 4-6 months for metastatic pancreatic cancer [18]. Recently borderline resectable pancreatic cancer has been defined as a subcategory of pancreatic cancer that is characterized by limited vascular involvement, where resection is technically possible but which carry a high risk of margin-positive resection unless preoperative (neoadjuvant) therapy is employed [71].

Table 2. Staging of pancreatic cancer [46].

STAGE	T	N	M	
Resectable (10-20%)				
IA	T1	N0	M0	Limited to pancreas; ≤2 cm in diameter
IB	T2	N0	M0	Limited to pancreas; >2 cm in diameter
IIA	T3	N0	M0	Extends beyond pancreas, no involvement of celiac axis or superior mesenteric artery
IIB	T1-T3	N1	M0	Regional lymph node metastasis
Locally advanced (30%)				
III	T4	N0-N1	M0	Tumor involves celiac axis or superior mesenteric artery
Metastatic (60%)				
IV	T1-T4	N0-N1	M1	Distant metastasis

N, regional lymph node metastasis; M, distant metastasis; T, primary tumor.

1.5.2 Single prognostic factors

The TNM staging system is currently the main method for estimating patient prognosis, but for patients undergoing resection for pancreatic cancer it is rather nondiscriminatory as it does not incorporate prognostic determinants other than the T, N, and M stages. By including additional prognostic factors, a prognostic model can be developed to better estimate an individual patient's survival.

The radicality of resection is certainly a powerful prognostic factor. Achieving a margin negative R0 resection with minimal postoperative complications has been identified as variables that can be affected by the surgeon, and which contribute to long-term survival in pancreatic cancer [16]. The importance of R0 resection is supported by several studies showing a strong survival advantage associated with complete tumor clearance [12, 72-74].

Tumor size has been linked to survival and is the only discriminant between T1 and T2 stages in the TNM classification of pancreatic cancer. The major problem is that the definition of the size after which a tumor becomes associated with poor prognosis is arbitrary from a biological point of view, and both a tumor diameter of 2 cm or more [75-78] or 3 cm or more [73, 79, 80] has been found to predict poor outcome after resection for pancreatic cancer.

Pancreatic cancers located in the body or tail of the pancreas are usually detected at a more advanced stage compared to tumors located in the head of the pancreas. However, for patients undergoing resection, the prognostic role of tumor location is controversial [81].

Lymphatic dissemination is one of the major patterns of tumor spread and one of the leading factors determining survival [73, 74, 82, 83].

Tumor grade based on the extent of glandular differentiation has been found to correlate significantly with postoperative survival [73, 84]. As grading systems are to a great extent subjective, reproducibility may though be low.

Tumors with perineural invasion [85] and peripancreatic fat invasion [86] have been reported to have a worse prognosis.

Postoperative adjuvant therapy prolongs survival in patients with resected pancreatic cancer [87-91].

The role of new prognostic factors like the activated stroma-index [92], histological necrosis [93], or molecular markers [94] need to be further investigated.

1.5.3 Different prognostic models

A prognostic nomogram for pancreatic cancer was developed from a large cohort of patients in the Memorial Sloan-Kettering Cancer Centre (MSKCC) in New York, USA [95]. The purpose of this nomogram was to estimate the probability that patients undergoing resection for pancreatic cancer would be alive at 1, 2, and 3 years postoperatively. Based on a Cox regression model, variables including age, sex, tumor location, type of resection, margin of resection, histologic differentiation, tumor size, T-stage, and N stage were selected. The nomogram predictions discriminated better than did the TNM stage (concordance index (C-index) 0.64 versus 0.56, $p<0.001$). This nomogram has been externally validated, with varying success [96-98].

Another group developed a multivariable prognostic model for resectable pancreatic cancer, incorporating age, histologic differentiation, tumor size, preoperative CA 19-9, serum albumin, and alkaline phosphatase. The results indicated that the addition of prognostic factors other than the traditional tumor-related ones could lead to a more accurate prognostic stratification of patients with resectable pancreatic cancer. The model classified patients with higher accuracy compared to the TNM system; C-indexes were equal to 0.73 and 0.59, respectively [99].

1.5.4 Validation of prognostic models

The assessment of the discriminatory ability of a survival analysis model is much more complex than evaluating the performance of a linear or logistic regression. Instead of two possible categories into which each subject falls, there are survival times and our predictions about them [100]. Several different measures have been proposed in the biostatistical literature. A requirement, which we want our

measure to satisfy, is that subjects with longer predicted survival time actually survive longer without experiencing the event of interest. Harrell et al. [101, 102] introduced the C-index, a measure of the separation of two survival distributions. Their measure has been widely adopted and extensively used for assessing prediction performance in survival analysis settings [103]. The C-index is a natural extension of the receiver operating characteristic (ROC) curve area to survival analysis. The C-index measures the probability that two patients, one with an event and one without, will be ranked correctly. This C-index is not related to any particular prognostic index threshold, but is integrated across all possible thresholds [104]. Once a prognostic model has been developed, internal validation is essential to establish whether the model is likely to provide useful classification of patient risk. External validation, preferably by external investigators, is an essential pre-requisite before the model can be applied in clinical practice.

1.5.5 Artificial neural networks

An artificial neural network (ANN) is a simplified model of the workings of the human brain. An ANN consists of a set of neurons (nodes) and synaptic connections (connection weights), which are capable of passing data through multiple layers. The end result is a system, which is capable of generalization, pattern recognition, and classification [105]. One of the most studied ANN architectures is the multilayer perceptron. It consists of an input-output network, which has one or more hidden layers of nodes, and where the flow of information is in a feed-forward direction. The learning is achieved by minimizing the error function of the input and target data. Computational power in a neural network does not derive from the complexity of each processing unit, but from the density and complexity of the interconnections [38, 106].

Conventional linear models may have limitations in terms of predictive ability when it comes to complex medical diseases. ANNs work in a non-linear fashion, which may better describe the interaction between different risk factors. ANNs have been used successfully in making predictions in complex medical scenarios such as automated electrocardiographic interpretation in the diagnosis of acute myocardial infarction [107]. Several authors have used ANNs to develop predictive models in oncology [108-110], but the use of ANNs as a prognostic tool in pancreatic cancer has not been previously described.

1.6 Treatment

1.6.1 Surgery

The anatomic location of the tumor within the pancreas dictates the type of resection. A lesion confined to the pancreatic head necessitates a pancreaticoduodenectomy, while lesions in the pancreatic body or tail may be suitable for a distal pancreatectomy. Nowadays, a total pancreatectomy is reserved for patients with multilocular or large tumors of the pancreas, but is seldom performed due to a high rate of postoperative complications such as diabetes mellitus [111].

Several technical aspects of the pancreaticoduodenectomy operation have been studied. Both standard Whipple's operation and pylorus-preserving pancreaticoduodenectomy are equally effective and have comparable complication rate, operative mortality rate, and overall long-term survival [112].

The pancreatic remnant can be joined to the jejunum or stomach. According to recent data a pancreaticogastrostomy may be a safer alternative to pancreaticojejunostomy, being associated with a reduced incidence of pancreatic fistula formation [113]. However, based on current evidence one technique cannot claim superiority over the other.

The extent of lymph node dissection has been a subject of discussion. It was hoped that extensive retroperitoneal lymphadenectomy and clearance of soft tissue around the pancreas (extended pancreaticoduodenectomy) would improve survival. However, available data do not demonstrate a benefit in long-term survival after extended lymphadenectomy also when dissecting the nerve plexus [114].

Vascular resection with pancreaticoduodenectomy is another area of debate. Portal or superior mesenteric vein resection and reconstruction is possible and can enable R0 resection without increased operative mortality [115].

Very convincing data exist concerning the volume-outcome relationship in pancreatic surgery. Nation-wide studies from Europe, the USA, and Japan convincingly proved the volume-outcome relationship in surgery of pancreatic cancer [15, 116-126]. The operative mortality rate at high-volume centers is reported to be in the range of 1-4%. There are also some data suggesting better long-term results in high-volume centers [127]. The surgeon volume and skill remain substantial, but not the most remarkable prognostic factors for complex surgical procedures, although high average level of surgical expertise in high-volume centers undoubtedly contributes to the overall improvement.

Most data regarding centralization of pancreaticoduodenectomy are derived from multi-institutional comparisons, and there is a lack of studies describing the effects of increased caseload of pancreaticoduodenectomy within the same unit. Furthermore, less is known regarding the effects of centralization on quality measures of pancreaticoduodenectomy such as operative blood loss, individual complications, and the need for reoperation. The process of centralization can be slow as demonstrated by a nationwide survey of pancreaticoduodenectomy in the USA [128]. In Sweden, gradual centralization of pancreaticoduodenectomy has occurred. To date, no information is available regarding the volume–outcome association for pancreaticoduodenectomy in Sweden.

1.6.2 Chemotherapy and radiation therapy

Currently, the standard of care for early-stage disease is surgery followed by adjuvant therapy. This is based on several randomized controlled trials. In the GITSG trial, 5-FU based chemoradiation was superior to observation [87]. The ESPAC-1 trial clearly established the survival advantage of adjuvant chemotherapy with 5-FU over no chemotherapy [88]. Chemoradiation failed to increase survival. In the CONKO-001 trial, adjuvant gemcitabine chemotherapy was superior to observation alone [89]. The ESPAC-3 trial demonstrated equivalence between 5-FU and gemcitabine in terms of survival parameters, though gemcitabine had a better toxicity profile [90]. The RTOG-9704 trial compared gemcitabine with 5-FU before and after 5-FU based chemoradiation and in an updated analysis of this trial the treatment arms did not differ by much [91].

For locally advanced pancreatic cancer, findings of trials in which attempts have been made to ascertain whether chemotherapy alone is preferable to chemoradiation have been inconclusive. Chemoradiation regimens containing gemcitabine yield similar results to those with 5-FU and it has been reported that chemoradiotherapy downstages about 30% of patients with locally advanced disease to resectable pancreatic cancer and these individuals go on to achieve median survival similar to that for those who are initially resectable without any preoperative treatment [18].

In the metastatic setting, the role of gemcitabine was established based on the pivotal paper from 1997 demonstrating a 23.8% clinical benefit and modest improvement in overall survival of 1.2 months over 5-FU [20]. The addition of erlotinib to gemcitabine resulted in a 0.3 month survival advantage [129], but this has not been accepted to be clinically relevant. More recent data indicated that FOLFIRINOX prolonged progression free survival and overall survival from 3.3 to 6.4 months and 6.8 to 11.1 months, respectively, compared to gemcitabine alone [21]. Additionally, the combination of gemcitabine and nab-paclitaxel

achieved a median overall survival of 8.5 months compared with 6.7 months with gemcitabine alone [22].

1.6.3 Mouse models of pancreatic cancer

There is an obvious need for the development of experimental models to study pancreatic cancer biology as it relates to what is seen in the clinic and for their potential utility for developing new therapeutic strategies.

The most commonly used preclinical animal models in pancreatic cancer research are tumor xenografts in immunodeficient mice and transgenic mouse models.

There are two main types of xenograft mouse models, the subcutaneous model in which human tumor cells are implanted into the animal between the dermis and underlying muscle, and the orthotopic model, in which human tumor cells are implanted directly into the pancreas.

The transgenic mouse model uses genetically engineered mice that express mutated oncogenes or tumor suppressor genes that give rise to mouse tumors. The creation of transgenic mouse models is challenging and traditional transgenic approaches failed to produce accurate models of pancreatic cancer in mice, potentially due to the non-physiological control of gene expression. However, in recent years as a result of important progress in gene targeting and a deeper understanding of the molecular and cellular events that occur during pancreatic neoplasia, these models are receiving increased attention [130].

The subcutaneous xenograft model still remains the standard for drug screening in pharmaceutical industries and the FDA considers a drug's effectiveness against xenografts sufficient for clinical trial approval [131]. This model is easily adaptable with a consistent tumor growth on the mouse side flank, and can be measured by a simple caliper. A concern that has been raised is that the use of subcutaneous mouse models might lead to exclusion of the unique tumor desmoplasia, which is a characteristic feature of pancreatic cancers [132]. On the other hand, it has been demonstrated that human pancreatic cancer cells are capable of creating their own desmoplastic microenvironment, beneficial for the cancer cell survival and progression [133, 134]. The stromal development in xenografts is, however, dependent on specific conditions and properties of the inoculated pancreatic cancer cells.

1.6.4 MUC4 as a molecular target in the therapy of pancreatic cancer

On the basis of molecular studies, mucins and particularly the MUC4 mucin have been proposed as markers of diagnosis, prognosis, and treatment in pancreatic

cancer [135]. Mucins are perceived as the biomolecules implicated in the protection and lubrication of epithelial surfaces. However, the recent realization that mucins can also function as signaling modulators and affect tumor cell phenotype has increased the interest in exploring their potential clinical usefulness.

The MUC4 gene is located on chromosome locus 3q29 and encodes a large apomucin (550-930 kDa) that is predicted to extend up to 2 μm above the cell surface [136, 137]. It is composed of two-subunits, MUC4α and MUC4β (Figure 6).

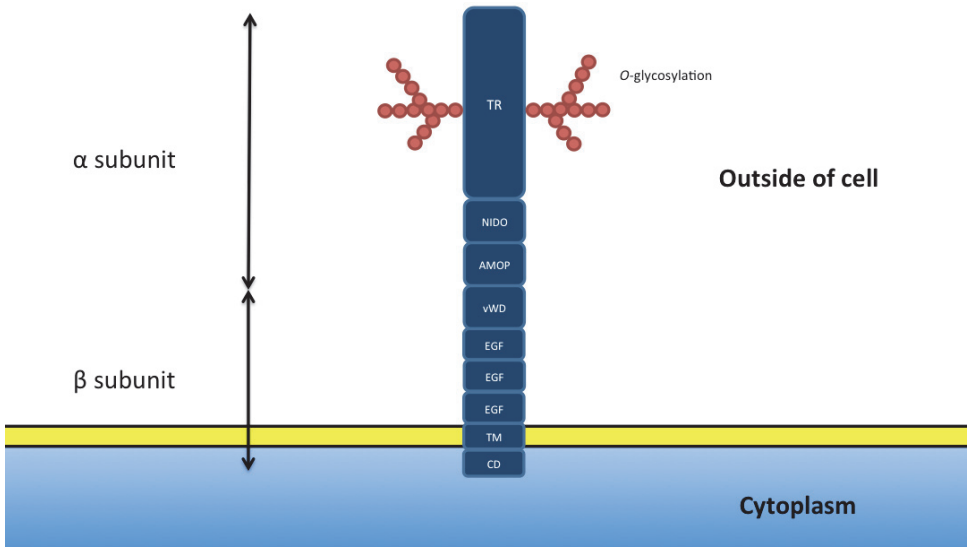

Figure 6. MUC4 domain structure. AMOP, adhesion-associated domain in MUC4 and other proteins; CD, cytoplasmic tail domain; EGF, epidermal growth factor-like domain; NIDO, nidogen-like domain; TM, transmembrane; TR, tandem repeat; vWD, von Willebrand factor D domain.

MUC4α is composed of the hallmark *O*-glycosylation characteristic of mucins and a tandem repeat (TR) rich in serine and threonine residues. The MUC4α subunit also harbors a nidogen-like domain (NIDO) and an adhesion-associated domain present in MUC4 and other proteins (AMOP) which are proposed to have important roles in cell-cell interaction and adhesion to extracellular matrix [136, 138, 139].

MUC4β tightly but non-covalently associates with MUC4α and possesses a single transmembrane segment and a cytoplasmic domain. Additionally, MUC4β contains other features in its extracellular regions such as 3 epidermal growth factor (EGF)-like domains and a von Willebrand D domain that mediate MUC4 interactions with other membrane or extracellular proteins [136, 140]. The interaction of MUC4 and HER2 via the EGF-like domains is the best characterized, likely serving as a regulator in signaling related to growth, motility,

or differentiating properties of the cell [141]. The MUC4-HER2 complex induces differentiation via activation of the cell cycle inhibitor p27kip, whereas formation of a quaternary complex of MUC4-HER2-HER3-neuregulin activates PKB/Akt and MAPK pathways leading to proliferation and inhibition of apoptosis [142, 143].

Under normal physiologic conditions, MUC4 is expressed in the epithelium of the respiratory, digestive, and urogenital tracts in varying levels [144]. Aberrant MUC4 overexpression has been implicated in a variety of carcinomas such as breast [145], lung [146], ovarian [147], colon [148], and pancreatic cancer [137], a phenomenon that has been shown to alter the biological properties of the tumor cells concerned. MUC4 was previously identified among the most differentially expressed genes in pancreatic cancer with an undetectable expression in the normal pancreas [149]. It was reported that MUC4 protein expression increases during pancreatic carcinogenesis from 17% in PanIN-1 to 89% in invasive ductal adenocarcinoma [150]. Moreover, several studies demonstrated that a high MUC4 expression is a predictor of poor outcome in patients with pancreatic cancer [151-153]. Experimental evidence suggests that MUC4 potentiates pancreatic tumor cell growth and metastasis through diverse mechanisms, such as altered proliferation, motility, adhesion, and HER2 signaling [154-157]. Importantly, MUC4 has been linked to gemcitabine resistance in pancreatic cancer [31-33].

The molecular mechanisms responsible for mucin gene activation in pancreatic cancer are slowly becoming known. Recent data indicate that mucin genes may be epigenetically regulated in pancreatic cancer [141]. An investigation of the detailed epigenetic mechanisms of MUC4 expression has shown that regulation of MUC4 expression involves both DNA methylation and histone H3 modification mediated by DNA methyltransferases and histone deacetylases (HDACs) in pancreatic cancer cells [158]. Therefore, one effective approach for the treatment of pancreatic cancer might be to specifically target MUC4 by epigenetic control and thereby alter tumor behavior.

Chapter 2 Aim of the Thesis

The general aim of this thesis was to investigate strategies to improve management of pancreatic cancer, with special reference to early detection, prognostic factors, and individualized treatment.

The specific aims were:

I. to identify serum protein biomarkers for resectable pancreatic cancer by using high-definition mass spectrometry ($HDMS^E$);
II. to develop a prognostic model for resectable pancreatic cancer by selecting and ranking clinical and histopathological risk factors for survival by using ANNs and high-performance computer clusters;
III. to assess whether the results of pancreaticoduodenectomy have improved following the transition from a low- to a high-volume center, especially with respect to duration of surgery, blood loss, complications, hospital stay and mortality;
IV. to determine the grade of concordance in terms of MUC4 tissue expression between primary pancreatic cancer and paired lymph node metastases, in order to elucidate the importance of this protein for treatment of disseminated disease;
V. to develop a biologically relevant in vivo model of pancreatic cancer that is suitable for the study of MUC4-directed therapy; and
VI. to investigate whether epigenetic control of MUC4 expression sensitizes pancreatic cancer cells to gemcitabine treatment.

Chapter 3 Material and Methods

3.1 Study population

All patients included in this thesis underwent elective pancreatic resection at the Department of Surgery, Skåne University Hospital, Sweden. This department consists of two units, Lund and Malmö. The two units were merged under one management team in 2010 and since then Lund provides the only tertiary level services for pancreatic diseases in the region.

The decision for surgical intervention was made at the weekly multidisciplinary pancreatic tumor conferences where each individual case was discussed and decided on optimal diagnostic and treatment measures based on best current evidence.

The pancreatic database included patient demographics, surgical information, pathology, referral to medical oncology, and follow-up.

The prospective blood and tissue sampling in its current form was initiated in 2012 by the author and his supervisors (BA and RA).

3.2 Study design

Table 3 shows a short summary of the study designs used in this thesis.

Table 3. Overview of design and participants in the papers of the thesis.

	I	**II**	**III**	**IV**	**V**	**VI**
Design	Prospective CS	Retrospective CS	Retrospective CS	Retrospective CS	Experimental animal study	Experimental in vitro study
Subjects	Humans	Humans	Humans	Humans	Mice	Cell lines
Method	$HDMS^E$	ANNs	Chart review	IHC	Xenograft tumor model	MTT assay, HCS
Number	27	84	221	17	15	2 cell lines
Location	Lund	Lund+Malmö	Lund	Lund	Lund	Lund
Study period	2012-2013	1995-2010	2000-2012	1999-2009	2013-2014	2014

ANN, artificial neural networks; CS, cohort study; HCS, high content screening; $HDMS^E$, high definition mass spectrometry; IHC, immunohistochemistry.

3.3 Biobank samples

Serum biofluids included in this study were prospectively sampled from patients with pancreatic cancer, benign pancreatic disease, as well as healthy controls. The study patients were undergoing treatment at the Department of Surgery, Skåne University Hospital, Lund, Sweden. Blood samples were taken at diagnosis, before start of treatment. Healthy control sera were obtained from blood donors at the local blood donation center. Blood samples were collected in BD SST II Advance tubes (serum separator tubes, 3.5 ml, product no. 368498; Becton Dickinson, Franklin Lakes, NJ, USA). The minimum clotting time was 30 min. The samples were centrifuged at 2000 x g at 25 °C for 10 min, serum collected and stored in aliquots at -80 °C in the local pancreatic biobank until further use. The ethical approval for the study was granted by the institutional review board at Lund University. All subjects gave written informed consent before taking part in the study. Formalin fixed paraffin embedded (FFPE) biospecimens, including tumor and lymph node specimens, were also collected for surgical cases.

3.5 Multiple affinity removal of high-abundant proteins in serum

To enrich for proteins of low-abundance, each sample was depleted of seven proteins that are highly abundant in serum (albumin, IgG, IgA, transferrin, haptoglobin, antitrypsin, and fibrinogen). Briefly, crude sera (10 µL) were diluted with 180 µL of Buffer A (product no. 5185-5987; Agilent Technologies, Santa Clara, CA, USA) and then filtered through 0.22 µm spin filter (product no. 5185-5990; Agilent Technologies) by spinning at 1000 x g at room temperature for 5 minutes. Diluted serum was injected on a multiple affinity removal system spin cartridge (product no. 5188-6408; Agilent Technologies) in Buffer A. The bound proteins were eluted with Buffer B (product no. 5185-5988; Agilent Technologies).

3.6 Trypsin digestion

The proteins were reduced with 10 mM dithiothreitol (Sigma-Aldrich, St. Louis, MO, USA) for 1 h at 56 °C and alkylated using 50 mM iodoacetamide (Sigma-Aldrich) for 30 min, kept dark at room temperature. Following this procedure, buffer exchange was performed with 50 mM ammonium bicarbonate buffer (pH 7.6) by using a 10 kDa cut-off spin filter (YM10 filter, AMICON, Millipore,

Billerica, MA, USA). The samples were digested with sequencing grade trypsin (Promega, Madison, WI, USA) in ratio 1:50 w/w (trypsin: protein) overnight at 37°C. The reaction was stopped by addition of 30 µL of 1% formic acid (Sigma-Aldrich). The resulting protein digests were dried on speed vacuum centrifugation and resuspended with 1% formic acid prior injection. Samples were diluted 1:1 with 10 fmol/µL of yeast alcohol dehydrogenase (ADH) internal standard tryptic digest (Waters, Milford, MA, USA) before analysis.

3.7 High definition mass spectrometry (HDMS^E)

Complex tryptic peptide mixtures were separated using nanoscale chromatography performed using a nanoACQUITY UPLC (Waters). One-dimensional reversed phase (RP) nanoACQUITY experiments with trapping were performed. Mobile phases A and B were 0.1% (v/v) formic acid in water and 0.1% (v/v) formic acid in acetonitrile, respectively. Following desalting of the peptides on a Symmetry C18 5 µm, 2 cm x 180 µm trap column (Waters), a reversed phase gradient was employed to separate peptides using 5 to 40% acetonitrile in water over 90 minutes on a 25 cm x 75 µm analytical RP column (Waters, USA) at a flow rate of 300 nL/min and a constant temperature of 35 °C.

Analysis of the complex peptide mixtures was performed using a SYNAPT G2-Si HDMS mass spectrometer (Waters, Manchester, UK) operated in a data-independent manner coupled with ion mobility (HDMS^E) [159]. The workflow is shown in Figure 7.

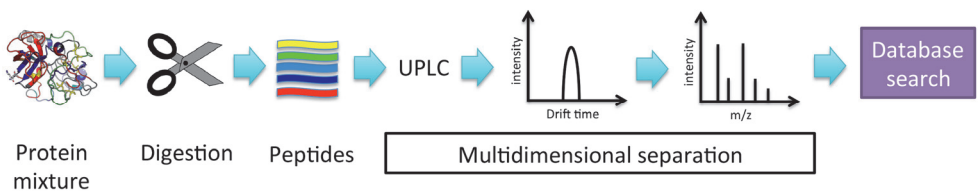

Figure 7. Experimental pipeline. UPLC, ultra performance liquid chromatography.

The mass spectrometer was operated in positive ESI resolution mode with resolution of >250,000 FWHM. In all experiments the mass spectrometer was programmed to step between low energy (4 eV) and elevated (14-40 eV) collision energies on the Triwave collision cell, using a scan time of 0.9 s per function over 50-2000 m/z.

HDMS^E data-independent analysis provides detection of all precursor and product ions with accurate mass measurement. Alignment of precursor and product ions by

drift and retention time aids peptide identification by assignment of product ions to parent ions during data processing and database searching [160, 161]. Protein identifications and quantification information were obtained by using UniProt human database Progenesis QI for Proteomics version 1.0 and a human UniProt database. Gene ontology annotations were retrieved from the PANTHER classification system [162].

3.8 Calibration and validation of the ANN model

Thirty-three input variables were collected and considered appropriate for analysis as potential risk variables. These included demographics (i.e., age and sex), clinical factors (i.e., body mass index (BMI), American Society of Anesthesiologists (ASA) grade, diabetes mellitus, smoking, jaundice, biliary drainage, and double duct sign), standard preoperative laboratory tests (i.e., white blood cell count, hemoglobin, platelet count, aspartate aminotransferase, alanine aminotransferase, alkaline phosphatase, γ-glutamyl transpeptidase, and total bilirubin), operative details (i.e., blood loss and blood transfusion), histopathological factors (i.e., tumor location, size, T stage, resection margin status, differentiation, lymph node metastasis, number of positive nodes, vascular invasion, perineural invasion, adipose tissue invasion, and peritumoral inflammation), major postoperative complications (i.e., Clavien grade ≥3), and treatment details (i.e., length of stay and adjuvant therapy).

A feed-forward ANN was used to construct the survival model (Figure 8) [163]. Several ANNs were combined into a single prediction model (i.e., a committee machine). To provide an estimation of the conditional probability of the event in question as a function of both risk variables and time, the model described by Biganzoli et al [164] as a generalization of the standard Cox proportional hazard model was used.

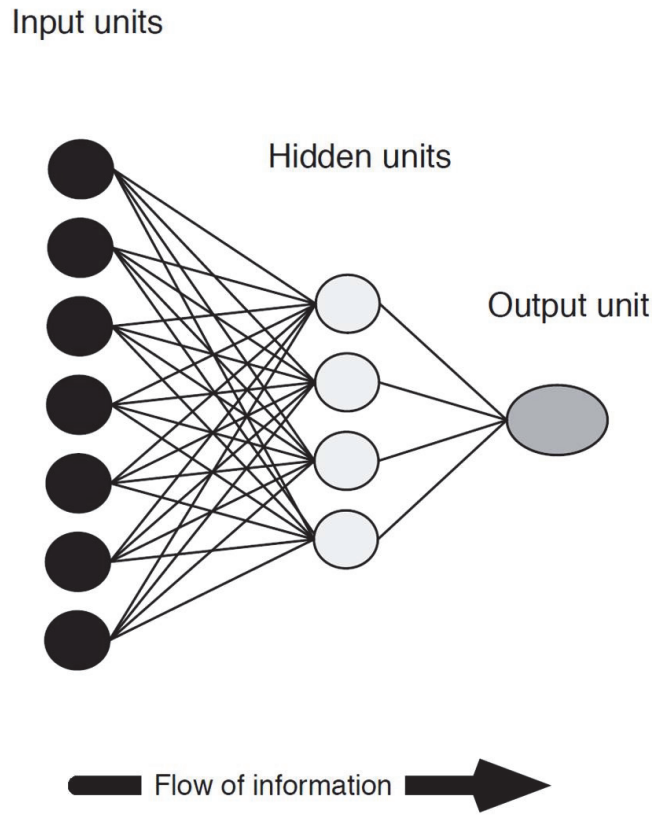

Figure 8. Schematic diagram of a multilalayer perceptron ANN.

Each multilayer perceptron was trained using conjugate gradient descent applied to an entropy error function. The number of hidden nodes and members in the committee machine were determined based on experiments, starting with a single node and increasing the number of nodes until the highest performance was found using the C-index [100]. To avoid overtraining and improve the generalization performance, a weight decay term was used. The calibration of the model was performed using a 10-fold cross-validation procedure [165]. To select the most important risk variables and to minimize the number of variables included in the final model, a ranking of risk variables was performed. A baseline C-index was calculated using all variables. The order of relevance was obtained by measuring the change in index when one risk variable was omitted from the model. This procedure was repeated for each of the variables included, and the least relevant variable was omitted from the model. To optimize the model, the bottomed ranked variable was eliminated, the ANNs were recalibrated using n-1 variables, and a new identification procedure of the least relevant variable was performed. This procedure was repeated until only one variable remained [165]. The final ranking

list was constructed from the top-ranked variables, which improved the performance of the model. Effective hazard ratios for the risk variables were determined in a similar way as described by Lippmann and Shahian [166].

3.9 Pancreaticoduodenectomy

The following text outlines the standard steps performed during pancreaticoduodenectomy at our institution for a tumor in the head of the pancreas without vessel involvement. It is important to remember that the order of the dissection may need to be modified to facilitate safe exposure and removal of the tumor, and anatomical variations are common.

The patient was placed in the supine position. General anesthesia was induced along with endotracheal intubation. A bilateral subcostal transverse incision was used and self-retaining retractors were placed for exposure. The abdomen was carefully explored to rule out extrapancreatic metastatic disease. Any suspicious lesions were biopsied and sent for frozen-section examination, and in the presence of metastases we did not proceed with tumor resection. Next, an extended Kocher maneuver was performed with mobilization of the duodenum and head of the pancreas followed by dissection of the superior mesenteric vein. The lesser omental sac was then entered. The hepatoduodenal ligament was dissected exposing the common bile duct, the hepatic artery branches, and the portal vein. The gallbladder was resected en bloc from the gallbladder fossa and the cystic artery was ligated. The bile duct was divided above the cystic duct entry across the common hepatic duct. Next, the gastroduodenal artery was divided, and the anterior surface of the portal vein was separated from the pancreas, creating a tunnel behind the pancreatic neck. The jejunum was divided approximately 20 cm distal to the ligament of Treitz and its respective mesentery was divided. The distal stomach was then transected. This was followed by transection of the pancreatic neck over the portal vein. To facilitate construction of a pancreaticogastrostomy, the pancreatic remnant was mobilized from the splenic vein (Figure 9). A double-layer pancreaticogastrostomy was achieved by anastomosing the pancreatic remnant to the posterior gastric wall midway between the lesser and greater curvature using interrupted sutures. The transected jejunum was brought retrocolic and a single-layer, end-to-side, hepaticojejunostomy was performed. Finally, a side-to-side gastrojejunostomy was performed between the proximal end of the jejunal loop and the distal end of the stomach. One or two suction drains were placed behind the anastomoses before the abdomen was closed.

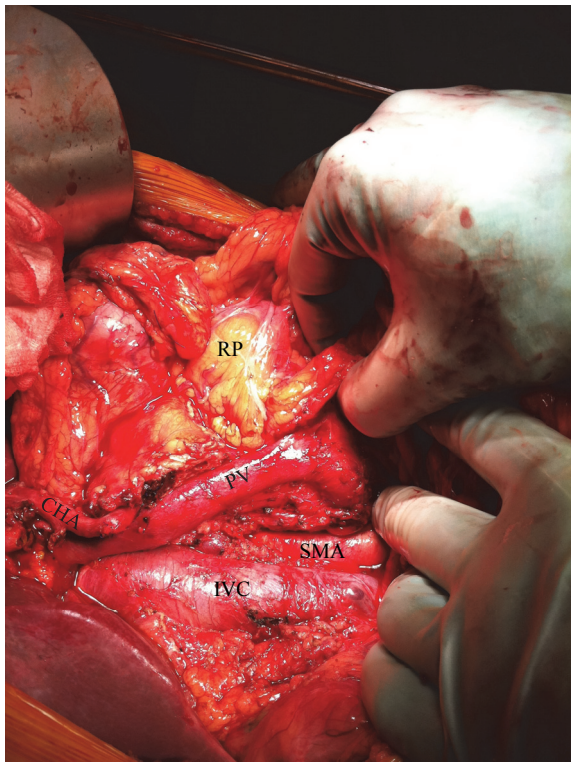

Figure 9. Pancreaticoduodenectomy. Mobilization of the remnant pancreas to prepare for the pancreatic anastomosis to the posterior gastric wall. CHA, common hepatic artery; IVC, inferior vena cava; PV, portal vein; RP, remnant pancreas; SMA, superior mesenteric artery.

The Clavien-Dindo classification of surgical complications was used to classify postoperative complications [167]. Major morbidity was defined as Clavien grade ≥III. Delayed gastric emptying (DGE) was defined according to the consensus definition proposed by the International Study Group of Pancreatic Surgery (ISGPS) [168]. Postpancreatectomy hemorrhage was defined according to ISGPS based on the time of onset, site of bleeding, severity, and clinical impact [169]. Pancreatic fistula was defined according to the definition from the International Study Group on Pancreatic Fistula (ISGPF) [170]. On the basis of the need for therapeutic intervention, only grade B and C pancreatic fistulas were included. Operative mortality was defined as death occurring in hospital or within 30 days of operation.

3.10 Targeting MUC4 expression in patient tumors

Patient tumor sections of 4 µm were automatically pretreated using the PT-link system (DAKO, Glostrup, Denmark) and then stained in an Autostainer Plus (DAKO) with the affinity-purified polyclonal anti-MUC4 antibody HPA 5895 (Atlas Antibodies, Stockholm, Sweden, diluted 1:150). The Envision Flex/HRP (K8010) kit (DAKO) was used for visualization of the staining. The specificity of this antibody has previously been validated using western blotting and protein arrays and MUC4 protein expression has been mapped by immunohistochemistry in 48 types of normal tissues and 20 common cancers (www.proteinatlas.org). The modified histochemical score (H-score) was used to grade expression of MUC4 in cancer cells by an experienced pathologist [152]. The intensity of staining (0=no staining, 1=weak, 2=medium strength, 3=strong) and percentage of stained cells (0=<5% cells stained, 25=5–25% stained, 50=26–50% stained, 75=51–75% stained, 100=>75% stained) were combined in order to calculate the H-score (0–300).

3.11 MUC4+ pancreatic cancer cell lines

Capan-1 (MUC4+) and CD18/HPAF (MUC4+) cells were provided by Professor Surinder Batra (University of Nebraska Medical Center, Omaha, Nebraska, USA) and HPAF-II (MUC4+) and Panc-1 (MUC4-) cells were obtained from ATCC®. Capan-1 was maintained in Iscove's modified Dulbecco's medium (Gibco, Life Technologies, Grand Island, NY, USA) supplemented with 10% fetal bovine serum and 1% penicillin-streptomycin (100 U/ml), respectively. The HPAF cell lines were maintained in minimum essential medium (Gibco) containing 1 mM sodium pyruvate, supplemented as described above. The Panc-1 cell line was maintained in Dulbecco's modified Eagle's medium (Gibco) supplemented with 10% fetal bovine serum and 1% penicillin-streptomycin (100 U/ml). All cells were cultured as a monolayer, kept in an incubator at 37 °C in 5% CO2 and passaged once a week using trypsin (0.25%)/EDTA (0.03%) (Gibco). For in vivo use, the cells were washed with DPBS without Ca^{2+} or Mg^{2+} (Gibco), trypsinized for 5 min, harvested and pelleted at 1,200 rpm for 3 min. After pellet dissociation by repeated gentle pipetting, cell density, and viability were determined using 0.06% trypan blue. $1x10^6$ cells from the respective cell lines were resuspended in 100 µl serum free Dulbecco's Modified Eagle's medium/Hams Nutrient Mix F12 medium (Gibco) and inoculated within 2 hours. For the in vitro experiments, the cells were seeded at a density of 5000 cells/well into 96-well plates in respective standard culture medium for 48 h before changing to serum-free media.

3.12 MUC4 expressing human xenograft model

Fifteen immunodeficient mice (Charles River, Sulzfeld, Germany and Barrier Department at Lund University, Sweden) were housed in standardized pathogen-free conditions in individually ventilated cages and provided free access to standard rodent chow, tap water and nesting material ad libitum. All procedures were performed in a dedicated animal operating room in accordance with the guidelines of the Swedish Government and Lund University, Sweden and were approved by the regional ethics committee.

In order to establish the xenograft tumors, fifteen animals were randomly divided in three groups of five animals in each group (Figure 10). Animals were shortly anesthetized by inhalation of Isofluran in at least 30% oxygen and injected subcutaneously through a $27^{3/4}$ G needle into the right flank with 100 µl fibroblast free cell suspension containing $1x10^6$ tumor cells [171]. Three MUC4+ human pancreatic carcinoma cell lines were used: Capan-1, HPAF-II, and CD18/HPAF.

After the cell inoculation, body weight and the tumor development were monitored once a week. When the tumor size reached about 10 mm in diameter, the animals were sacrificed and examined for metastases. The subcutaneous tumors were resected, fixed in 4% paraformaldehyde for at least 24 h and paraffin-embedded for sectioning and staining for histology or antigen expression.

Figure 10. Subcutaneous model of human pancreatic cancer established in nude mouse.

The tumor size was measured with digital caliper and the volume was calculated using the following formula: Volume (mm^3) = (Length x $Width^2$)/2 [172]. In multi-lobed tumors, the volume of individual lobes were calculated and summarized to obtain the final volume. Quantitative analysis of expressed MUC4 or α-smooth muscle actin (α-SMA) biomarkers was performed on digital microscope slides created by the ScanScope® microscope slide scanner using Aperio Image Scope software version 11 (Aperio Technologies, Inc., Vista, CA, USA). Briefly, for analysis of MUC4 expression, six optical fields (20x

magnification) were randomly selected on the digital slides from specimens stained with the 8G7 antibody. The number of strongly positive cells was counted in each field and summarized for each specimen in the respective group. The results are presented as the median of the total amount of positively stained cells for each specimen in the respective group. The extent of α-SMA expression or sirius red staining was determined as percentage of the strongly positive stained region in relation to the total area of the specimen using Positive Pixel Count 2004-08-11 algorithm, version 8.100.

The tumor sections of 4 µm were deparaffinized in xylene and rehydrated in graded ethanol. The slides were pretreated with 5% normal goat serum in TBS (25 mM Tris, 75mM NaCl, 0.025% TritonX-100 [pH 7.4]) with 2% BSA to minimize the cross-reaction of the secondary antibody with endogenous immunoglobulins in the tissue. The sections were then incubated overnight at 4 °C with the monoclonal antibody 8G7 (Abcam, Cambridge, MA, USA) which recognizes tandem repeat peptide regions of human MUC4 or monoclonal antibody 1A4 (Dako, Glostrup, Denmark) recognizing α-SMA. Primary antibody was diluted 1:50 or 1:100, respectively, in antibody dilution buffer (TBS with 2% BSA). In order to block the endogenous peroxidase activity, the sections were incubated for 15 min with 0.3% H_2O_2 in TBS in room temperature. After washing with TBS, primary antibody detection was performed with a HRP-conjugated secondary antibody (Sigma-Aldrich, St. Louis, MO, USA) diluted 1:200 in antibody dilution buffer. DAB was used as the chromogen for colored visualization of the antigens. The sections were then counterstained with hematoxylin for 20 seconds, dehydrated, cleared and mounted with pertex. Negative controls were treated in a similar way with the exception of primary antibody.

Additionally, all specimens were also stained with picro-sirius red (Abcam, Cambridge, MA, USA) to visualize collagen accumulation in the tissue or hematoxylin and eosin (H&E) for histological evaluation.

3.13 Compound library screening

All tested chemical compounds (Table 4) were obtained from Enzo Life Sciences, Farmingdale, NY, USA (Epigenetics library BML-2836 och Phosphatase inhibitor library BML-2834) and screened at low dose (0.5 µM) or high dose (10 µM) in Capan-1 (MUC4+) and Panc-1 (MUC4-) cell lines. Cells were seeded in respective 96-well plates with one plate for each concentration and cell line. The individual plates were incubated with compounds for 72 h at 37°C. Cell viability was then determined using a tetrazolium salt-based colorimetric assay (MTT kit: Promega, Madison, WI, USA). The absorbance of the dissolved purple formazan

product was measured at 590 nm on a Labsystems Multiscan Plus plate reader using the DeltaSoft JV software (BioMetallics Inc., Princeton, NJ, USA).

Table 4. The combined epigenetics and phosphatase small-molecule inhibitor library.

NAME	PLATE DESCRIPTION	COMPOUND DESCRIPTION
2,4-Pyridinedicarboxylic acid	Epigenetics library	Histone demethylase inhibitor
5-Aza-2'-deoxycytidine (Decitabine)	Epigenetics library	DNA methyltransferase inhibitor
9,10-Phenanthrenequinone	Phosphatase inhibitor library	CD45 tyrosine phosphatase
AGK2	Epigenetics library	SIRT2 inhibitor
Alendronate	Phosphatase inhibitor library	Tyrosine phosphatases
Alexidine·2HCl	Phosphatase inhibitor library	PTPMT1
Aminoresveratrol sulfate	Epigenetics library	SIRT1 activator
Anacardic acid	Epigenetics library	HAT inhibitor
Apicidin	Epigenetics library	HDAC inhibitor
B2	Epigenetics library	SIRT2 inhibitor
B4-Rhodanine	Phosphatase inhibitor library	PRL3
Benzylphosphonic acid	Phosphatase inhibitor library	Tyrosine phosphatases
BIX-01294·3HCl	Epigenetics library	Histone methyltransferase inhibitor
BML-210	Epigenetics library	HDAC inhibitor
BML-260	Phosphatase inhibitor library	JSP-1
BML-266	Epigenetics library	SIRT2 inhibitor
BML-267	Phosphatase inhibitor library	PTP1B
BML-267 ester	Phosphatase inhibitor library	PTP1B (cell permeable)
BML-278	Epigenetics library	SIRT1 actvator
BML-281	Epigenetics library	HDAC-6 inhibitor
BN-82002	Phosphatase inhibitor library	CDC25
Butyrolactone 3	Epigenetics library	HAT inhibitor
BVT-948	Phosphatase inhibitor library	Tyrosine phosphatases
Cantharidic acid	Phosphatase inhibitor library	PP1 and PP2A
Cantharidin	Phosphatase inhibitor library	PP1 and PP2A
CI-994	Epigenetics library	HDAC inhibitor
CinnGel	Phosphatase inhibitor library	PTP1B
CTPB	Epigenetics library	HAT activator
Cyclosporin A	Phosphatase inhibitor library	Calcineurin (PP2B)
Cypermethrin	Phosphatase inhibitor library	Calcineurin (PP2B)
Deltamethrin	Phosphatase inhibitor library	Calcineurin (PP2B)
Endothall	Phosphatase inhibitor library	PP2A
EX-527	Epigenetics library	SIRT1 inhibitor
Fenvalerate	Phosphatase inhibitor library	Calcineurin (PP2B)
Fluoro-SAHA	Epigenetics library	HDAC inhibitor
Garcinol	Epigenetics library	HAT inhibitor
Gossypol	Phosphatase inhibitor library	Calcineurin (PP2B)
Isonicotinamide	Epigenetics library	Nicotinamide antagonist
ITSA-1	Epigenetics library	Inhibitor of TSA activity
L-p-Bromotetramisole oxalate	Phosphatase inhibitor library	Tyrosine phosphatases
Levamisole HCl	Phosphatase inhibitor library	Mammalian alkaline phosphatase
M-344	Epigenetics library	HDAC inhibitor
MC-1293	Epigenetics library	HDAC inhibitor
NCH-51	Epigenetics library	HDAC inhibitor
Nicotinamide	Epigenetics library	SIRT inhibitor
NSC-3852	Epigenetics library	HDAC inhibitor
NSC-663284	Phosphatase inhibitor library	CDC25
NSC-95397	Phosphatase inhibitor library	CDC25
Nullscript	Epigenetics library	Scriptaid Neg control
OBA	Phosphatase inhibitor library	Tyrosine phosphatases
OBA Ester	Phosphatase inhibitor library	Tyrosine phosphatases (cell permeable)
Oxamflatin	Epigenetics library	HDAC inhibitor
Pentamidine	Phosphatase inhibitor library	PRL1
Phenylbutyrate·Na	Epigenetics library	HDAC inhibitor
Piceatannol	Epigenetics library	SIRT activator
Resveratrol	Epigenetics library	SIRT1 activator
RK-682	Phosphatase inhibitor library	Tyrosine phosphatases
RWJ-60475	Phosphatase inhibitor library	CD45 tyrosine phosphatase
RWJ-60475 (AM)3	Phosphatase inhibitor library	CD45 tyrosine phosphatase (cell permeable)
Salermide	Epigenetics library	SIRT inhibitor

Sanguinarine chloride	Phosphatase inhibitor library	PP2C
Scriptaid	Epigenetics library	HDAC inhibitor
Shikonin	Phosphatase inhibitor library	
Sirtinol	Epigenetics library	SIRT inhibitor
Splitomicin	Epigenetics library	SIRT-2 inhibitor
Suberoyl bis-hydroxamic acid	Epigenetics library	HDAC inhibitor
Suramin·6Na	Epigenetics library	SIRT1 inhibitor
Tetramisole HCl	Phosphatase inhibitor library	Mammalian alkaline phosphatase
Tranylcypromine hemisulfate	Epigenetics library	Lysine demethylase inhibitor
Triacetylresveratrol	Epigenetics library	SIRT1 activator
Trichostatin A	Epigenetics library	HDAC inhibitor
Tyrphostin 8	Phosphatase inhibitor library	Calcineurin (PP2B)
Valproic acid	Epigenetics library	HDAC inhibitor
Valproic acid hydroxamate	Epigenetics library	HDAC inhibitor
Vorinostat (SAHA)	Epigenetics library	HDAC inhibitor
Zebularine	Epigenetics library	DNA methyltransferase inhibitor

3.14 Dose-response study

The cells were seeded in 96-well plates as described above, one plate for each time point. Cells were treated with either apicidin, gemcitabine or vehicle control at 10-fold serial increasing concentrations (0.05 μM to 50 μM) for 24, 48 and 72 h. Cell viability was determined as described above. For each treatment and cell line, the experiments were performed in six replicates to determine the concentration required to cause 50% growth inhibition (LD_{50}). Combined treatments of a sub-therapeutic concentration of apicidin (0.05 μM) together with gemcitabine at concentrations of 0.05, 0.5, 1.0, 5, 10, 20 and 50 μM for 72 h were tested to evaluate whether apicidin synergistically increased gemcitabine-induced cell growth inhibition.

3.15 High content screening (HCS) of protein expression

The plated cells were treated with 0.05 μM apicidin or 5 μM gemcitabine alone, or in combination for 72 h. Cell viability was determined as described above. For HCS, cells were fixed with 4% paraformaldehyde, permeabilized with 0.5% TritonX-100/PBS, incubated for 30 min with 5% donkey serum for antibody raised in rabbit or 5% goat serum for antibody raised in mouse to block nonspecific protein interactions followed by primary antibodies to MUC4, hepatocyte nuclear factor 4α (HNF4α), GATA-binding factor 6 (GATA6), and forkhead box protein A2 (FOXA2) (Table 5), all at 1:100 dilution, overnight. Alexa® Fluor 488-conjugated anti-mouse, made in goat or anti-rabbit made in donkey (Molecular Probes, Life Technologies) were used at a dilution of 1:200 as secondary antibody. Cells were co-stained with DAPI (0.1 mg/ml; Molecular probes) to determine the location of nuclei and stored at 4ºC in 50 μl of anti-fading mounting medium until analysis. All experiments were performed in six replicates.

Plates were scanned on a Cellomics ArrayScan PlatformVTI HCS Reader (Thermo Fisher Scientific, Rockford, IL, USA) to determine the mean total intensity per cell. Image quantification analysis was performed using Cellomics Morphology Explorer software (www.cellomics.com).

Table 5. Antibodies used for high content screening.

PRIMARY ANTIBODY	PROTEIN NAME	COMPANY	SECONDARY ANTIBODY
8G7	Mucin 4	Abcam (ab52263)	Goat anti-mouse
F.674.9	Hepatocyte nuclear factor 4α	Thermo Scientific (MA5-14891)	Donkey anti-rabbit
C-20	GATA-binding factor 6	Santa Cruz Biotechnology (sc-7244)	Donkey anti-rabbit
M-20	Forkhead box protein A2	Santa Cruz Biotechnology (sc-6554)	Donkey anti-rabbit

3.16 Statistics

In study I, the experiment was normalized using the peptides of the added internal standard protein ADH from yeast. Statistical analysis was performed using log2-transformed normalized abundances. Hierarchical clustering and principal component analysis (PCA) were employed to visualize any statistically significant differences between the groups. Multiple group comparison was conducted with the ANOVA test. Protein interaction maps were obtained from the Search Tool for the Retrieval of Interacting Genes/Proteins (STRING) database version 9.1 containing known and predicted physical and functional protein-protein interactions [173].

In study II, multivariate analysis by Cox proportional hazard model was performed using stepwise Cox regression. Inclusion criterion for the full model was $p<0.250$. The limit for stepwise backward elimination was $p<0.100$. The Kaplan-Meier method was used to estimate long-term survival. The performance of the survival model was determined using C-index [100]. Missing data were handled using multiple imputation techniques [174]. High-performance computing clusters were used to train and evaluate the ANNs.

In study III, univariate analysis for continuous variables was conducted with the Kruskal-Wallis test. The Mantel-Haenszel χ^2 test was used to assess trends in mortality and other categorical variables across volume groups [3,12].

In study IV, concordance between MUC4 expression in primary and metastatic samples was calculated as the ratio of concordant cases to total cases. McNemar's test was used to evaluate differences in dichotomized staining results. The

Wilcoxon signed-rank test and Spearman's rank correlation test was used to compare H-scores between primary and paired lymph node metastases.

In study V, the nonparametric Kruskal-Wallis test was used for multiple group comparisons. When significant, post hoc tests were performed using the Dunn's test. Data were analyzed using SPSS version 22.0 (IBM, Armonk, NY, USA) and GraphPad Prism version 6.0 (GraphPad Software, San Diego, CA, USA). Significance was assumed with a p-value <0.05.

In study VI, the LD_{50} was calculated by a variable slope dose–response curve fitting. One-way ANOVA was used for comparisons of protein expression levels between groups followed by Dunnett's post hoc test to compare the mean of each treatment group with the mean of the control group. Data were analyzed using GraphPad Prism version 6.0 (GraphPad Software, San Diego, CA, USA). Significance was assumed with a p-value <0.05.

Protein lists were processed and statistically analyzed using Qlucore Omics Explorer version 3.0. For the other studies, statistical analyses were performed using SPSS (versions 20 and 22; IBM, Armonk, New York, USA), Stata MP (version 11.1; StataCorp LP, College Station, TX, USA) and GraphPad Prism version 6.0 (GraphPad Software, San Diego, CA, USA). The ANN calibration and analyses were performed with MatLab Distribution Computing Server 2010a, Neural Network Toolbox (MathWorks, Natick, MA, USA). A p-value less than 0.05 was considered statistically significant.

Chapter 4 Results

Study I – Protein deep sequencing applied to biobank samples from patients with pancreatic cancer

Mass spectrometry and proteomic analysis was performed on a total of 27 serum samples from Lund. The sera were from 9 patients with resectable pancreatic cancer, 9 patients with benign pancreatic disease, and 9 healthy blood donors. Among the benign group, the patients had chronic pancreatitis (n=4), IPMN (n=3), serous cystadenoma (n=1), and benign biliary stricture (n=1).

System solution reproducibility

In the first development phase of the study, single samples from each group were injected in triplicate. The HDMS^E platform generates high peak capacity that maximizes the protein identification, whilst retaining label-free quantification capabilities. To assess the analytical reproducibility of the LC/MS acquisition and data processing, we calculated the intensity differences between peaks from triplicate acquisitions of the same serum sample. Some 4,801 peptides were identified within the data, for each cycle run. The MS data from the different replicates were clustered tightly and showed that there is a high reproducibility. All triplicate data points showed less than 4% variation in intensity, while the chromatographic reproducibility was found to have 2-4% RSD. These shotgun analysis data are illustrated in Figure 11, with triplicate LC-MS overlayed BPI chromatograms where the platform performance can be viewed to be highly constant over the entire cycle run, going from hydrophilic to hydrophobic peptide sequences.

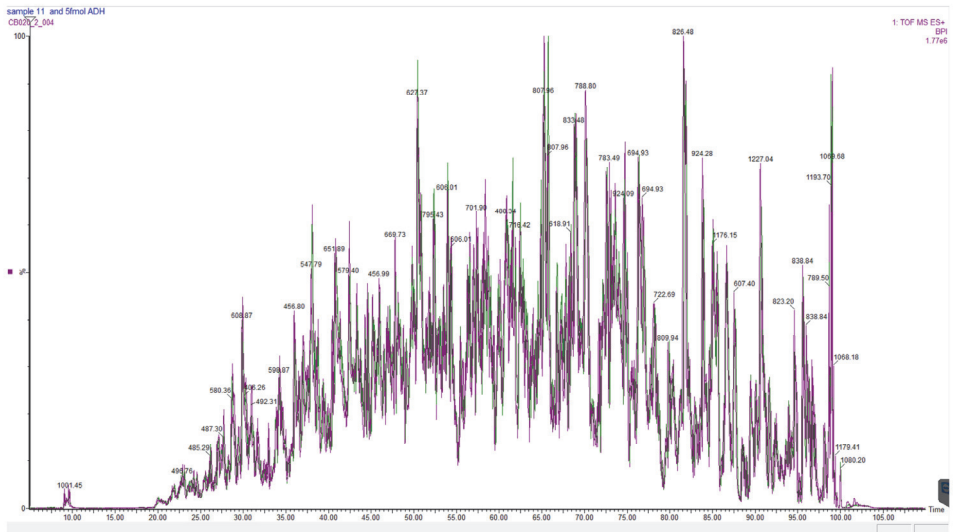

Figure 11. Raw HDMS^E data overlayed tripled injections.

Peptide sequence identification and quantification

In the second part of the assay development, we continued analyzing all 27 patient samples by duplicate injections. Within this part of the study, we generated a data output of 71,209 distinct features. The HDMS^E data files were interrogated with Progenesis QI for Proteomics for protein identification and quantification. The resulting proteins were then subjected to stringent independent validation within the software. By using an identification criterion of 80% peptide probability and 99% protein probability, a total number of 7,947 unique peptides and 715 unique proteins were identified using a false discovery rate <0.5%. The differential protein quantification was performed by calculating the sum of all unique normalized peptide ion abundances for a specific protein on each run and then comparing mean values between samples. As the study was conducted over a substantial time period, a normalization procedure was important, utilizing ADH, as an internal control in all clinical samples. We also performed the study by having the quality control (QC) run as the calibrant within the assay, at frequency as the 8th sample within the analysis cycle.

Gene ontology

Gene ontology analysis was undertaken to assess the holistic biological role and molecular function of the identified proteins. The annotation highlighted a

significant portion of species involved in both binding and catalytic processes. In terms of biological process the proteins were represented most highly by those involved in metabolic and cellular processes (Figure 12). This is in line with what the pancreas study team was expecting. Similar ontology groupings were identified by other research groups in recent studies [175, 176].

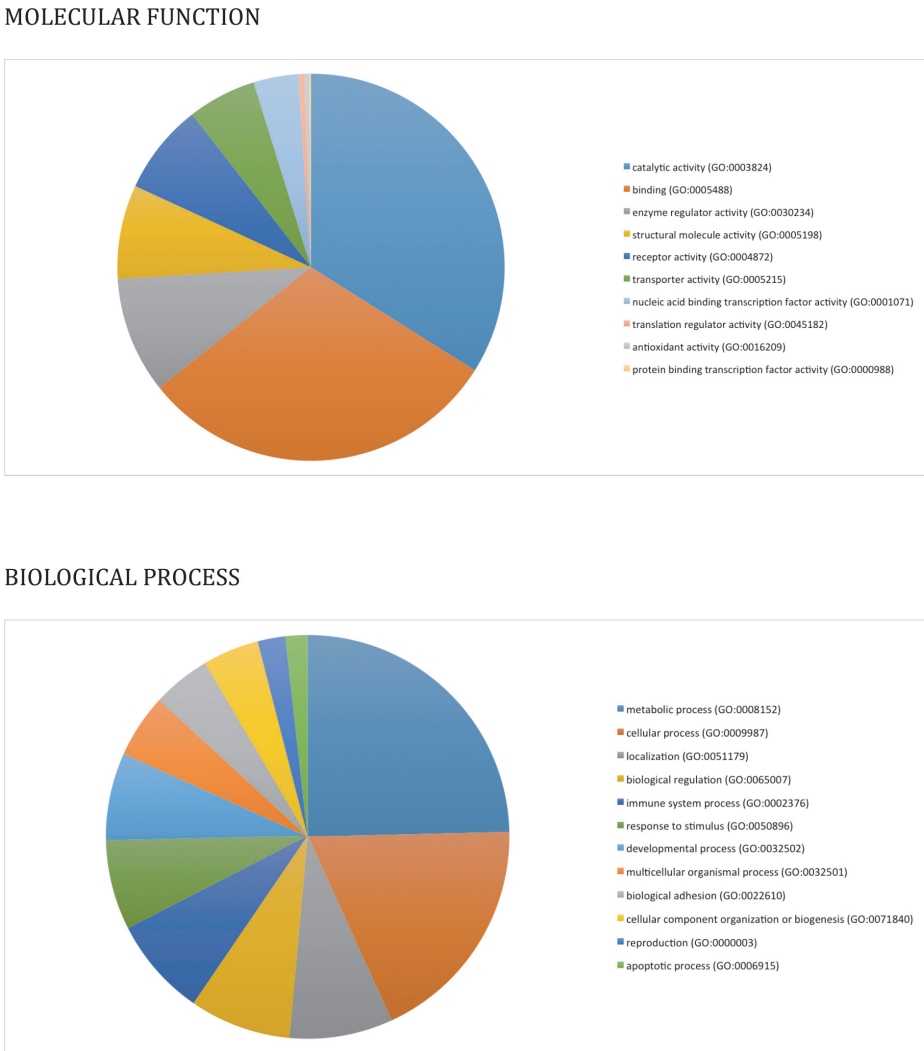

Figure 12. Gene ontology classification of proteins identified in the serum samples.

Hierarchical clustering

To define if protein expression profiles were distinct between pancreatic cancer and control samples, we performed unsupervised hierarchical clustering on log-transformed baseline protein concentrations, as outlined in Figure 13. A two-way clustering approach was applied in order to allow a meaningful clustering of both proteins and samples. We were able to find group specific regulation in each study group in the resulting heat-map for 134 differentially expressed proteins ($p<0.0009$), where the red color indicates up-regulation and the green down-regulation of protein expression over the mean values. Further, the analysis showed several clusters that could be used for classification purposes. In particular, one cluster containing 40 proteins showed a significant up-regulation in the pancreatic cancer group. By these statistical calculations, low q-values (all below 0.005), were provided indicating a low false discovery rate.

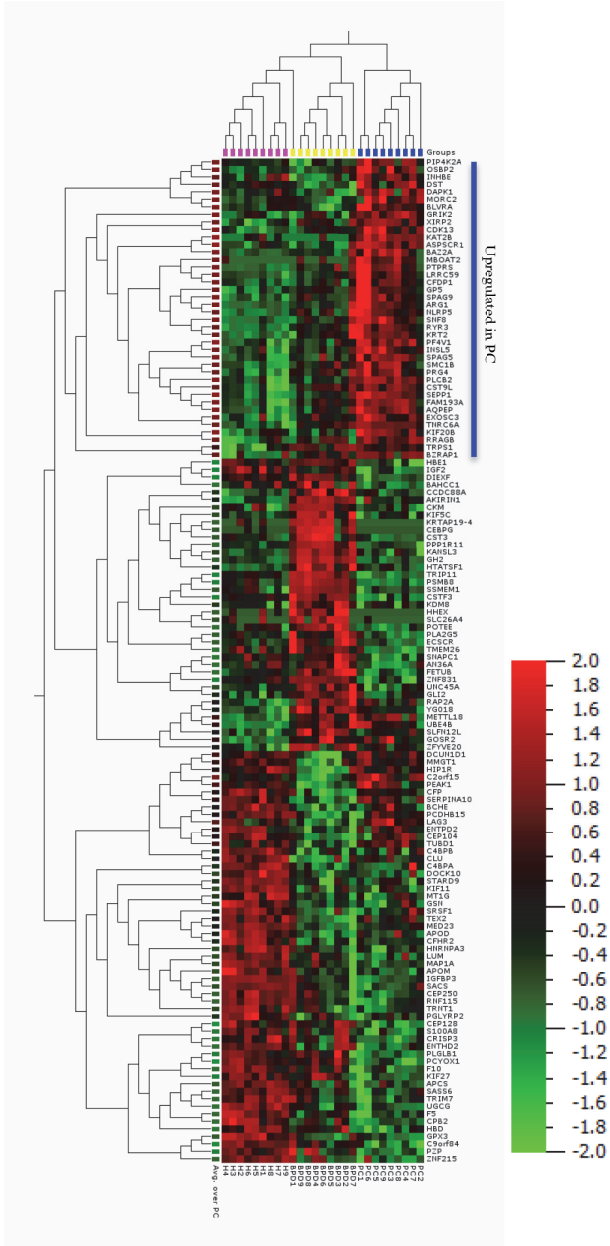

Figure 13. Heat map diagram with two-way unsupervised hierarchical clustering of proteins and serum samples. Each row represents a protein and each column represents a sample. The protein clustering tree is shown on the left, and the sample clustering tree appears at the top. The color scale shown in the map illustrates the relative expression level of a protein across all samples: red represents an expression level above the mean; green represents expression lower than the mean. This analysis identified 134 differentially expressed proteins ($p<0.0009$). There was clustering of 40 proteins up-regulated in pancreatic cancer as compared to patients with benign pancreatic disease and healthy controls. Blue, pancreatic cancer; yellow, benign pancreatic disease; pink, healthy.

Principal component analysis - PCA

These distinct protein profile signatures observed between pancreatic cancer and control phenotypes after clustering analyses were further confirmed by PCA. In the PCA score plot (Figure 14), samples that have similar protein expression profiles fall close to each other. This was found to correlate well with the clinical stratification. We also observed a larger variation in the protein expressions among the pancreatic cancer and benign cases compared with the healthy samples. This is illustrated in the PCA plot by the more scattered distribution of cancer samples (blue) and benign cases (yellow) compared with healthy samples (pink). These findings suggest that the cancer and benign population are more heterogeneous than the corresponding healthy population. Furthermore, as can be seen in the plot, the first principal component contains 38% of the total variance and clearly sets the pancreatic cancer group apart from the rest of the subtypes. Overall, these data provide evidence that the pancreatic cancer cohort can be stratified by our unique group of proteins.

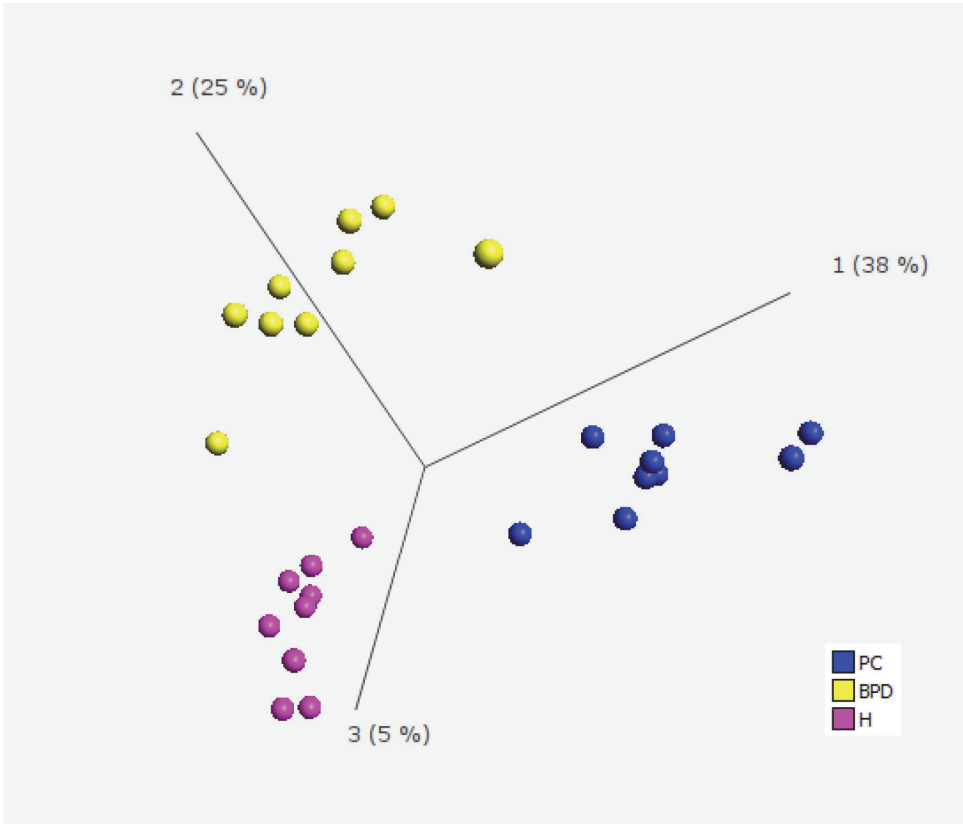

Figure 14. Principal component analysis on the differentially expressed proteins between pancreatic cancer, benign pancreatic disease, and healthy controls.

Protein network analysis

Protein network analysis using the STRING system was applied for the subset of differentially regulated proteins identified within the study. The STRING database builds clusters of known and predicted protein interactions. The network is presented under confidence view, where the thicker lines represent stronger associations as shown in Figure 15. Proteins from the experiments are represented as colored nodes. Ten additional interacting proteins (white nodes) representing nodes of a higher iteration/depth were automatically generated by STRING to maximize existing interactions. The overall analysis resulted in several distinct protein networks including a total of 75 unique interactions (p=1.44e-7).

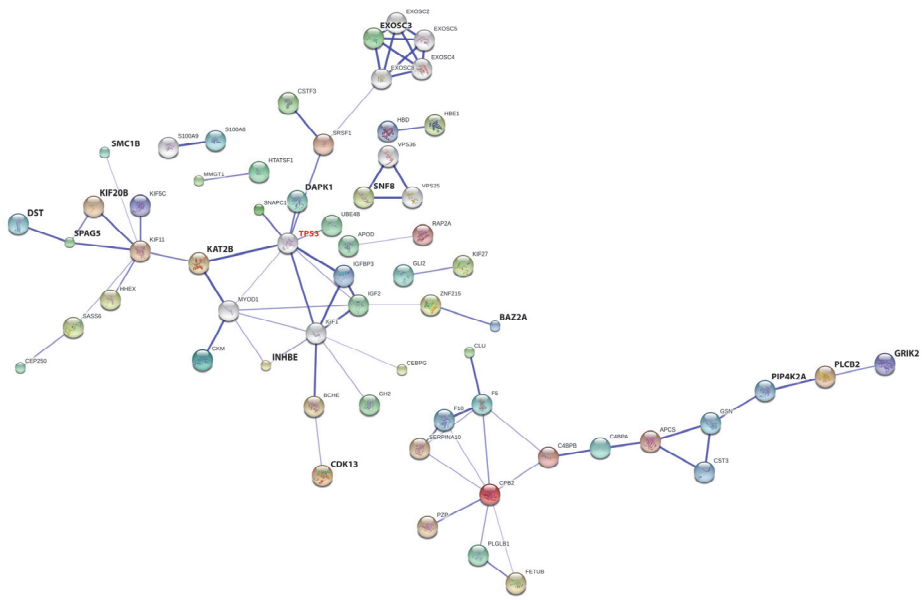

Figure 15. STRING network showing the association between differentially expressed proteins. The interaction map was generated using default settings. We used medium confidence (0.4) and standard criteria for linkage including neighborhood, gene fusion, co-occurrence, co-expression, experiments, databases, and textmining. Ten additional interplay proteins (white nodes) were also added to the network. Bold text indicated significant up-regulation in pancreatic cancer samples. Stronger associations are represented by thicker lines.

As illustrated in Figure 15, we found that most proteins clustered in a tight interaction network centered on TP53 (p53 protein). It is known that alterations in the p53 tumor suppressor are found in the majority of early stage pancreatic cancers [177], which strengthens the overall evaluation of the protein complex data. It is also known that activation of the p53 signaling pathway overrules as master regulator of pancreatic cancer development. The p53 mechanism of action occurs through a diverse process procedure, such as cell cycle regulation,

apoptosis, senescence, and autophagy [177-180]. The up-regulated proteins in pancreatic cancer that showed significant interactions with p53 included; BAZ2A, CDK13, DAPK1, DST, EXOSC3, INHBE, KAT2B, KIF20B, SMC1B, and SPAG5. The specific expression profiles of each of the 10 proteins within the study groups, are shown in Figure 16.

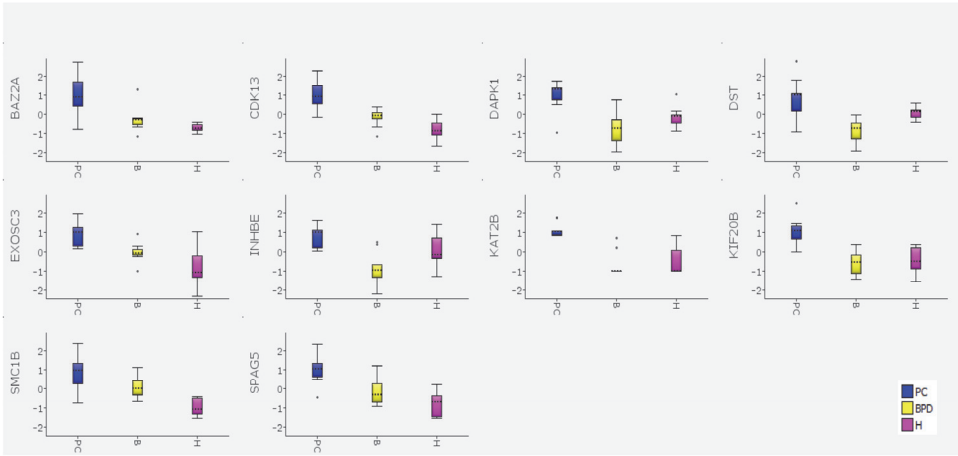

Figure 16. Examples of protein expression changes for the diagnosis of pancreatic cancer: BAZ2A, CDK13, DAPK1, DST, EXOSC3, INHBE, KAT2B, KIF20B, SMC1B, and SPAG5. Values represent log2 fold change.

Study II – Artificial neural networks predict survival from pancreatic cancer after radical surgery

This study included 84 patients that underwent macroscopically radical resection for pancreatic cancer in Lund and Malmö. Forty-five patients received adjuvant gemcitabine, capecitabine, or 5-FU–based chemotherapy after surgical resection. The median survival of the entire cohort was 19 months.

ANN architecture

Six million different ANN models were validated using a high-performance computer cluster. The architecture of the final ANN consisted of 4 hidden nodes and 1 output node. This ANN architecture was used to identify the most influential risk variables that can be associated with survival.

Performance and accuracy

Figure 17 shows the change in the performance of the ANN model with the number of input variables plotted on the x-axis and C-index on the y-axis. The first peak was achieved when the 7 top-ranked variables were selected. Included herein were lymph node metastasis, poor differentiation, BMI, age, positive resection margin, peritumoral inflammation, and ASA grade (Table 6). The Cox regression model selected 3 variables: lymph node metastasis, tumor location, and preoperative white blood cell count. The ANN model was more accurate than Cox regression in predicting survival. The C-index was 0.79 for the ANN and 0.67 for Cox regression.

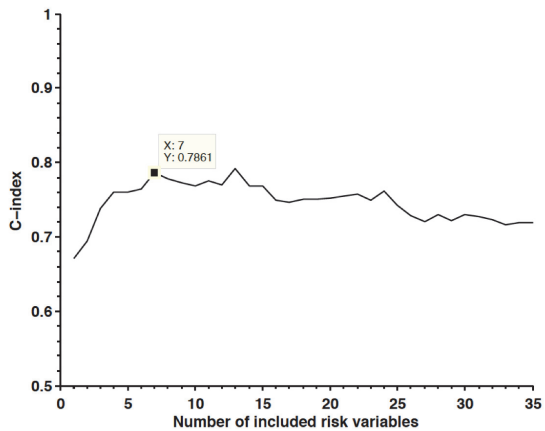

Figure 17. Performance of the ANN (y-axis) plotted against the number of input variables (x-axis).

Table 6. Variables used to construct the ANN

RANK	VARIABLE	HAZARD RATIO	PERFORMANCE (C-index)
1	Lymph node metastasis	1.481	0.672
2	Poor differentiation	1.299	0.694
3	BMI	0.852	0.738
4	Age	0.949	0.760
5	Positive resection margin	1.349	0.760
6	Peritumoral inflammation	2.206	0.765
7	ASA grade	1.472	0.786

Time dependence of hazard ratios

In Cox regression, it is assumed that the hazard ratio proportion remains constant throughout the time period of the analysis. However, a more accurate representation of time is to include it as a covariate. This approach is shown in

Figure 18. For example, the hazard ratio for lymph node metastasis was relatively stable over time. In contrast, the hazard for ASA grade gradually increased.

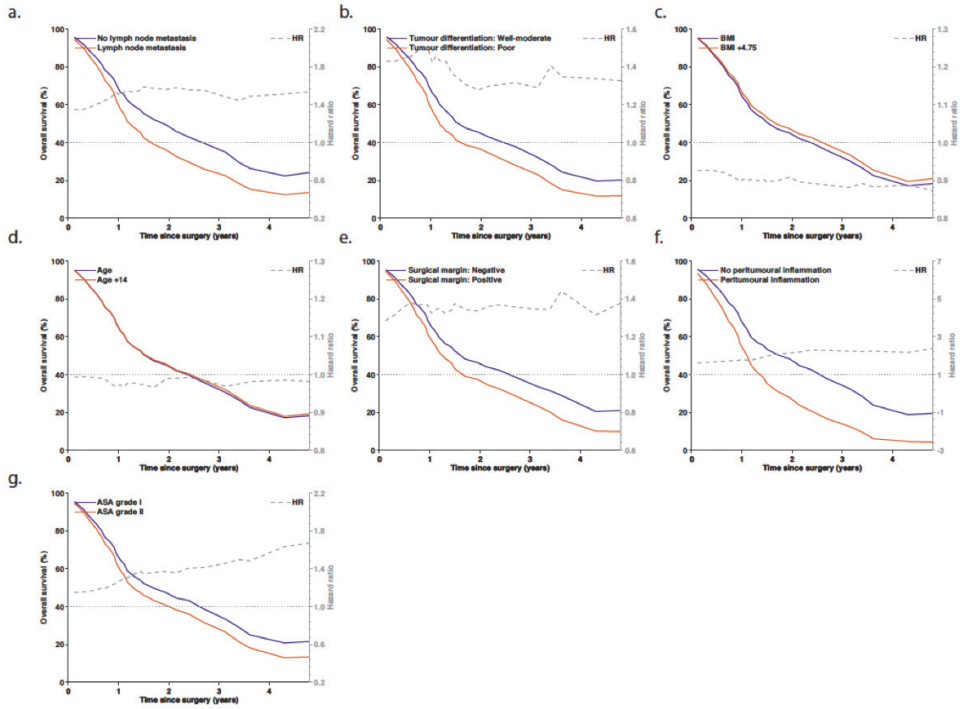

Figure 18. Survival curves and time-dependent hazard ratios for the 7 top-ranked variables. For continuous variables (BMI and age), the time-dependent hazard ratio was calculated using the interquartile range instead of a unit difference.

Individualized survival prediction

The ANN survival predictions were compared with observed survival using the Kaplan-Meier method. Figure 19 shows that ANN and Kaplan-Meier survival curves were similar, which indicated that predicted survival did not considerably differ from observed survival. This finding was further supported by the C-index. Over time, the agreement between the ANN and Kaplan-Meier decreased because the analysis was affected by the limited number of patients with actual long-term follow-up.

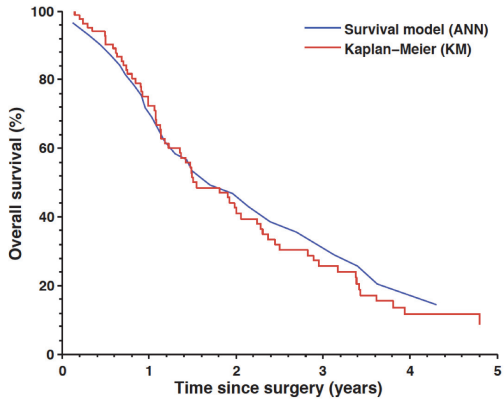

Figure 19. A comparison of ANN survival prediction and Kaplan-Meier estimates.

Study III – Pancreaticoduodenectomy - the transition from a low- to a high-volume center

This study included 221 patients that underwent pancreaticoduodenectomy for pancreatic cancer and other periampullary tumors in Lund. The annual number of PDs increased from 5 in 2000 to 39 in 2012 (Figure 20). Hospital volume was categorized by the number of pancreaticoduodenectomies performed annually into low-volume (<10 procedures/year), years 2000-2004, n=25; medium-volume (10-24 procedures/year), years 2005–2009, n=86; and high-volume (≥25 procedures/year), years 2010–2012, n=110 based on established cut-off values [122].

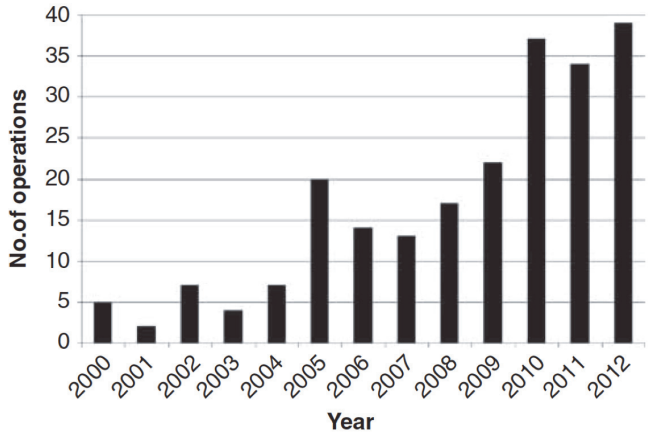

Figure 20. Pancreaticoduodenectomies performed between January 2000 and December 2012 at Skåne University Hospital, Lund, Sweden.

The most common indication for surgery was pancreatic ductal adenocarcinoma (Table 7).

Table 7. Indications for pancreaticoduodenectomy

HISTOPATHOLOGICAL DIAGNOSIS	n (%)
Pancreatic ductal adenocarcinoma	66 (29.9)
Cholangiocarcinoma	42 (19.0)
Ampullary adenocarcinoma	36 (16.3)
Duodenal adenocarcinoma	22 (10.0)
Intraductal papillary mucinous neoplasm	15 (6.8)
Neuroendocrine tumor	10 (4.5)
Chronic pancreatitis	10 (4.5)
Serous cystadenoma	5 (2.3)
Mucinous cystadenoma	3 (1.4)
Mucinous cystadenocarcinoma	2 (0.9)
Solid pseudopapillary neoplasm	2 (0.9)
Ampullary adenoma	2 (0.9)
Duodenal adenoma	1 (0.5)
Gastrointestinal stromal tumor	1 (0.5)
Metastatic renal cell carcinoma	1 (0.5)
Metastatic non-small cell carcinoma	1 (0.5)
Benign bile stricture	1 (0.5)
Duodenal ulcer	1 (0.5)

Median age at the time of surgery (p=0.143), percentage of female patients (p=0.218), and preoperative comorbidity (p=0.225) did not change during the study period (Table 8).

The median operative duration decreased significantly over the volume categories ($p<0.001$), ranging from 523 min in the low-volume period to 451 min in the high-volume period. Intraoperative blood loss also dropped ($p<0.001$). The need for blood transfusion decreased progressively with increasing hospital volume ($p<0.001$).

The most common complication was DGE. There was no significant difference in the rate of DGE across volume groups. There was a reduced incidence of postoperative hemorrhage according to hospital volume ($p=0.022$). Pancreatic fistula did not differ significantly between volume groups. Infectious complications were similar between groups. Additionally, major morbidity and intensive care unit requirement remained unaltered.

Reoperation was required in six patients, reasons being postoperative hemorrhage in five patients and ileus in one patient. The need for reoperation significantly decreased when comparing the volume categories ($p=0.041$). Postoperative length of stay dropped significantly ($p=0.010$), ranging from 16 days in the low-volume period to 13 days in the high-volume period. There were three postoperative deaths. Causes were sepsis-associated multiple organ failure in one patient, hemorrhage in one patient, and unknown in one patient. The mortality rates for the low-, medium-, and high-volume periods were 4.0%, 2.3%, and 0%, respectively ($p=0.066$).

Table 8. Hospital volume and outcome for pancreaticoduodenectomy.

	LOW-VOLUME <10 PDs/year 2000-2004, n=25	MEDIUM-VOLUME 10-24 PDs/year 2005-2009, n=86	HIGH-VOLUME ≥25 PDs/year 2010-2012, n=110	p-value
Age	63 (15-76)	67 (17-83)	67 (25-81)	0.143
Female gender	14 (56.0)	41 (47.7)	47 (42.7)	0.218
ASA score	2 (1-3)	2 (1-3)	2 (1-3)	0.225
Operative time (min)	523 (300-758)	534 (278-945)	451 (235-820)	<0.001
Blood loss (ml)	1150 (200-3600)	800 (100-2800)	500 (100-4600)	<0.011
Blood transfusion	13 (56.5)	24 (31.6)	10 (9.7)	<0.001
Delayed gastric emptying	9 (37.5)	29 (33.7)	45 (40.9)	0.588
Grade A	1 (4.2)	6 (7.0)	25 (22.7)	
Grade B	2 (8.3)	14 (16.3)	12 (10.9)	
Grade C	6 (25.0)	9 (10.5)	8 (7.3)	
Hemorrhage	5 (20.8)	14 (16.3)	8 (7.3)	0.022
Grade A	1 (4.2)	4 (4.7)	4 (3.6)	
Grade B	2 (8.3)	4 (4.7)	2 (1.8)	
Grade C	2 (8.3)	6 (7.0)	2 (1.8)	
Pancreatic fistula	4 (16.7)	13 (15.1)	11 (10.0)	0.238
Grade B	4 (16.7)	5 (5.8)	8 (7.3)	
Grade C	0 (0.0)	8 (9.3)	3 (2.7)	
Wound infection	6 (25.0)	18 (20.9)	25 (22.7)	0.970
Intra-abdominal infection	2 (8.3)	13 (15.1)	10 (9.1)	0.578
Major morbidity	5 (20.0)	14 (16.3)	19 (17.3)	0.872
ICU requirement	3 (13.6)	5 (5.8)	8 (7.3)	0.582
Reoperation	2 (8.3)	3 (3.5)	1 (0.9)	0.041
Postoperative LOS	16 (9-89)	15 (8-62)	13 (6-78)	0.010
Mortality	1 (4.0)	2 (2.3)	0 (0.0)	0.066

ASA = American Society of Anesthesiologists score; ICU = intensive care unit; LOS, length of stay; PD, pancreaticoduodenectomy. Analysis is based on the available patient data.

Study IV – Comparison of MUC4 expression in primary pancreatic cancer and paired lymph node metastases

This study included 17 patients with resected pancreatic and synchronous lymph node metastases.

Distribution of MUC4 expression in primary and matched lymph node metastases (categorical)

Following assessment of MUC4 immunoreactivity, 15 (88%) primary tumor samples were classified as positive. Of lymph node metastases, 14 (82%) were positive. One representative case is shown in Figure 21.

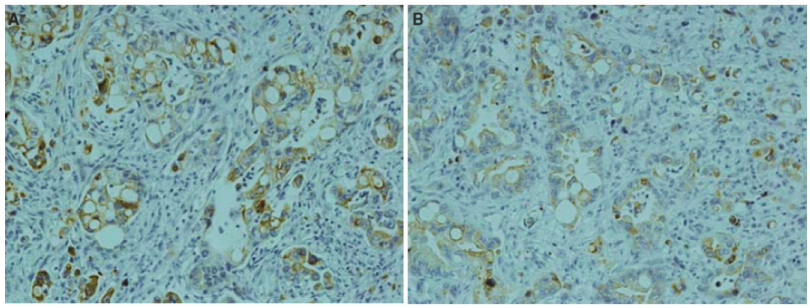

Figure 21. Representative immunohistochemical staining of MUC4. Positive labeling for MUC4 in primary pancreatic cancer (a) and paired lymph node metastasis (b) from the same patient. Original magnification 20x for all images.

Distribution of MUC4 in primary and matched lymph node metastases (continuous)

In the primary tumors, the median H-score was 100 (0–225). In the matched lymph node metastases, the median H-score was 75 (0–225). The H-score for distribution of MUC4 expression is shown in Figure 22.

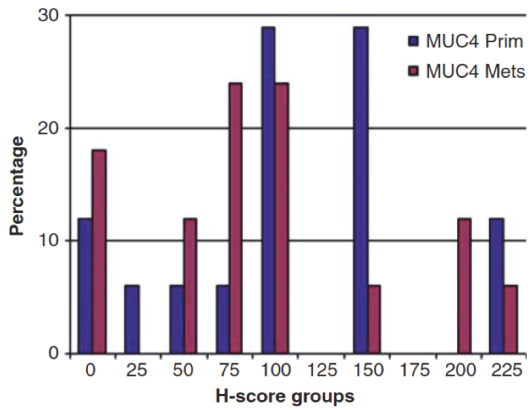

Figure 22. MUC4 distribution in matched pairs of primary tumors and lymph node metastases (n=17).

Comparison of MUC4 status between paired tumors

The overall MUC4 concordance rate between primary and paired metastatic tumors was 82% (14/17; Table 9). The p-value for skewness (McNemar's test) was 1.000. Of the three discordant cases, two were positive in the primary tumor and negative in the metastases and one was negative in the primary tumor and

positive in the metastasis. There was no significant difference between primary tumors and their matched lymph node metastases regarding H-score (Wilcoxon signed rank test, p=0.285).

Table 9. Matched tumor samples have high concordance when using a pre-defined definition of positive vs negative MUC4 (categorical).

		Primary		
		Positive	**Negative**	
Metastatic	Positive	13	1	14
	Negative	2	1	3
		15	2	17

The distribution of H-score for expression of MUC4 significantly correlated (Spearman's rank correlation, r=0.615; p=0.009) between tumors and paired metastatic lesions (Figure 23).

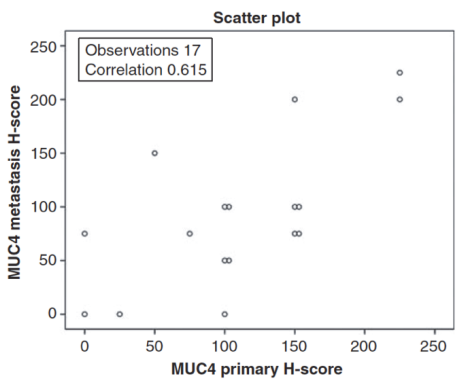

Figure 23. Good correlation between matched primary tumors and corresponding lymph node metastases. p = 0.009.

Study V – Analysis of MUC4 expression in human pancreatic cancer xenografts in immunodeficient mice

All 15 animals developed solid subcutaneous tumors within two weeks after inoculation. Tumor volume varied in a similar matter in all groups with no

significant differences between groups (p=0.796; Table 10). No metastases were found.

Table 10. Capan-1, HPAF-II and CD18/HPAF tumors, MUC4+ cell amount, α-SMA staining extent.

	CAPAN-1 TUMORS (n=5)	HPAF-II TUMORS (n=5)	CD18/HPAF TUMORS (n=5)	p-value
Tumor volume (mm^3)	540 (290-800)	400 (230-580)	460 (120-650)	0.796
MUC4+ cells	576 (553-599)	94 (62-131)	0	0.002
α-SMA extent (%)	38.80 (13.26-56.70)	25.62 (20.99-45.01)	8.95 (3.19-16.33)	0.018

Histology

Capan-1 cells formed poorly differentiated solid tumors without duct structures. The tumor consisted of epithelial cells with irregular nuclei rich of mitosis and a eosinophil cytoplasm with focal vacuolar degeneration. Cells set in nests were supported by a fibrous stroma. The tumor area had pseudocyst formation with protein rich liquid in the lumen. CD18/HPAF cells formed solid tumors characterized by epithelial-like structures with a delicate fibrous stroma around and poorly defined necrosis. Moderate pleomorphism, numerous mitosis and an eosinophilic cytoplasm were prominent. Tumors derived from HPAF-II cells were composed of poorly formed glands infiltrated by poorly differentiated epithelial cells and abundant fibrous stroma. Necrosis could occasionally be noted in individual large tumors, exceeding a volume of 500 mm^3. Examples of histological findings in the respective tumors are presented in Figure 24.

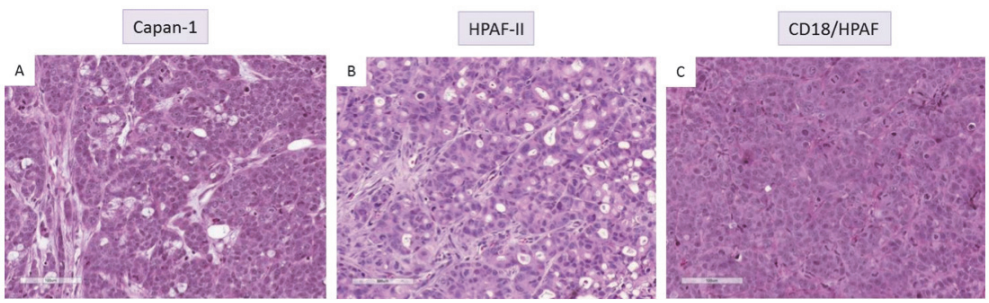

Figure 24. Representative histological examples. Capan-1 tumor (A), HPAF-II tumor (B), and CD18/HPAF tumor (C) (H&E staining). Original magnification 20x for all images.

MUC4 expression

Significant differences between the groups were detected by quantitative analysis of MUC4+ cells. The highest amount of MUC4+ cells was estimated in specimens

from Capan-1 xenografts (Kruskal-Wallis, p=0.002). The ratio between the variations in staining intensity was, however, proportionally distributed between Capan-1 and HPAF-II groups. No expression of MUC4 was identified in the xenografts derived from CD18/HPAF cells (Figures 25 and 26).

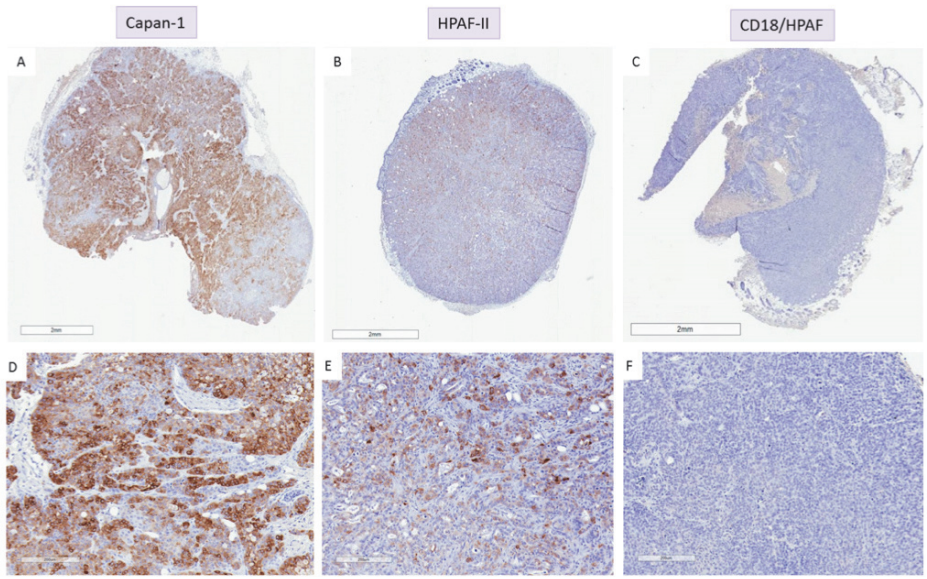

Figure 25. Representative examples of the surface MUC4 antigen expression in Capan-1 derived tumor (A, D), HPAF-II tumor (B, E), and CD18/HPAF tumor (C, F). Photographs were taken at 1x and 10x magnification.

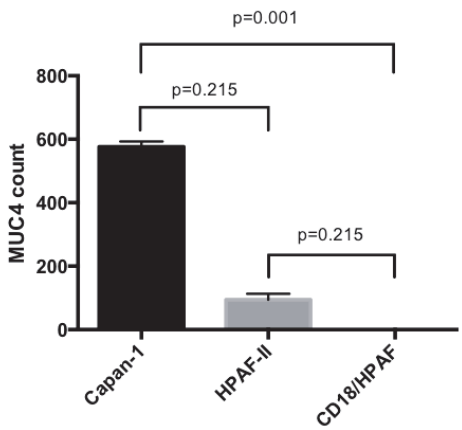

Figure 26. Capan-1 tumors have the highest MUC4 count. Kruskal-Wallis test, p=0.002; Dunn's post hoc, Capan-1 vs. CD18/HPAF (p=0.001), Capan-1 vs. HPAF-II (p=0.215), HPAF-II vs. CD18/HPAF (p=0.215). n=5 mice per group.

α-SMA expression and collagen accumulation

The extent of α-SMA or picro-sirius red staining differed between the groups. A significantly larger extent of α-SMA immunoreactivity, covering up to 38.80% of the tumor area, was uniformly distributed in all sections from Capan-1 xenografts (Kruskal-Wallis, p=0.018; Dunn's post hoc, Capan-1 vs. CD18/HPAF (p=0.027), Capan-1 vs. HPAF-II (p=1.000), HPAF-II vs. CD18/HPAF (p=0.071)). No variation in staining intensity was observed between the groups (Figure 27). The staining pattern of α-SMA and sirius red revealed a positive correlation with the grade of α-SMA expression and collagen accumulation in all groups (Figure 27).

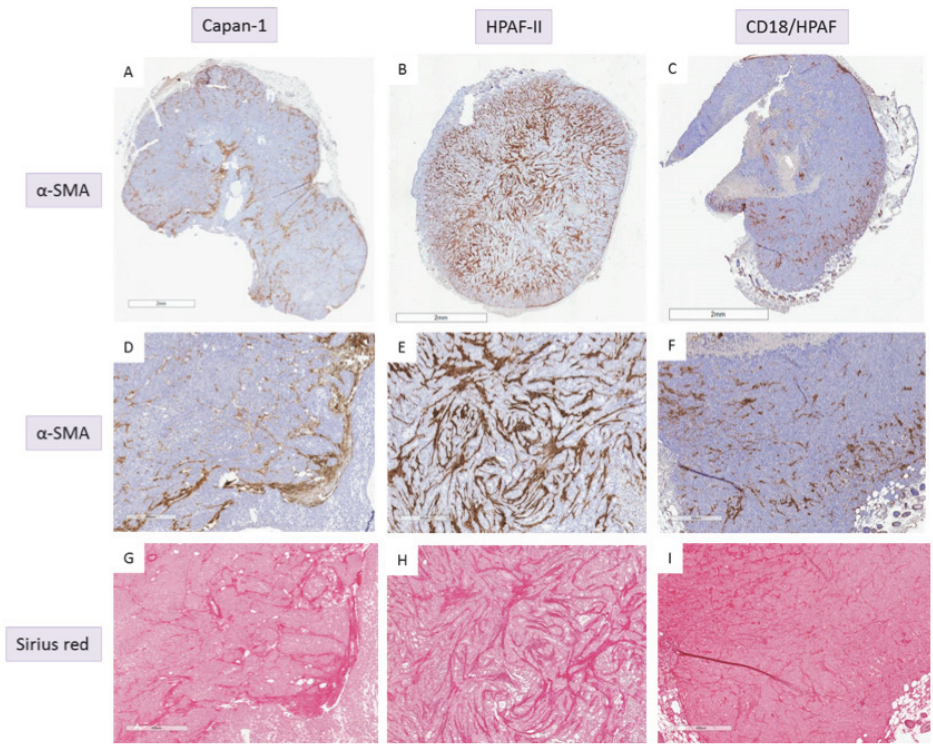

Figure 27. Representative examples of the α-SMA antigen expression (A-F) and sirius red staining (G-I) in Capan-1 tumor (A, D, G), HPAF-II tumor (B, E, H), and CD18/HPAF tumor (C, F, I). Photographs were taken at 1x and 10x magnification.

Study VI – Apicidin sensitizes pancreatic cancer cells to gemcitabine by epigenetically regulating MUC4 expression

Compound screening results

The ten compounds from the compound library screen yielding the highest growth inhibition are shown in Table 11.

Table 11. Top 10 most effective substances from the compound library screen. The data values represent percentage inhibition of proliferation compared to controls.

NAME	PLATE DESCRIPTION	COMPOUND DESCRIPTION	Capan-1 (MUC4+)		Panc-1 (MUC4-)	
			10 µM	0.5 µM	10 µM	0.5 µM
Apicidin	Epigenetics library	HDAC inhibitor	-76,5	-78,4	-49,5	-9,9
Trichostatin A	Epigenetics library	HDAC inhibitor	-43,7	-48,4	-39,7	0,7
Vorinostat (SAHA)	Epigenetics library	HDAC inhibitor	-23,6	-29,8	-19,2	15,8
Fenvalerate	Phosphatase inhibitor library	Calcineurin (PP2B)	-9,8	-11,9	-23,5	9,2
Fluoro-SAHA	Epigenetics library	HDAC inhibitor	-9,0	-15,7	-10,8	4,3
Scriptaid	Epigenetics library	HDAC inhibitor	-7,3	-15,1	-32,4	-12,9
Suramin·6Na	Epigenetics library	SIRT1 inhibitor	-6,3	-8,8	-3,1	5,1
Alexidine·2HCl	Phosphatase inhibitor library	PTPMT1	-6,3	-15,3	-97,9	-22,2
Cantharidic acid	Phosphatase inhibitor library	PP1 and PP2A	-4,8	-12,2	-33,6	-0,5
Valproic acid hydroxamate	Epigenetics library	HDAC inhibitor	-4,7	-7,2	-11,9	4,3

Apicidin (Figure 28) was found to reduce Capan-1 proliferation by 78%, a pharmacological effect that greatly exceed those of the other library members. Interestingly, the other the most effective compound, trichostatin A, was been reported in a previous study on colon cancer cells to induce inhibition of the transcription factor HNF4α, leading to down-regulation of its downstream target MUC4 [148]. On the other hand, apicidin induces a long-lasting hyperacetylation of histones H3 and H4 while that induced by trichostatin A is transient [181-183]. Given the superior antiproliferative activity of apicidin over trichostatin A, the former was further tested to discern its full inhibitory potential.

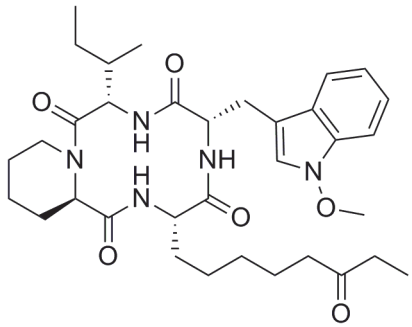

Figure 28. Cyclo-L-(2-amino-8-oxodecanoyl)-L-(N-methoxy-tryptophan)-L-isoleucyl-D-pipecolinyl, cyclo(N-O-methyl-L-tryptophanyl-L-isoleucinyl-D-pipecolinyl-L-2-amino-8-oxodecanoyl).

Dose-response to apicidin and gemcitabine at 24, 48, and 72 hours

As shown in Figure 29, both Capan-1 and Panc-1 cells responded to apicidin treatment after concentrations that exceeded 0.05 μM. The LD50 value for apicidin treatment at 72 hours was 5.17 μM in Capan-1 cells and 0.52 μM in Panc-1 cells. Capan-1 cells were resistant to gemcitabine treatment and the LD50 was not reached. The Panc-1 cells were more sensitive to gemcitabine treatment with an LD50 value of 50 μM at 72 hours.

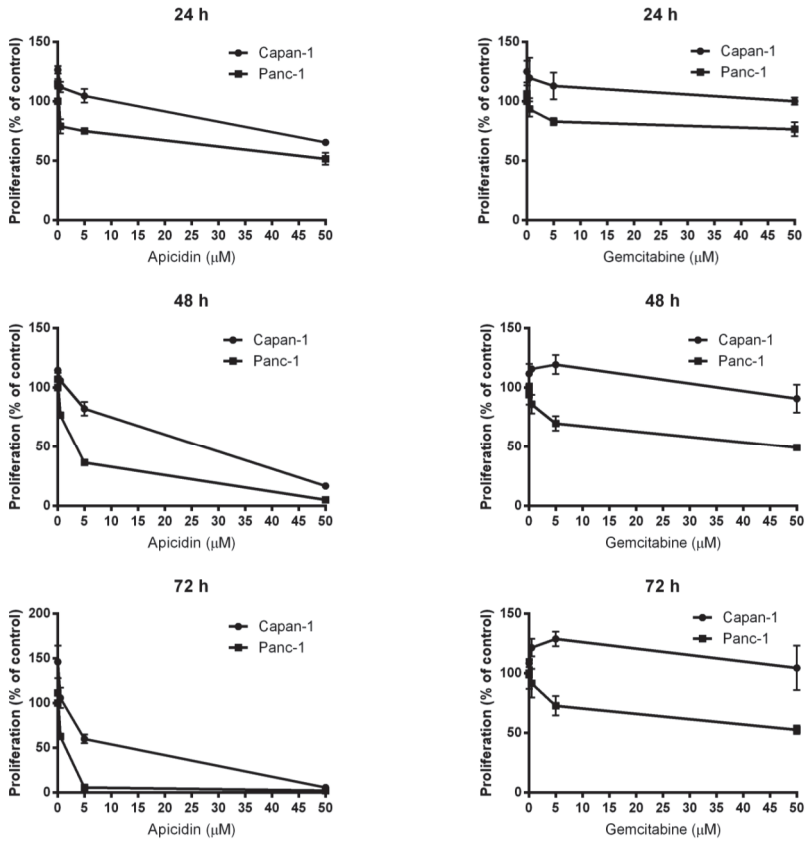

Figure 29. Dose response test results for apicidin and gemcitabine at 24, 48, and 72 hours.

Expression of MUC4 and HNF4α in untreated and treated Capan-1 cells

The protein expression analysis in Capan-1 cells showed that treated cells had significantly lower MUC4 expression compared to controls (ANOVA, $p<0.0001$). *Post-hoc* analyses revealed that MUC4 expression levels were significantly lower in all treatment groups compared to the control, as shown in Figure 30.

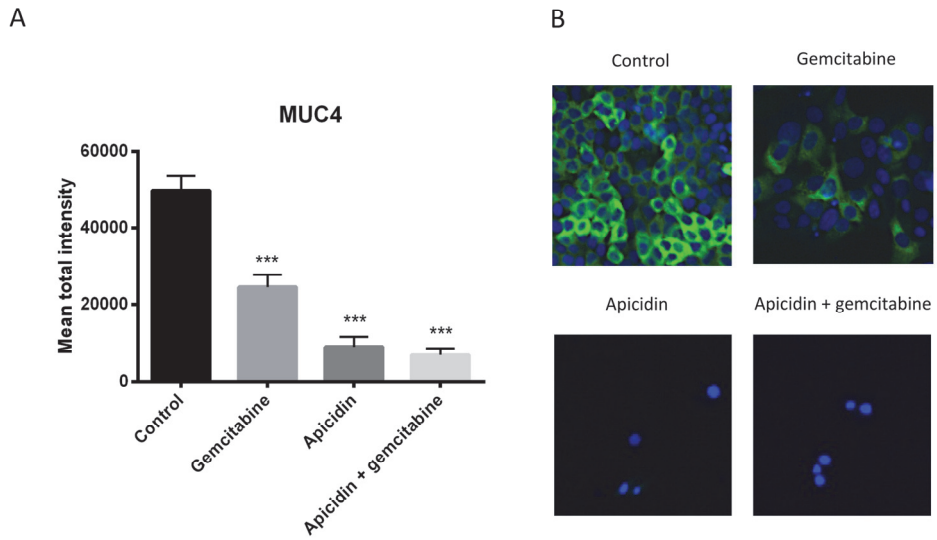

Figure 30. High content screening of MUC4 expression in control Capan-1 cells and after treatment with gemcitabine (5 μM), apicidin (0.05 μM), and gemcitabine plus apicidin. A: Mean MUC4 total intensity per cell. B: Immunofluorescence staining of MUC4. Original magnification 10x for all images. Significant differences at ***p<0.001 compared to the control group.

In addition, the levels of the transcription factor HNF4α were lower in treated cells (ANOVA, p=0.0026). *Post-hoc* analyses revealed that significance was reached only for cells treated with apicidin, and with apicidin plus gemcitabine treated cells, as shown in Figure 31. Expression of the transcription factors GATA6 and FOXA2 was undetectable in the nuclei of Capan-1 cells and these factors were not analyzed further.

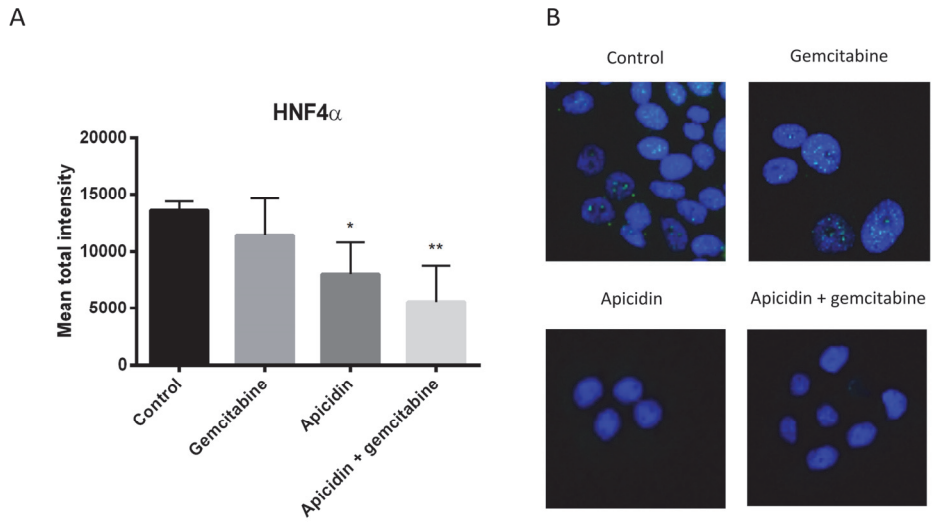

Figure 31. High content screening of hepatocyte nuclear factor 4α (HNF4α) expression in control Capan-1 cells and after treatment with gemcitabine (5 μM), apicidin (0.05 μM) and gemcitabine plus apicidin. A: Mean HNF4α total intensity per cell. B: Immunofluorescence staining of HNF4α. Original magnification 40x for all images. Significant differences at *p<0.05 and **p<0.01 compared to the control group.

Apicidin sensitizes Capan-1 cells to gemcitabine treatment

The lowest concentration of apicidin used in the dose-response study, 0.05 μM, which is a subtherapeutic dose, was chosen to investigate the effects of combination treatment with gemcitabine in chemoresistant Capan-1 cells. It was found that apicidin and gemcitabine synergistically inhibited proliferation of Capan-1 cells, as shown in Figure 32, compared to the drugs when used alone.

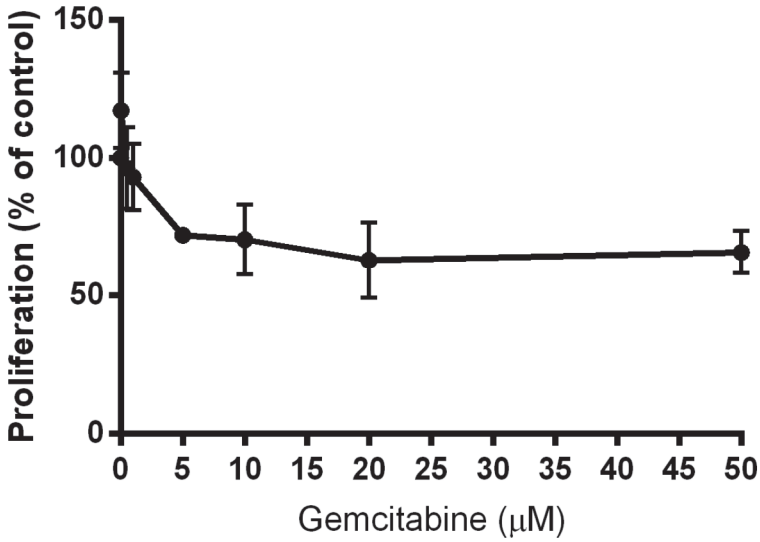

Figure 32. Effect of apicidin (0.05 μM) and gemcitabine (0.05-50 μM) combination treatment on Capan-1 cell proliferation after 72 h.

Chapter 5 General Discussion

Pancreatic cancer detection and treatment is hampered by the lack of accurate diagnostic biomarkers. To reduce the mortality of pancreatic cancer patients, detection of cancer at curable stages is the best approach at present. Patients with pancreatic cancer have a poor survival, even when they are fortunate enough to undergo resection of their tumor, but their cancers have different biological characteristics, and their survival is not uniform. Patient prognosis is currently estimated on the basis of the TNM staging system, which does not factor in prognostic determinants other than the T, N, and M stages. By integrating additional significant prognostic factors, a prognostic model can be developed to better assess an individual patient's survival. With technical advances and centralization of care, pancreatic surgery has become a safe procedure. However, the poor response rates of pancreatic cancer patients to current systemic treatment options indicate that more effective intervention measures need to be developed.

Early detection

In study I, we attempted a systematic approach for the discovery of pancreatic cancer biomarkers: (1) dedicated sample preparation in serum, (2) $HDMS^E$ for global protein expression profiling with label-free quantification using an internal standard, (3) hierarchical clustering and PCA, and (4) protein network analyses. In this feasibility study, we demonstrated that $HDMS^E$ can be used to discover biomarkers in sera from pancreatic cancer patients. The platform provides resolution in three dimensions and allows for high peak capacity analyses maximizing protein identification whilst retaining label-free quantification capabilities. Relative quantification analysis of the three conditions was performed using a label free approach. Hierarchical clustering and PCA of the data showed a clear differentiation between the pancreatic cancer and control phenotypes. Our study led to the identification of a 40-protein panel that distinguishes pancreatic cancer from benign and healthy controls. To better understand potential underlying mechanisms of importance in pancreatic cancer, a series of protein network analyses was performed using the differentially regulated proteins that were identified in the experiments. Among this protein set, examples of proteins whose abundance were found to be the increased in pancreatic cancer included BAZ2A,

CDK13, DAPK1, DST, EXOSC3, INHBE, KAT2B, KIF20B, SMC1B, and SPAG5. These proteins are intracellular proteins located in the cytoplasm or nucleus present at low concentrations in the blood stream, thus revealing the successful potential of our strategy to identify tissue-leakage proteins as candidate biomarkers. The interplay between these proteins and p53 indicate that they are promising biomarker candidates with a clear link to pancreatic cancer pathology [177-180].

Methodological considerations (I)

This was a prospective cohort study. The identified protein candidates warrant further investigation in independent sample sets to test their performance as early detection markers of pancreatic cancer, a work that is in progress. The recent advances in proteomic methods have enabled the systematic characterization of complex proteomes and identification of differentially expressed proteins in cells, tissue and biofluids. To find possible cancer biomarkers, great care must be taken to define the clinical application and to select relevant specimens for proteomic analysis [184]. When analyzing serum or plasma by proteomic methods there are several sources of variability that may occur. One of the most important factors leading to false discovery begins with the choice of adequate controls. Changes in inflammation and acute phase proteins often occur in malignant conditions including pancreatic cancer [185]. These changes may reflect the underlying chronic condition (e.g. chronic pancreatitis) in contrast to cancer-specific changes. Therefore nonspecific changes in serum or plasma need to be differentiated from potentially specific biomarkers. This is why, in addition to healthy control specimens, specimens from patients with chronic pancreatitis and other benign pancreatic diseases also were included to adequately identify disease-perturbed proteins.

Prognostic factors

In study II, we showed for the first time the application of ANNs for predicting survival in pancreatic cancer. The C-index was 0.79, indicating a good discriminatory power. Although the current TNM staging system continues to be the standard determinant of prognosis after resection for pancreatic cancer, the heterogeneity of tumor biology and patient characteristics results in significant variation of outcome within each staging category. Thus, incorporating other important prognostic variables in addition to the TNM classification might improve the prediction of outcomes. Several studies have investigated ANNs in the prediction of survival from other cancer types [108-110]. Many of these used

receiver operating characteristic curves to describe the accuracy and the discrimination for the different models. We used Harrell's C-index, which is similar to receiver operating characteristic analysis in the logistic model but appropriate for censored data. The C-index provides the probability that given 2 patients, one who will die before the other, the model will assign a higher probability of death to the former [101]. The C-index of previous ANN models for survival prediction in cancer has ranged from 0.66 to 0.81 [186-190]. Thus, in comparison with these studies, our ANN model had good predictive ability. Consistent with previous reports [81], we confirmed that lymph node metastasis, tumor differentiation, and margin status were correlated with outcome for patients undergoing resection for pancreatic cancer. BMI was also considered an important prognostic factor in the ANN. Recently, the beneficial impact of high BMI on the survival of patients undergoing pancreaticoduodenectomy for pancreatic cancer has been reported [191]. The median BMI at operation was 24.5 in the present study, with 39.5% being obese or overweight. The patients with a high BMI may have more physiologic reserve than lower BMI patients and may tolerate better the effects of surgical resection and other therapies [192]. In the present series, young patients had a tendency to have a worse prognosis than older patients. This has not been previously documented in the context of pancreatic cancer. However, in other types of cancer, clinical and biomarker data suggest that early-onset cancers may grow faster and be biologically more aggressive than late-onset cancers [193, 194]. Several mechanisms have been proposed concerning the role of inflammation in the development and progression of pancreatic cancer [195]. The presence of peritumoral inflammation was associated with a decrease in survival in our series. Other authors have also noted the prognostic value of histologic inflammation by using the ratio of Th2/Th1 tumor-infiltrating lymphoid cells [196]. Concerning the influence of preoperative comorbid conditions, we found that the ASA grade had a significant impact on the performance of the ANN model. In the future, biomarkers such as genes, microRNAs, or proteins can be incorporated into the ANN in order to increase its predictive ability.

Methodological considerations (II)

This was a retrospective cohort study. All the data were analyzed over a relatively long time frame, with potential changes in imaging and histopathological and treatment approaches over time. The adjuvant chemotherapy regimens were heterogeneous during the time period. There may also have been a selection bias as to which patients received adjuvant treatment [197]. This may explain why adjuvant chemotherapy was not included in either the ANN or the Cox regression model. The percentage of missing data per variable ranged from 0% to 12% in this study. We used multiple imputation techniques to substitute missing values. Data imputation has been shown to be superior to complete case analysis and the

missing indicator method in multivariable models [198]. ANNs have suffered difficulties with generalization, producing models that can overfit (‘‘overtrain’’) the data. To improve the generalization, an internal crossvalidation was performed; however, external validation would have been beneficial.

Treatment

The results from study III demonstrated that the transition from a low- to a high-volume center optimized the outcomes of pancreaticoduodenectomy. The relationship between hospital volume and mortality after pancreaticoduodenectomy has been known for many years. Previous studies have reported lower mortality rates at high-volume centers [15, 116-126]. Most data regarding centralization of pancreticoduodenectomy are derived from multi-institutional comparisons, and there is a lack of studies describing the effects of increased caseload of pancreaticoduodenectomy within the same unit. Furthermore, less is known regarding the effects of centralization on quality measures of pancreaticoduodenectomy such as operative blood loss, individual complications, and the need for reoperation. Between 2000 and 2012, our hospital caseload of pancreaticoduodenectomy increased by eightfold. The core staff of senior pancreatic surgeons was stable over time with four senior pancreatic surgeons during the first period and six senior pancreatic surgeons during periods 2 and 3. One senior pancreatic surgeon was recruited during the first period, otherwise the increase in core staff was managed by internal training. There was a tendency toward a decrease in mortality from 4% in the low-volume period to 0% in the high-volume period. Reduced need for reoperation and shorter length of stay in the high-volume period also suggest that centralization may be associated with less costs. Two main theories have been put forth to explain the volume–outcome relationship in surgery [199]. The “practice makes perfect” concept suggests that repetition increases the ability of surgeons and hospitals to perform a given procedure, which may be especially relevant when it comes to complex and high-risk operations. The underlying factors are multifactorial and include improved technical skill of the operating surgeon, more careful patient selection criteria, better postoperative and intensive care units, and improved multidisciplinary care. The “selective referral” concept suggests that centers that have good outcomes receive more referrals leading to higher volumes. However, this concept requires that referring doctors and their patients can choose hospital, but in Sweden, which has a mainly government-funded health care system, this is rarely the case.

Switching the emphasis from large to small, it has been found that mucins are overall increasingly being recognized for their role in the therapy of pancreatic cancer due to their aberrant expression [200]. In study IV, we showed that both

primary pancreatic tumors and matched metastatic lymph nodes display MUC4 expression. Although three cases showed discordance, in general, a similar pattern of MUC4 expression was observed in the primary and matched metastatic lesions, using either categorical or continuous scoring. Patients who expressed MUC4 in the primary tumor also expressed MUC4 in the lymph node metastases, indicating that MUC4 is retained during metastatic progression. Upregulation of MUC4 is a common feature of pancreatic cancer and according to a recent study MUC4 is expressed in a high percentage of early pancreatic intraepithelial neoplasia and metastatic disease, while silenced in the normal pancreas [201]. In experimental studies, it has been shown that MUC4-positive pancreatic cancer cells metastasize more often than MUC4-negative cells [154]. Induction of epithelial-mesenchymal transition (EMT) together with facilitated cell cycle progression and reduced apoptosis are some of the proposed mechanisms that drive the MUC4-associated metastatic process in pancreatic cancer. MUC4 induces EMT and metastasis in pancreatic cancer cells through FAK activation by acting as an intramembrane ligand for receptor tyrosine kinases such as HER2 [156, 157, 202]. This causes downstream activation of MKK7, JNK1/2, and c-Jun leading to upregulation of N-cadherin. The upregulation of N-cadherin induces the EMT process but also increased cell invasion through ERK and MMP9 and reduced apoptosis and increased cell mobility through Akt [202]. The unchanged expression pattern of membrane proteins has been demonstrated in several other studies when comparing primary pancreatic cancer and metastatic sites [203, 204]. The assertion that pancreatic tumors maintain MUC4 expression also during metastatic spread, points to the role of MUC4 as a potential therapeutic target also for pancreatic cancer cell dissemination.

In study V, we generated subcutaneous pancreatic tumors in mice by inoculation of cells from MUC4 expressing human pancreatic cancer cell lines, Capan-1, HPAF-II, or CD18/HPAF. It is important that the *in vivo* model exhibits characteristics translatable to the human pathological scenario of pancreatic cancer with respect to parameters intended to study. Transplanted MUC4+ tumor cells created well-defined tumor nodules with a similar growth pattern in immunodeficient mouse. Morphologically, the tumor xenografts in general consisted of poorly differentiated epithelial-like formations surrounded by a more or less pronounced fibrotic tissue stroma and could therefore represent an experimental tool to recapitulate conditions found clinically in pancreatic cancer. MUC4 expression, however, was only detected in Capan-1 and HPAF-II xenografts. These results are indicating that the MUC4 expression is maintained through the in vivo tumor progression process, which is in agreement with and mimics the clinical scenario. Even though the amount of labeled MUC4 antigen expressed in both in vivo models well reflects the human situation, the MUC4 expression in xenografts derived from Capan-1 cells was supreme. Desmoplastic reaction, which is one of the representative histological findings in pancreatic

cancer, was present in all tumors to various degrees. Based on the α-SMA staining analysis of tissue specimens, we speculated that local host dermal fibroblasts became activated in response to mechanical tension [205] caused by the growing xenograft, acquiring contractile stress fibers and adopting the migratory myofibroblast-like phenotype [206], which enabled the activated fibroblasts to invade the tumor. De novo expression of α-SMA together with the characteristic spindle shaped morphology is commonly used for identification of cancer associated fibroblasts (CAFs) [207]. CAFs represent a source of various types of factors and mediators enhancing the tumor progression, including extracellular matrix components, such as various types of collagen. CAFs are thought to be responsible for the dense stroma production, which is one of the hallmarks for pancreatic adenocarcinoma [207-210]. These findings indicate that xenograft tumors are self-sufficient in creating a favorable microenvironment for further tumor progression, i.e. in agreement with the clinical situation [211, 212].

In study VI, we screened a combined epigenetics and phosphatase small-molecule inhibitor library to discover substances that might epigenetically modify MUC4 expression. The compounds in this collection are involved in epigenetic regulation of chromatin such as lysine-modifying enzymes and DNA methylation inhibitors, which in turn have been shown to alter gene expression. Our findings indicate that the HDAC inhibitor apicidin has potent antitumor activity against pancreatic cancer cells, which has not been demonstrated previously. Moreover, we discovered that subtherapeutic levels of apicidin significantly down-regulated MUC4 expression and sensitized pancreatic cancer cells to gemcitabine treatment.

HDAC inhibitors can affect gene expression by either down- or up-regulation of target genes. Although it is counterintuitive for HDAC inhibitors to repress gene transcription, this phenomenon is frequently observed and may result from the acetylation of histones that are normally unacetylated, resulting in blockage of the necessary transcription machinery; alternatively, hyperacetylation may result in the transcription of a regulatory factor that negatively regulates gene transcription [148]. The MUC4 gene is controlled at the transcriptional level by HNFs, FOXA, GATA, and caudal-related homeobox in a cell type-specific manner [213]. In a previous study, it was found that HDAC inhibitors affect HNF4α expression in colonic cancer cell lines. Specifically, trichostatin A was found to inhibit binding of SP1 to the *HNF4α* promoter, an epigenetic cascade that directly suppresses HNF4α expression, which in turn down-regulates the expression of the MUC4 protein and concomitantly reduces cancer cell proliferation [148]. As apicidin also functions through the SP1-binding site [214], this indicates that apicidin and trichostatin A may affect MUC4 expression in a similar manner.

Gemcitabine resistance in pancreatic cancer is related to several mechanisms, including alteration of apoptosis-regulating genes, low expression of nucleoside transporters, and reduced levels of metabolic enzymes [215]. Previous studies have shown that MUC4 protects pancreatic cancer cells against gemcitabine-

induced apoptosis through the activation of anti-apoptotic pathway MUC4-HER2-ERK [31]. Other mechanisms of pancreatic cancer cell resistance to gemcitabine that are linked to MUC4 have been proposed and include involvement of the NF-κB pathway that leads to modulation of apoptosis and the regulation of hCNT1 [32]. Moreover, it has been reported that silencing of the *MUC4* gene in pancreatic cancer cells increases sensitivity to gemcitabine treatment [31-33]. These findings suggest that MUC4 plays an important role in the biological properties of pancreatic cancer cells and that repressing MUC4 expression may be one way to potentiate existing therapy or develop new treatments for pancreatic cancer.

Methodological considerations (III-VI)

Study III was a retrospective cohort study. The strength of this study was that volume groups were compared within the same surgical unit. This design eliminates several biased variables affecting interhospital comparisons. We also provided a detailed analysis of individual patient characteristics and clinical course, which most of the previous volume–outcome studies lack as they are based on administrative data and not medical records. It has been shown that other variables besides volume such as age, male gender, and comorbidity are positive predictors of complications and death following pancreaticoduodenectomy [216, 217]. However, these factors were similar across volume groups in this study.

Study IV was also a retrospective cohort study. Full-face sections of metastatic lesions in pancreatic cancer are few in the clinical setting. The matched primary and metastatic lesions used in this study, although few in number, represent a valuable source for the study of biomarker expression during pancreatic cancer progression. The population was of sufficient size to observe trends and tendencies regarding MUC4 expression in humans, although further investigations, with more cases, are needed to confirm these findings.

Study V was an experimental in vivo study. In order to evaluate the potential of MUC4 as an adequate therapeutic target as well as investigate novel MUC4-directed therapies, biologically relevant preclinical models are necessary. The standard method for generating human solid tumors in mice is by inoculation of cancer cells. A concern has been raised, that this approach might lead to exclusion of the unique tumor desmoplasia, which is a characteristic feature of the majority of pancreatic cancers. Our results show that a biologically relevant preclinical model of pancreatic cancer can be developed with the characteristic desmoplastic microenvironment, expressing MUC4 with a comparable intensity as the human counterpart.

Study VI was an experimental in vitro study. We identified the HDAC inhibitor apicidin, which markedly inhibits the growth of pancreatic cancer cells and down-regulates MUC4 expression, an effect mediated by HNF4α. Although we did not

test the toxicity of apicidin in normal cells, previous data indicate that normal cells, e.g. endometrial or colonic cells, are viable after the treatment with the same doses of apicidin that induce growth inhibition of cancer cells [181, 218]. Following these initial very promising in vitro data, we are planning to use apicidin in the Capan-1 in vivo model presented within this thesis in order to evaluate biodistribution, safety, and anti-tumor activity.

Chapter 6 Conclusions

The major conclusions reached in the studies included in this thesis were:

I. 134 differentially expressed serum proteins were identified between resectable pancreatic cancer, benign pancreatic disease and healthy controls, of which 40 proteins showed a significant up-regulation in the pancreatic cancer group. 10 protein candidates were linked to the tumor suppressor p53 by protein network analyses. These protein candidates may provide new avenues of research for a non-invasive blood based diagnosis of pancreatic cancer.

II. A model for survival prediction in resectable pancreatic cancer with artificial neural networks was developed, identifying 7 risk factors, and showed high accuracy. This model could be used in the future to inform clinical decision-making.

III. The transition from a low- to a high-volume center optimized the outcome for patients undergoing pancreaticoduodenectomy. Operative duration, blood loss, hemorrhagic complications, reoperations and length of stay decreased after the transition to a high-volume center. There was a tendency toward reduced operative mortality reaching 0% in the more than 100 pancreaticoduodenectomies performed in the high-volume period.

IV. MUC4 positivity was detected in most primary pancreatic cancers and matched metastatic lymph nodes with a high level of concordance. This suggests that MUC4 expression is retained during pancreatic cancer progression and that MUC4 expression could serve as target also for pancreatic cancer cell dissemination.

V. The Capan-1 pancreatic cancer xenograft tumor model in immunodeficient mice is suitable for the study of MUC4-directed therapy in the experimental setting.

VI. Apicidin sensitizes Capan-1 pancreatic cancer cells to gemcitabine by epigenetic regulation of MUC4 expression.

Future Perspectives

Pancreatic research today carries many challenges, but also presents great opportunities to improve outcomes for the patients.

The present thesis provides a novel serum-based diagnostic tool for pancreatic cancer detection, which may be our most important result. A validation study is ongoing to investigate if pre-diagnostic levels of the identified protein candidates are associated with subsequent pancreatic cancer risk. From a large cohort of subjects that have participated in a health screening program in Malmö, Sweden, we have obtained serum samples from pancreatic cancer cases that were collected 1-5 years prior to cancer diagnosis. These cases are matched to 2 healthy controls each. Preferably, our protein candidates will be evaluated using multiple reaction monitoring allowing for targeted protein assay development. In the future, the increased knowledge of non-inherited and inherited risk factors for pancreatic cancer may allow more targeted screening on an individual basis in asymptomatic patients.

As shown in the studies, a prognostic stratification of pancreatic cancer patients is possible. An external cohort would be desirable to further develop this model and validate the findings. It would also be interesting to include new variables in the ANN model to increase its predictive ability. The ANN may in the future also become a tool that could aid in the diagnostic setting especially when integrating clinical and biomarker data.

The centralization of pancreatic surgery has been successful in southern Sweden with operative mortality close to 0%. This implies that patients should continue to be directed to regional centers. It also indicates that surgery alone is not enough to improve the prognosis of pancreatic cancer patients given the poor long-term survival.

The fact that we do not have any effective systemic treatment for pancreatic cancer is challenging and demands translational research in order to link clinical and

experimental findings. When developing individualized treatment, potential drug targets need to be stable in metastatic disease in order to effectively target the disseminated cancer cell population. The ability of HDAC inhibitors such as apicidin to selectively inhibit growth of tumor cells have made them promising anticancer drugs, particularly given their ability to be combined with other agents. Apicidin may thus prove clinically useful as a novel therapy for pancreatic tumors, which express high levels of MUC4 and show resistance to gemcitabine or other anticancer agents, either as a sensitizing agent or as monotherapy.

Acknowledgements

The completion of this thesis would not have been possible without the support of colleagues, friends, and family. I would like to express my sincere gratitude to the following people:

Roland Andersson, Professor of Surgery, main supervisor, for supporting my interest in surgery and associated research. His experience and wide knowledge of clinical and experimental pancreatology coupled with dedication, enthusiasm, visionary thinking, and timely advice, have been of great benefit when writing this thesis. I will always cherish his belief and trust in me.

Bodil Andersson, Associate Professor of Surgery, co-supervisor, for help and guidance since my start in pancreatic cancer research, and for excellent support when building the local pancreatic biobank.

György Marko-Varga, Professor of Clinical Protein Science and Imaging, co-supervisor, for introducing me to the field of mass spectrometry and for sharing his vast knowledge of biomarker research.

Johan Nilsson, Associate Professor of Cardiothoracic Surgery, for excellent collaboration in the ANN study. His expertise in machine learning algorithms has been a great asset and I look forward to future projects.

Monika Posaric Bauden, researcher, for important technical and intellectual contributions to the experimental studies.

Katarzyna Said Hilmersson, laboratory engineer, for support when performing the in vitro studies and for collecting the serum samples used in the protein deep sequencing study.

Bobby Tingstedt, Associate Professor of Surgery, for valuable contributions to the clinical papers.

Gert Lindell, Associate Professor of Surgery, Head of the Section of Hepato-Pancreato-Biliary Surgery, for sharing his knowledge and experience in pancreatic surgery, and for his continuous encouragement.

Caroline Williamsson, pancreatic surgeon, for support with the classification and grading of postoperative complications after pancreaticoduodenectomy.

Sara Regnér, Associate Professor of Surgery, for help with the inclusion of patients from Malmö in the ANN study. Her extensive knowledge of pancreatic diseases was much appreciated when interpreting the results.

Agata Sasor, consultant pancreatic pathologist, for classifying the biobank samples and for providing images of H&E-stained tissues shown in this thesis.

Charlotte Welinder, Associate Professor of Experimental Oncology, for teaching me the sample preparation steps used in the protein deep sequencing study.

Joanne B. Connolly, PhD, Waters Corporation, for support with the HDMS^{E} data analyses and interpretations.

Fredrik Ek, PhD, and Roger Olsson, Professor of Medicinal Chemistry, for excellent ideas and for providing access to the small molecule library.

Anna Hammarberg, PhD, for technical support when performing the HCS analyses.

Monica Keidser, research administrator, for assistance in processing manuscripts and applications.

Marie-Louise Pendse, research nurse, for maintaining our pancreatic registry.

Peter Svensson, Professor, and his staff, including Pia Johansson and Åsa Andersson, for providing continuous support and also dedicated research time during my clinical training that allowed me to complete this thesis.

Colleagues and friends in the laboratory, including Carlos Urey, Chinmay Gundewar, Emelie Karnevie, Yutaka Sugihara, Toshihide Nishimura, Melinda Rezeli, Thomas Fehniger, and Roger Appelqvist, for their support and friendship.

Furthermore, I would like to thank Folke Johnsson, Associate Professor of Surgery, Chief of the Surgical Department, and Tobias Axmarker, specialist surgeon, for offering me the opportunity to work as a surgeon at Skåne University Hospital. I also thank my colleagues Magnus Bergenfeldt, Christian Sturesson, Jenny Rystedt, Peter Strandberg Holka, Karolin Isaksson, and Daniel Åkerberg, for their encouragement and for sharing their vast knowledge and expertise in general surgery. My thanks are also due to Inger Keussen and Wojciech Cwikiel, at the Department of Radiology, for their help and support.

Finally, I would like to thank my mother, father, and brother. I love you.

References

1. Morgagni GB. De sedibus, et causis morborum per anatomen indagatis libri quinque. Venetiis: Typog Remondiniana; 1761.
2. Da Costa JM. On the morbid anatomy and symptoms of cancer of the pancreas. Philadelphia: J. B. Lippincott & Company; 1858.
3. Codivilla A. Rendiconto statistico della sezione chirurgica dell'ospedale di Imola. 1898.
4. Halsted WS. Contributions to the surgery of the bile passages, especially of the common bile-duct. Boston Med Surg J 1899;141:645–54.
5. Kocher T. Mobilisierung des duodenum und gastroduodenostomie. Zentralbl Chir 1903;30:33-8.
6. Kausch W. Das carcinom der papilla duodeni und seine radikale entfernung. Beitr Klin Chir 1912;78:439–86.
7. Hirschel G. Die resektion des duodenums mit der papille wegen karzinoms. Munch Med Wochenschr 1914;61:1728–9.
8. Whipple AO, Parsons WB, Mullins CR. Treatment of carcinoma of the ampulla of vater. Ann Surg 1935;102:763-79.
9. Whipple AO. Observations on radical surgery for lesions of the pancreas. Surg Gynecol Obstet 1946;82:623-31.
10. Whipple AO. A reminiscence: pancreaticduodenectomy. Rev Surg 1963;20:221-5.
11. Brunschwig A. Resection of the head of pancreas and duodenum for carcinoma - pancreatoduodenectomy. Surg Gynecol Obstet 1937;65:681-4.
12. Cameron JL, Riall TS, Coleman J, Belcher KA. One thousand consecutive pancreaticoduodenectomies. Ann Surg 2006;244:10-5.
13. Fernandez-del Castillo C, Morales-Oyarvide V, McGrath D, Wargo JA, Ferrone CR, Thayer SP, et al. Evolution of the Whipple procedure at the Massachusetts General Hospital. Surgery 2012;152:S56-63.

14. Yeo CJ, Cameron JL, Sohn TA, Lillemoe KD, Pitt HA, Talamini MA, et al. Six hundred fifty consecutive pancreaticoduodenectomies in the 1990s: pathology, complications, and outcomes. Ann Surg 1997;226:248-57; discussion 57-60.

15. Yoshioka R, Yasunaga H, Hasegawa K, Horiguchi H, Fushimi K, Aoki T, et al. Impact of hospital volume on hospital mortality, length of stay and total costs after pancreaticoduodenectomy. Br J Surg 2014;101:523-9.

16. Howard TJ, Krug JE, Yu J, Zyromski NJ, Schmidt CM, Jacobson LE, et al. A margin-negative R0 resection accomplished with minimal postoperative complications is the surgeon's contribution to long-term survival in pancreatic cancer. J Gastrointest Surg 2006;10:1338-45; discussion 45-6.

17. Wray CJ, Ahmad SA, Matthews JB, Lowy AM. Surgery for pancreatic cancer: recent controversies and current practice. Gastroenterology 2005;128:1626-41.

18. Vincent A, Herman J, Schulick R, Hruban RH, Goggins M. Pancreatic cancer. Lancet 2011;378:607-20.

19. Moertel CG, Childs DS, Jr., Reitemeier RJ, Colby MY, Jr., Holbrook MA. Combined 5-fluorouracil and supervoltage radiation therapy of locally unresectable gastrointestinal cancer. Lancet 1969;2:865-7.

20. Burris HA, 3rd, Moore MJ, Andersen J, Green MR, Rothenberg ML, Modiano MR, et al. Improvements in survival and clinical benefit with gemcitabine as first-line therapy for patients with advanced pancreas cancer: a randomized trial. J Clin Oncol 1997;15:2403-13.

21. Conroy T, Desseigne F, Ychou M, Bouche O, Guimbaud R, Becouarn Y, et al. FOLFIRINOX versus gemcitabine for metastatic pancreatic cancer. N Engl J Med 2011;364:1817-25.

22. Von Hoff DD, Ervin T, Arena FP, Chiorean EG, Infante J, Moore M, et al. Increased survival in pancreatic cancer with nab-paclitaxel plus gemcitabine. N Engl J Med 2013;369:1691-703.

23. Ma J, Siegel R, Jemal A. Pancreatic cancer death rates by race among US men and women, 1970-2009. J Natl Cancer Inst 2013;105:1694-700.

24. Rahib L, Smith BD, Aizenberg R, Rosenzweig AB, Fleshman JM, Matrisian LM. Projecting cancer incidence and deaths to 2030: the unexpected burden of thyroid, liver, and pancreas cancers in the United States. Cancer Res 2014;74:2913-21.

25. Simard EP, Ward EM, Siegel R, Jemal A. Cancers with increasing incidence trends in the United States: 1999 through 2008. CA Cancer J Clin 2012.

26. Ma J, Jemal A. The rise and fall of cancer mortality in the USA: why does pancreatic cancer not follow the trend? Future Oncol 2013;9:917-9.

27. Cardin DB, Berlin JD. Pancreas cancer on the rise: are we up to the challenge? J Natl Cancer Inst 2013;105:1675-6.

28. Siegel R, Ma J, Zou Z, Jemal A. Cancer statistics, 2014. CA Cancer J Clin 2014;64:9-29.

29. Schniewind B, Christgen M, Kurdow R, Haye S, Kremer B, Kalthoff H, et al. Resistance of pancreatic cancer to gemcitabine treatment is dependent on mitochondria-mediated apoptosis. Int J Cancer 2004;109:182-8.

30. Andersson R, Aho U, Nilsson BI, Peters GJ, Pastor-Anglada M, Rasch W, et al. Gemcitabine chemoresistance in pancreatic cancer: molecular mechanisms and potential solutions. Scand J Gastroenterol 2009;44:782-6.

31. Bafna S, Kaur S, Momi N, Batra SK. Pancreatic cancer cells resistance to gemcitabine: the role of MUC4 mucin. Br J Cancer 2009;101:1155-61.

32. Skrypek N, Duchene B, Hebbar M, Leteurtre E, van Seuningen I, Jonckheere N. The MUC4 mucin mediates gemcitabine resistance of human pancreatic cancer cells via the Concentrative Nucleoside Transporter family. Oncogene 2013;32:1714-23.

33. Wissniowski TT, Meister S, Hahn EG, Kalden JR, Voll R, Ocker M. Mucin production determines sensitivity to bortezomib and gemcitabine in pancreatic cancer cells. Int J Oncol 2012;40:1581-9.

34. Fisher W, Andersen D, Bell Jr R, Saluja A, Brunicardi F. Pancreas. In: Brunicardi F, Andersen D, Billiar T, Dunn D, Hunter J, Matthews J, et al., editors. Schwartz's principles of surgery. 9th ed. New York: McGraw-Hill; 2009.

35. Isaji S, Kawarada Y, Uemoto S. Classification of pancreatic cancer: comparison of Japanese and UICC classifications. Pancreas 2004;28:231-4.

36. Bockman DE. Anatomy and fine structure. In: Beger HG, Warshaw AL, Büchler MW, Kozarek RA, Lerch MM, Neoptolemos JP, et al., editors. The pancreas: an integrated textbook of basic science, medicine, and surgery. 2nd ed. Malden: Wiley-Blackwell; 2008.

37. Sherwood L. The digestive system. 8th ed. Belmont: Cengage Learning; 2010.

38. Andersson B. Acute pancreatitis - severity classification, complications and outcome [Dissertation]. Lund: Lund University; 2010.

39. Poruk KE, Firpo MA, Adler DG, Mulvihill SJ. Screening for pancreatic cancer: why, how, and who? Ann Surg 2013;257:17-26.

40. Tingstedt B, Weitkamper C, Andersson R. Early onset pancreatic cancer: a controlled trial. Ann Gastroenterol 2011;24:206-12.

41. Aho U, Zhao X, Lohr M, Andersson R. Molecular mechanisms of pancreatic cancer and potential targets of treatment. Scand J Gastroenterol 2007;42:279-96.

42. Klöppel G, Hruban RH, Longnecker DS, Adler G, Kern SE, Partanen TJ. Ductal adenocarcinoma of the pancreas. In: Hamilton SR, Aaltonen LA, editors. World health organization classification of tumours, pathology and genetics of tumours of the digestive system. Lyon: IARC Press; 2000.

43. Zhu Z, Friess H, diMola FF, Zimmermann A, Graber HU, Korc M, et al. Nerve growth factor expression correlates with perineural invasion and pain in human pancreatic cancer. J Clin Oncol 1999;17:2419-28.

44. Bartosch-Härlid A, Andersson R. Cachexia in pancreatic cancer - mechanisms and potential intervention. e-SPEN Journal 2009;4:e337-e43.

45. Bartosch-Harlid A, Andersson R. Diabetes mellitus in pancreatic cancer and the need for diagnosis of asymptomatic disease. Pancreatology 2010;10:423-8.

46. Hidalgo M. Pancreatic cancer. N Engl J Med 2010;362:1605-17.

47. Carney CP, Jones L, Woolson RF, Noyes R, Jr., Doebbeling BN. Relationship between depression and pancreatic cancer in the general population. Psychosom Med 2003;65:884-8.

48. Smith EB. Carcinoma of the pancreas--early diagnostic presumptive signs. J Natl Med Assoc 1974;66:496-8.

49. Kennedy EP, Yeo CJ. Pancreatic cancer: clinical aspects, assessment, and management. In: Jarnagin WR, editor. Blumgart's surgery of the liver, pancreas and biliary tract (Volume 1). 5th ed. Philadelphia: Elsevier Saunders; 2012.

50. Khorana AA, Fine RL. Pancreatic cancer and thromboembolic disease. Lancet Oncol 2004;5:655-63.

51. Miura F, Takada T, Amano H, Yoshida M, Furui S, Takeshita K. Diagnosis of pancreatic cancer. HPB (Oxford) 2006;8:337-42.

52. Andersson R, Vagianos CE, Williamson RC. Preoperative staging and evaluation of resectability in pancreatic ductal adenocarcinoma. HPB (Oxford) 2004;6:5-12.

53. Yachida S, Jones S, Bozic I, Antal T, Leary R, Fu B, et al. Distant metastasis occurs late during the genetic evolution of pancreatic cancer. Nature 2010;467:1114-7.

54. Glenn J, Steinberg WM, Kurtzman SH, Steinberg SM, Sindelar WF. Evaluation of the utility of a radioimmunoassay for serum CA 19-9 levels in patients before and after treatment of carcinoma of the pancreas. J Clin Oncol 1988;6:462-8.

55. Goonetilleke KS, Siriwardena AK. Systematic review of carbohydrate antigen (CA 19-9) as a biochemical marker in the diagnosis of pancreatic cancer. Eur J Surg Oncol 2007;33:266-70.

56. Bosman FT, Carneiro F, Hruban RH, Theise ND, editors. World Health Organization classification of tumours of the digestive system. Lyon: IARC Press; 2010.

57. Kim CG, Jo S, Kim JS. Impact of surgical volume on nationwide hospital mortality after pancreaticoduodenectomy. World J Gastroenterol 2012;18:4175-81.

58. Goggins M. Development of novel pancreatic tumor biomarkers. In: Neoptolemos J, Urrutia R, Abbruzzese J, Büchler MW, editors. Pancreatic cancer. 1st ed. New York: Springer; 2010.

59. Anderson NL, Anderson NG. The human plasma proteome: history, character, and diagnostic prospects. Mol Cell Proteomics 2002;1:845-67.

60. Aebersold R, Mann M. Mass spectrometry-based proteomics. Nature 2003;422:198-207.

61. Tessitore A, Gaggiano A, Cicciarelli G, Verzella D, Capece D, Fischietti M, et al. Serum biomarkers identification by mass spectrometry in high-mortality tumors. Int J Proteomics 2013;2013:125858.

62. Langley SR, Dwyer J, Drozdov I, Yin X, Mayr M. Proteomics: from single molecules to biological pathways. Cardiovasc Res 2013;97:612-22.

63. Domon B, Aebersold R. Options and considerations when selecting a quantitative proteomics strategy. Nat Biotechnol 2010;28:710-21.

64. Kim MS, Pinto SM, Getnet D, Nirujogi RS, Manda SS, Chaerkady R, et al. A draft map of the human proteome. Nature 2014;509:575-81.

65. Wilhelm M, Schlegl J, Hahne H, Moghaddas Gholami A, Lieberenz M, Savitski MM, et al. Mass-spectrometry-based draft of the human proteome. Nature 2014;509:582-7.

66. Ansari D, Aronsson L, Sasor A, Welinder C, Rezeli M, Marko-Varga G, et al. The role of quantitative mass spectrometry in the discovery of pancreatic cancer biomarkers for translational science. J Transl Med 2014;12:87.

67. Bond NJ, Shliaha PV, Lilley KS, Gatto L. Improving qualitative and quantitative performance for MS(E)-based label-free proteomics. J Proteome Res 2013;12:2340-53.

68. Karmazanovsky G, Fedorov V, Kubyshkin V, Kotchatkov A. Pancreatic head cancer: accuracy of CT in determination of resectability. Abdom Imaging 2005;30:488-500.

69. Tempero MA, Arnoletti JP, Behrman SW, Ben-Josef E, Benson AB, 3rd, Casper ES, et al. Pancreatic Adenocarcinoma, version 2.2012: featured updates to the NCCN Guidelines. J Natl Compr Canc Netw 2012;10:703-13.

70. Ansari D, Keussen I, Andersson R. Positron emission tomography in malignancies of the liver, pancreas and biliary tract - indications and potential pitfalls. Scand J Gastroenterol 2013;48:259-65.

71. Cooper AB, Tzeng CW, Katz MH. Treatment of borderline resectable pancreatic cancer. Curr Treat Options Oncol 2013;14:293-310.

72. Wagner M, Redaelli C, Lietz M, Seiler CA, Friess H, Buchler MW. Curative resection is the single most important factor determining outcome in patients with pancreatic adenocarcinoma. Br J Surg 2004;91:586-94.

73. Winter JM, Cameron JL, Campbell KA, Arnold MA, Chang DC, Coleman J, et al. 1423 pancreaticoduodenectomies for pancreatic cancer: A single-institution experience. J Gastrointest Surg 2006;10:1199-210; discussion 210-1.

74. Richter A, Niedergethmann M, Sturm JW, Lorenz D, Post S, Trede M. Long-term results of partial pancreaticoduodenectomy for ductal adenocarcinoma of the pancreatic head: 25-year experience. World J Surg 2003;27:324-9.

75. Cameron JL, Crist DW, Sitzmann JV, Hruban RH, Boitnott JK, Seidler AJ, et al. Factors influencing survival after pancreaticoduodenectomy for pancreatic cancer. Am J Surg 1991;161:120-4; discussion 4-5.

76. Franko J, Hugec V, Lopes TL, Goldman CD. Survival among pancreaticoduodenectomy patients treated for pancreatic head cancer <1 or 2 cm. Ann Surg Oncol 2013;20:357-61.

77. Kuhlmann KF, de Castro SM, Wesseling JG, ten Kate FJ, Offerhaus GJ, Busch OR, et al. Surgical treatment of pancreatic adenocarcinoma; actual survival and prognostic factors in 343 patients. Eur J Cancer 2004;40:549-58.

78. Lim JE, Chien MW, Earle CC. Prognostic factors following curative resection for pancreatic adenocarcinoma: a population-based, linked database analysis of 396 patients. Ann Surg 2003;237:74-85.

79. Moon HJ, An JY, Heo JS, Choi SH, Joh JW, Kim YI. Predicting survival after surgical resection for pancreatic ductal adenocarcinoma. Pancreas 2006;32:37-43.

80. Sohn TA, Yeo CJ, Cameron JL, Koniaris L, Kaushal S, Abrams RA, et al. Resected adenocarcinoma of the pancreas-616 patients: results, outcomes, and prognostic indicators. J Gastrointest Surg 2000;4:567-79.

81. Garcea G, Dennison AR, Pattenden CJ, Neal CP, Sutton CD, Berry DP. Survival following curative resection for pancreatic ductal adenocarcinoma. A systematic review of the literature. JOP 2008;9:99-132.

82. Schnelldorfer T, Ware AL, Sarr MG, Smyrk TC, Zhang L, Qin R, et al. Long-term survival after pancreatoduodenectomy for pancreatic adenocarcinoma: is cure possible? Ann Surg 2008;247:456-62.

83. Raut CP, Tseng JF, Sun CC, Wang H, Wolff RA, Crane CH, et al. Impact of resection status on pattern of failure and survival after pancreaticoduodenectomy for pancreatic adenocarcinoma. Ann Surg 2007;246:52-60.

84. Wasif N, Ko CY, Farrell J, Wainberg Z, Hines OJ, Reber H, et al. Impact of tumor grade on prognosis in pancreatic cancer: should we include grade in AJCC staging? Ann Surg Oncol 2010;17:2312-20.

85. Chen JW, Bhandari M, Astill DS, Wilson TG, Kow L, Brooke-Smith M, et al. Predicting patient survival after pancreaticoduodenectomy for malignancy: histopathological criteria based on perineural infiltration and lymphovascular invasion. HPB (Oxford) 2010;12:101-8.

86. Jamieson NB, Foulis AK, Oien KA, Dickson EJ, Imrie CW, Carter R, et al. Peripancreatic fat invasion is an independent predictor of poor outcome following pancreaticoduodenectomy for pancreatic ductal adenocarcinoma. J Gastrointest Surg 2011;15:512-24.

87. Kalser MH, Ellenberg SS. Pancreatic cancer. Adjuvant combined radiation and chemotherapy following curative resection. Arch Surg 1985;120:899-903.

88. Neoptolemos JP, Stocken DD, Friess H, Bassi C, Dunn JA, Hickey H, et al. A randomized trial of chemoradiotherapy and chemotherapy after resection of pancreatic cancer. N Engl J Med 2004;350:1200-10.

89. Oettle H, Post S, Neuhaus P, Gellert K, Langrehr J, Ridwelski K, et al. Adjuvant chemotherapy with gemcitabine vs observation in patients undergoing curative-intent resection of pancreatic cancer: a randomized controlled trial. JAMA 2007;297:267-77.

90. Neoptolemos JP, Stocken DD, Bassi C, Ghaneh P, Cunningham D, Goldstein D, et al. Adjuvant chemotherapy with fluorouracil plus folinic acid vs gemcitabine following pancreatic cancer resection: a randomized controlled trial. JAMA 2010;304:1073-81.

91. Regine WF, Winter KA, Abrams RA, Safran H, Hoffman JP, Konski A, et al. Fluorouracil vs gemcitabine chemotherapy before and after fluorouracil-based chemoradiation following resection of pancreatic adenocarcinoma: a randomized controlled trial. JAMA 2008;299:1019-26.

92. Erkan M, Michalski CW, Rieder S, Reiser-Erkan C, Abiatari I, Kolb A, et al. The activated stroma index is a novel and independent prognostic marker in pancreatic ductal adenocarcinoma. Clin Gastroenterol Hepatol 2008;6:1155-61.

93. Hiraoka N, Ino Y, Sekine S, Tsuda H, Shimada K, Kosuge T, et al. Tumour necrosis is a postoperative prognostic marker for pancreatic cancer patients with a high interobserver reproducibility in histological evaluation. Br J Cancer 2010;103:1057-65.

94. Ansari D, Rosendahl A, Elebro J, Andersson R. Systematic review of immunohistochemical biomarkers to identify prognostic subgroups of patients with pancreatic cancer. Br J Surg 2011;98:1041-55.

95. Brennan MF, Kattan MW, Klimstra D, Conlon K. Prognostic nomogram for patients undergoing resection for adenocarcinoma of the pancreas. Ann Surg 2004;240:293-8.

96. Clark EJ, Taylor MA, Connor S, O'Neill R, Brennan MF, Garden OJ, et al. Validation of a prognostic nomogram in patients undergoing resection for pancreatic ductal adenocarcinoma in a UK tertiary referral centre. HPB (Oxford) 2008;10:501-5.

97. de Castro SM, Biere SS, Lagarde SM, Busch OR, van Gulik TM, Gouma DJ. Validation of a nomogram for predicting survival after resection for adenocarcinoma of the pancreas. Br J Surg 2009;96:417-23.

98. Ferrone CR, Kattan MW, Tomlinson JS, Thayer SP, Brennan MF, Warshaw AL. Validation of a postresection pancreatic adenocarcinoma nomogram for disease-specific survival. J Clin Oncol 2005;23:7529-35.

99. Botsis T, Anagnostou VK, Hartvigsen G, Hripcsak G, Weng C. Modeling prognostic factors in resectable pancreatic adenocarcinomas. Cancer Inform 2010;7:281-91.

100. Pencina MJ, D'Agostino RB. Overall C as a measure of discrimination in survival analysis: model specific population value and confidence interval estimation. Stat Med 2004;23:2109-23.

101. Harrell FE, Jr., Lee KL, Mark DB. Multivariable prognostic models: issues in developing models, evaluating assumptions and adequacy, and measuring and reducing errors. Stat Med 1996;15:361-87.

102. Harrell FE, Jr., Califf RM, Pryor DB, Lee KL, Rosati RA. Evaluating the yield of medical tests. JAMA 1982;247:2543-6.

103. Koziol JA, Jia Z. The concordance index C and the Mann-Whitney parameter Pr(X>Y) with randomly censored data. Biom J 2009;51:467-74.

104. Mallett S, Royston P, Waters R, Dutton S, Altman DG. Reporting performance of prognostic models in cancer: a review. BMC Med 2010;8:21.

105. Curran D, O'Riordan C. Neural network evolution and artificial life research. Tosh C, Ruxton G, editors. Cambridge: Cambridge University Press; 2010.

106. Nilsson J. Risk stratification in cardiac surgery: algorithms and applications [Dissertation]. Lund: Lund University; 2005.

107. Heden B, Ohlin H, Rittner R, Edenbrandt L. Acute myocardial infarction detected in the 12-lead ECG by artificial neural networks. Circulation 1997;96:1798-802.

108. Lundin M, Lundin J, Burke HB, Toikkanen S, Pylkkanen L, Joensuu H. Artificial neural networks applied to survival prediction in breast cancer. Oncology 1999;57:281-6.

109. Dolgobrodov SG, Moore P, Marshall R, Bittern R, Steele RJ, Cuschieri A. Artificial neural network: predicted vs observed survival in patients with colonic cancer. Dis Colon Rectum 2007;50:184-91.

110. Sato F, Shimada Y, Selaru FM, Shibata D, Maeda M, Watanabe G, et al. Prediction of survival in patients with esophageal carcinoma using artificial neural networks. Cancer 2005;103:1596-605.

111. Bachmann J, Michalski CW, Martignoni ME, Buchler MW, Friess H. Pancreatic resection for pancreatic cancer. HPB (Oxford) 2006;8:346-51.

112. Diener MK, Fitzmaurice C, Schwarzer G, Seiler CM, Antes G, Knaebel HP, et al. Pylorus-preserving pancreaticoduodenectomy (pp Whipple) versus pancreaticoduodenectomy (classic Whipple) for surgical treatment of periampullary and pancreatic carcinoma. Cochrane Database Syst Rev 2011:CD006053.

113. Liu FB, Chen JM, Geng W, Xie SX, Zhao YJ, Yu LQ, et al. Pancreaticogastrostomy is associated with significantly less pancreatic fistula than pancreaticojejunostomy reconstruction after pancreaticoduodenectomy: a meta-analysis of seven randomized controlled trials. HPB (Oxford) 2014; June 3 [Epub ahead of print].

114. Jang JY, Kang MJ, Heo JS, Choi SH, Choi DW, Park SJ, et al. A prospective randomized controlled study comparing outcomes of standard resection and extended resection, including dissection of the nerve plexus and various lymph nodes, in patients with pancreatic head cancer. Ann Surg 2014;259:656-64.

115. Liles JS, Katz MH. Pancreaticoduodenectomy with vascular resection for pancreatic head adenocarcinoma. Expert Rev Anticancer Ther 2014:1-11.

116. Balzano G, Zerbi A, Capretti G, Rocchetti S, Capitanio V, Di Carlo V. Effect of hospital volume on outcome of pancreaticoduodenectomy in Italy. Br J Surg 2008;95:357-62.

117. Birkmeyer JD, Finlayson SR, Tosteson AN, Sharp SM, Warshaw AL, Fisher ES. Effect of hospital volume on in-hospital mortality with pancreaticoduodenectomy. Surgery 1999;125:250-6.

118. Birkmeyer JD, Siewers AE, Finlayson EV, Stukel TA, Lucas FL, Batista I, et al. Hospital volume and surgical mortality in the United States. N Engl J Med 2002;346:1128-37.

119. de Wilde RF, Besselink MG, van der Tweel I, de Hingh IH, van Eijck CH, Dejong CH, et al. Impact of nationwide centralization of pancreaticoduodenectomy on hospital mortality. Br J Surg 2012;99:404-10.

120. Finks JF, Osborne NH, Birkmeyer JD. Trends in hospital volume and operative mortality for high-risk surgery. N Engl J Med 2011;364:2128-37.

121. Gordon TA, Bowman HM, Tielsch JM, Bass EB, Burleyson GP, Cameron JL. Statewide regionalization of pancreaticoduodenectomy and its effect on in-hospital mortality. Ann Surg 1998;228:71-8.

122. Gouma DJ, van Geenen RC, van Gulik TM, de Haan RJ, de Wit LT, Busch OR, et al. Rates of complications and death after pancreaticoduodenectomy: risk factors and the impact of hospital volume. Ann Surg 2000;232:786-95.

123. Ho V, Heslin MJ. Effect of hospital volume and experience on in-hospital mortality for pancreaticoduodenectomy. Ann Surg 2003;237:509-14.

124. Nordback L, Parviainen M, Raty S, Kuivanen H, Sand J. Resection of the head of the pancreas in Finland: effects of hospital and surgeon on short-term and long-term results. Scand J Gastroenterol 2002;37:1454-60.

125. Topal B, Van de Sande S, Fieuws S, Penninckx F. Effect of centralization of pancreaticoduodenectomy on nationwide hospital mortality and length of stay. Br J Surg 2007;94:1377-81.

126. Urbach DR, Bell CM, Austin PC. Differences in operative mortality between high- and low-volume hospitals in Ontario for 5 major surgical procedures: estimating the number of lives potentially saved through regionalization. CMAJ 2003;168:1409-14.

127. La Torre M, Nigri G, Ferrari L, Cosenza G, Ravaioli M, Ramacciato G. Hospital volume, margin status, and long-term survival after pancreaticoduodenectomy for pancreatic adenocarcinoma. Am Surg 2012;78:225-9.

128. Learn PA, Bach PB. A decade of mortality reductions in major oncologic surgery: the impact of centralization and quality improvement. Med Care 2010;48:1041-9.

129. Moore MJ, Goldstein D, Hamm J, Figer A, Hecht JR, Gallinger S, et al. Erlotinib plus gemcitabine compared with gemcitabine alone in patients with advanced pancreatic cancer: a phase III trial of the National Cancer Institute of Canada Clinical Trials Group. J Clin Oncol 2007;25:1960-6.

130. Lockley M, Tuveson D. Mouse models of pancreatic exocrine cancer. In: Neoptolemos JP, Urrutia R, Abbruzzese J, Büchler MW, editors. Pancreatic cancer: Springer; 2010.

131. Garber K. Realistic rodents? Debate grows over new mouse models of cancer. J Natl Cancer Inst 2006;98:1176-8.

132. Duner S, Lopatko Lindman J, Ansari D, Gundewar C, Andersson R. Pancreatic cancer: the role of pancreatic stellate cells in tumor progression. Pancreatology 2010;10:673-81.

133. Kyriazis AP, Kyriazis AA, Scarpelli DG, Fogh J, Rao MS, Lepera R. Human pancreatic adenocarcinoma line Capan-1 in tissue culture and the nude mouse: morphologic, biologic, and biochemical characteristics. Am J Pathol 1982;106:250-60.

134. Lohr M, Trautmann B, Gottler M, Peters S, Zauner I, Maillet B, et al. Human ductal adenocarcinomas of the pancreas express extracellular matrix proteins. Br J Cancer 1994;69:144-51.

135. Singh AP, Chaturvedi P, Batra SK. Emerging roles of MUC4 in cancer: a novel target for diagnosis and therapy. Cancer Res 2007;67:433-6.

136. Chaturvedi P, Singh AP, Batra SK. Structure, evolution, and biology of the MUC4 mucin. FASEB J 2008;22:966-81.

137. Kaur S, Kumar S, Momi N, Sasson AR, Batra SK. Mucins in pancreatic cancer and its microenvironment. Nat Rev Gastroenterol Hepatol 2013;10:607-20.

138. Ciccarelli FD, Doerks T, Bork P. AMOP, a protein module alternatively spliced in cancer cells. Trends Biochem Sci 2002;27:113-5.

139. Senapati S, Gnanapragassam VS, Moniaux N, Momi N, Batra SK. Role of MUC4-NIDO domain in the MUC4-mediated metastasis of pancreatic cancer cells. Oncogene 2012;31:3346-56.

140. Chang CY, Chang HW, Chen CM, Lin CY, Chen CP, Lai CH, et al. MUC4 gene polymorphisms associate with endometriosis development and endometriosis-related infertility. BMC Med 2011;9:19.

141. Jonckheere N, Skrypek N, Van Seuningen I. Mucins and pancreatic cancer. Cancers (Basel) 2010;2:1794-812.

142. Jepson S, Komatsu M, Haq B, Arango ME, Huang D, Carraway CA, et al. Muc4/sialomucin complex, the intramembrane ErbB2 ligand, induces specific phosphorylation of ErbB2 and enhances expression of p27(kip), but does not activate mitogen-activated kinase or protein kinaseB/Akt pathways. Oncogene 2002;21:7524-32.

143. Carraway KL, Perez A, Idris N, Jepson S, Arango M, Komatsu M, et al. Muc4/sialomucin complex, the intramembrane ErbB2 ligand, in cancer and epithelia: to protect and to survive. Prog Nucleic Acid Res Mol Biol 2002;71:149-85.

144. Workman HC, Sweeney C, Carraway KL, 3rd. The membrane mucin Muc4 inhibits apoptosis induced by multiple insults via ErbB2-dependent and ErbB2-independent mechanisms. Cancer Res 2009;69:2845-52.

145. Workman HC, Miller JK, Ingalla EQ, Kaur RP, Yamamoto DI, Beckett LA, et al. The membrane mucin MUC4 is elevated in breast tumor lymph node metastases relative to matched primary tumors and confers aggressive properties to breast cancer cells. Breast Cancer Res 2009;11:R70.

146. Tsutsumida H, Goto M, Kitajima S, Kubota I, Hirotsu Y, Wakimoto J, et al. MUC4 expression correlates with poor prognosis in small-sized lung adenocarcinoma. Lung Cancer 2007;55:195-203.

147. Singh AP, Senapati S, Ponnusamy MP, Jain M, Lele SM, Davis JS, et al. Clinical potential of mucins in diagnosis, prognosis, and therapy of ovarian cancer. Lancet Oncol 2008;9:1076-85.

148. Algamas-Dimantov A, Yehuda-Shnaidman E, Peri I, Schwartz B. Epigenetic control of HNF-4alpha in colon carcinoma cells affects MUC4 expression and malignancy. Cell Oncol (Dordr) 2013;36:155-67.

149. Andrianifahanana M, Moniaux N, Schmied BM, Ringel J, Friess H, Hollingsworth MA, et al. Mucin (MUC) gene expression in human pancreatic adenocarcinoma and chronic pancreatitis: a potential role of MUC4 as a tumor marker of diagnostic significance. Clin Cancer Res 2001;7:4033-40.

150. Swartz MJ, Batra SK, Varshney GC, Hollingsworth MA, Yeo CJ, Cameron JL, et al. MUC4 expression increases progressively in pancreatic intraepithelial neoplasia. Am J Clin Pathol 2002;117:791-6.

151. Saitou M, Goto M, Horinouchi M, Tamada S, Nagata K, Hamada T, et al. MUC4 expression is a novel prognostic factor in patients with invasive ductal carcinoma of the pancreas. J Clin Pathol 2005;58:845-52.

152. Aloysius MM, Zaitoun AM, Awad S, Ilyas M, Rowlands BJ, Lobo DN. Mucins and CD56 as markers of tumour invasion and prognosis in periampullary cancer. Br J Surg 2010;97:1269-78.

153. Zhu Y, Zhang JJ, Zhu R, Zhu Y, Liang WB, Gao WT, et al. The increase in the expression and hypomethylation of MUC4 gene with the progression of pancreatic ductal adenocarcinoma. Med Oncol 2011;28 Suppl 1:S175-84.

154. Chaturvedi P, Singh AP, Moniaux N, Senapati S, Chakraborty S, Meza JL, et al. MUC4 mucin potentiates pancreatic tumor cell proliferation, survival, and

invasive properties and interferes with its interaction to extracellular matrix proteins. Mol Cancer Res 2007;5:309-20.

155. Rachagani S, Macha MA, Ponnusamy MP, Haridas D, Kaur S, Jain M, et al. MUC4 potentiates invasion and metastasis of pancreatic cancer cells through stabilization of fibroblast growth factor receptor 1. Carcinogenesis 2012;33:1953-64.

156. Chaturvedi P, Singh AP, Chakraborty S, Chauhan SC, Bafna S, Meza JL, et al. MUC4 mucin interacts with and stabilizes the HER2 oncoprotein in human pancreatic cancer cells. Cancer Res 2008;68:2065-70.

157. Jonckheere N, Skrypek N, Merlin J, Dessein AF, Dumont P, Leteurtre E, et al. The mucin MUC4 and its membrane partner ErbB2 regulate biological properties of human CAPAN-2 pancreatic cancer cells via different signalling pathways. PLoS One 2012;7:e32232.

158. Vincent A, Ducourouble MP, Van Seuningen I. Epigenetic regulation of the human mucin gene MUC4 in epithelial cancer cell lines involves both DNA methylation and histone modifications mediated by DNA methyltransferases and histone deacetylases. FASEB J 2008;22:3035-45.

159. Rodriguez-Suarez E, Hughes C, Gethings L, Giles K, Wildgoose J, Stapels M, et al. An ion mobility assisted data independent LC-MS strategy for the analysis of complex biological samples. Curr Anal Chem 2013;9:199-211.

160. Silva JC, Denny R, Dorschel CA, Gorenstein M, Kass IJ, Li GZ, et al. Quantitative proteomic analysis by accurate mass retention time pairs. Anal Chem 2005;77:2187-200.

161. Silva JC, Gorenstein MV, Li GZ, Vissers JP, Geromanos SJ. Absolute quantification of proteins by LCMSE: a virtue of parallel MS acquisition. Mol Cell Proteomics 2006;5:144-56.

162. Mi H, Muruganujan A, Casagrande JT, Thomas PD. Large-scale gene function analysis with the PANTHER classification system. Nat Protoc 2013;8:1551-66.

163. Cross SS, Harrison RF, Kennedy RL. Introduction to neural networks. Lancet 1995;346:1075-9.

164. Biganzoli E, Boracchi P, Mariani L, Marubini E. Feed forward neural networks for the analysis of censored survival data: a partial logistic regression approach. Stat Med 1998;17:1169-86.

165. Andersson B, Andersson R, Ohlsson M, Nilsson J. Prediction of severe acute pancreatitis at admission to hospital using artificial neural networks. Pancreatology 2011;11:328-35.

166. Lippmann RP, Shahian DM. Coronary artery bypass risk prediction using neural networks. Ann Thorac Surg 1997;63:1635-43.

167. Dindo D, Demartines N, Clavien PA. Classification of surgical complications: a new proposal with evaluation in a cohort of 6336 patients and results of a survey. Ann Surg 2004;240:205-13.

168. Wente MN, Bassi C, Dervenis C, Fingerhut A, Gouma DJ, Izbicki JR, et al. Delayed gastric emptying (DGE) after pancreatic surgery: a suggested definition by the International Study Group of Pancreatic Surgery (ISGPS). Surgery 2007;142:761-8.

169. Wente MN, Veit JA, Bassi C, Dervenis C, Fingerhut A, Gouma DJ, et al. Postpancreatectomy hemorrhage (PPH): an International Study Group of Pancreatic Surgery (ISGPS) definition. Surgery 2007;142:20-5.

170. Bassi C, Dervenis C, Butturini G, Fingerhut A, Yeo C, Izbicki J, et al. Postoperative pancreatic fistula: an international study group (ISGPF) definition. Surgery 2005;138:8-13.

171. Masamune A, Hamada S, Kikuta K, Takikawa T, Miura S, Nakano E, et al. The angiotensin II type I receptor blocker olmesartan inhibits the growth of pancreatic cancer by targeting stellate cell activities in mice. Scand J Gastroenterol 2013;48:602-9.

172. Tomayko MM, Reynolds CP. Determination of subcutaneous tumor size in athymic (nude) mice. Cancer Chemother Pharmacol 1989;24:148-54.

173. Franceschini A, Szklarczyk D, Frankild S, Kuhn M, Simonovic M, Roth A, et al. STRING v9.1: protein-protein interaction networks, with increased coverage and integration. Nucleic Acids Res 2013;41:D808-15.

174. Schemper M, Smith TL. Efficient evaluation of treatment effects in the presence of missing covariate values. Stat Med 1990;9:777-84.

175. Chen R, Pan S, Brentnall TA, Aebersold R. Proteomic profiling of pancreatic cancer for biomarker discovery. Mol Cell Proteomics 2005;4:523-33.

176. Polanski M, Anderson NL. A list of candidate cancer biomarkers for targeted proteomics. Biomark Insights 2007;1:1-48.

177. Oshima M, Okano K, Muraki S, Haba R, Maeba T, Suzuki Y, et al. Immunohistochemically detected expression of 3 major genes (CDKN2A/p16, TP53, and SMAD4/DPC4) strongly predicts survival in patients with resectable pancreatic cancer. Ann Surg 2013;258:336-46.

178. Jones S, Zhang X, Parsons DW, Lin JC, Leary RJ, Angenendt P, et al. Core signaling pathways in human pancreatic cancers revealed by global genomic analyses. Science 2008;321:1801-6.

179. Morton JP, Timpson P, Karim SA, Ridgway RA, Athineos D, Doyle B, et al. Mutant p53 drives metastasis and overcomes growth arrest/senescence in pancreatic cancer. Proc Natl Acad Sci U S A 2010;107:246-51.

180. Rosenfeldt MT, O'Prey J, Morton JP, Nixon C, MacKay G, Mrowinska A, et al. p53 status determines the role of autophagy in pancreatic tumour development. Nature 2013;504:296-300.

181. Han JW, Ahn SH, Park SH, Wang SY, Bae GU, Seo DW, et al. Apicidin, a histone deacetylase inhibitor, inhibits proliferation of tumor cells via induction of p21WAF1/Cip1 and gelsolin. Cancer Res 2000;60:6068-74.

182. Hong J, Ishihara K, Yamaki K, Hiraizumi K, Ohno T, Ahn JW, et al. Apicidin, a histone deacetylase inhibitor, induces differentiation of HL-60 cells. Cancer Lett 2003;189:197-206.

183. Ishihara K, Hong J, Zee O, Ohuchi K. Possible mechanism of action of the histone deacetylase inhibitors for the induction of differentiation of HL-60 clone 15 cells into eosinophils. Br J Pharmacol 2004;142:1020-30.

184. Hanash SM, Pitteri SJ, Faca VM. Mining the plasma proteome for cancer biomarkers. Nature 2008;452:571-9.

185. Tingstedt B, Johansson P, Andersson B, Andersson R. Predictive factors in pancreatic ductal adenocarcinoma: role of the inflammatory response. Scand J Gastroenterol 2007;42:754-9.

186. Damato B, Eleuteri A, Fisher AC, Coupland SE, Taktak AF. Artificial neural networks estimating survival probability after treatment of choroidal melanoma. Ophthalmology 2008;115:1598-607.

187. Eleuteri A, Aung MS, Taktak AF, Damato B, Lisboa PJ. Continuous and discrete time survival analysis: neural network approaches. Conf Proc IEEE Eng Med Biol Soc 2007;2007:5420-3.

188. Faraggi D, Simon R. A neural network model for survival data. Stat Med 1995;14:73-82.

189. Hoang T, Trinh QA, Asselain B. Construction and validation of a prognostic model for metastatic breast cancer using bayesian neural network and regression tree. Intelligent data analysis in medicine and pharmacology The european conference on artificial intelligence; 23rd July; Lyon, France: ECAI; 2002. p. 37–43.

190. Taktak AFG, Eleuteri A, Aung MSH, Lisboa PJG, Desjardins L, Damato BE. Survival analysis in cancer using a partial logistic neural network model with Bayesian regularisation framework: a validation study. Int J Knowledge Engineering Soft Data Paradigms 2009;1:277–95.

191. Tsai S, Choti MA, Assumpcao L, Cameron JL, Gleisner AL, Herman JM, et al. Impact of obesity on perioperative outcomes and survival following pancreaticoduodenectomy for pancreatic cancer: a large single-institution study. J Gastrointest Surg 2010;14:1143-50.

192. Mathur AK, Ghaferi AA, Sell K, Sonnenday CJ, Englesbe MJ, Welling TH. Influence of body mass index on complications and oncologic outcomes following hepatectomy for malignancy. J Gastrointest Surg 2010;14:849-57.

193. Benz CC. Impact of aging on the biology of breast cancer. Crit Rev Oncol Hematol 2008;66:65-74.

194. Etzel CJ, Lu M, Merriman K, Liu M, Vaporciyan A, Spitz MR. An epidemiologic study of early onset lung cancer. Lung Cancer 2006;52:129-34.

195. Li N, Grivennikov SI, Karin M. The unholy trinity: inflammation, cytokines, and STAT3 shape the cancer microenvironment. Cancer Cell 2011;19:429-31.

196. De Monte L, Reni M, Tassi E, Clavenna D, Papa I, Recalde H, et al. Intratumor T helper type 2 cell infiltrate correlates with cancer-associated fibroblast thymic stromal lymphopoietin production and reduced survival in pancreatic cancer. J Exp Med 2011;208:469-78.

197. Russ AJ, Weber SM, Rettammel RJ, Mahvi DM, Rikkers LF, Cho CS. Impact of selection bias on the utilization of adjuvant therapy for pancreas adenocarcinoma. Ann Surg Oncol 2010;17:371-6.

198. van der Heijden GJ, Donders AR, Stijnen T, Moons KG. Imputation of missing values is superior to complete case analysis and the missing-indicator method in multivariable diagnostic research: a clinical example. J Clin Epidemiol 2006;59:1102-9.

199. Lee CN, Daly JM. Provider volume and clinical outcomes in surgery: issues and implications. Bull Am Coll Surg 2002;87:21-6.

200. Chakraborty S, Jain M, Sasson AR, Batra SK. MUC4 as a diagnostic marker in cancer. Expert Opin Med Diagn 2008;2:891-910.

201. Remmers N, Anderson JM, Linde EM, DiMaio DJ, Lazenby AJ, Wandall HH, et al. Aberrant expression of mucin core proteins and o-linked glycans associated with progression of pancreatic cancer. Clin Cancer Res 2013;19:1981-93.

202. Ponnusamy MP, Lakshmanan I, Jain M, Das S, Chakraborty S, Dey P, et al. MUC4 mucin-induced epithelial to mesenchymal transition: a novel mechanism for metastasis of human ovarian cancer cells. Oncogene 2010;29:5741-54.

203. Yachida S, Iacobuzio-Donahue CA. The pathology and genetics of metastatic pancreatic cancer. Arch Pathol Lab Med 2009;133:413-22.

204. Nichols LS, Ashfaq R, Iacobuzio-Donahue CA. Claudin 4 protein expression in primary and metastatic pancreatic cancer: support for use as a therapeutic target. Am J Clin Pathol 2004;121:226-30.

205. Hinz B, Gabbiani G. Mechanisms of force generation and transmission by myofibroblasts. Curr Opin Biotechnol 2003;14:538-46.

206. Tomasek JJ, Gabbiani G, Hinz B, Chaponnier C, Brown RA. Myofibroblasts and mechano-regulation of connective tissue remodelling. Nat Rev Mol Cell Biol 2002;3:349-63.

207. Sugimoto H, Mundel TM, Kieran MW, Kalluri R. Identification of fibroblast heterogeneity in the tumor microenvironment. Cancer Biol Ther 2006;5:1640-6.

208. Hwang RF, Moore T, Arumugam T, Ramachandran V, Amos KD, Rivera A, et al. Cancer-associated stromal fibroblasts promote pancreatic tumor progression. Cancer Res 2008;68:918-26.

209. Joyce JA, Pollard JW. Microenvironmental regulation of metastasis. Nat Rev Cancer 2009;9:239-52.

210. Levental KR, Yu H, Kass L, Lakins JN, Egeblad M, Erler JT, et al. Matrix crosslinking forces tumor progression by enhancing integrin signaling. Cell 2009;139:891-906.

211. Bachem MG, Schunemann M, Ramadani M, Siech M, Beger H, Buck A, et al. Pancreatic carcinoma cells induce fibrosis by stimulating proliferation and matrix synthesis of stellate cells. Gastroenterology 2005;128:907-21.

212. Cortez E, Roswall P, Pietras K. Functional subsets of mesenchymal cell types in the tumor microenvironment. Semin Cancer Biol 2014;25C:3-9.

213. Jonckheere N, Vincent A, Perrais M, Ducourouble MP, Male AK, Aubert JP, et al. The human mucin MUC4 is transcriptionally regulated by caudal-related homeobox, hepatocyte nuclear factors, forkhead box A, and GATA endodermal transcription factors in epithelial cancer cells. J Biol Chem 2007;282:22638-50.

214. Kim S, Kang JK, Kim YK, Seo DW, Ahn SH, Lee JC, et al. Histone deacetylase inhibitor apicidin induces cyclin E expression through Sp1 sites. Biochem Biophys Res Commun 2006;342:1168-73.

215. Donadelli M, Costanzo C, Beghelli S, Scupoli MT, Dandrea M, Bonora A, et al. Synergistic inhibition of pancreatic adenocarcinoma cell growth by trichostatin A and gemcitabine. Biochim Biophys Acta 2007;1773:1095-106.

216. Eeson G, Chang N, McGahan CE, Khurshed F, Buczkowski AK, Scudamore CH, et al. Determination of factors predictive of outcome for patients undergoing a pancreaticoduodenectomy of pancreatic head ductal adenocarcinomas. HPB (Oxford) 2012;14:310-6.

217. Venkat R, Puhan MA, Schulick RD, Cameron JL, Eckhauser FE, Choti MA, et al. Predicting the risk of perioperative mortality in patients undergoing pancreaticoduodenectomy: a novel scoring system. Arch Surg 2011;146:1277-84.

218. Ueda T, Takai N, Nishida M, Nasu K, Narahara H. Apicidin, a novel histone deacetylase inhibitor, has profound anti-growth activity in human endometrial and ovarian cancer cells. Int J Mol Med 2007;19:301-8.